doi:10.1038/nature18933

Supplementary Neuroanatomical Results For A Multi-modal Parcellation of Human Cerebral Cortex

Matthew F. Glasser[1], Timothy S. Coalson[1]*, Emma C. Robinson[2,3]*, Carl D. Hacker[4]*, John Harwell[1], Essa Yacoub[5], Kamil Ugurbil[5], Jesper Andersson[2], Christian F. Beckmann[6], Mark Jenkinson[2], Stephen M. Smith[2], David C. Van Essen[1]

[1]Department of Neuroscience, Washington University Medical School, Saint Louis, Missouri 63110, USA. [2]FMRIB Centre, Nuffield Department of Clinical Neurosciences, John Radcliffe Hospital, University of Oxford, Oxford OX3 9DU, UK. [3]Department of Computing, Imperial College, London SW7 2AZ, UK. [4]Department of Biomedical Engineering, Washington University, Saint Louis, Missouri 63110, USA. [5]Center for Magnetic Resonance Research (CMRR), University of Minnesota, Minneapolis, Minnesota 55455, USA. [6]Donders Institute for Brain, Cognition and Behavior, Radboud University, Nijmegen 6525 EN, The Netherlands. [7]Department of Cognitive Neuroscience, Radboud University Medical Centre Nijmegen, Postbus 9101, Nijmegen 6500 HB, The Netherlands.

**These authors contributed equally to this work.*

Introduction and Overview

The Supplementary Neuroanatomical Results presented below provide extensive documentation describing our identification of 180 human neocortical areas and the evidence used to delineate their boundaries based on the 210P group average multi-modal data. This introductory section gives an overview of the Supplementary Neuroanatomical Results and general comments covering the subsequent 22 region-by-region sections that describe the boundary between each pair of cortical areas. Each boundary is described only once, in the first section where it is encountered.

Grouping by Regions

For organizational purposes, we grouped the 180 cortical areas into 22 regions based on several criteria: Each region includes a set of geographically contiguous areas that can be seen in their entirety from a single viewing perspective on the inflated cortical surface or in some cases on a flatmap. In addition, the areas within a region often share common properties, based on architecture, task-fMRI profiles, and/or functional connectivity. Figure 1 shows each region in a different color, with areal boundaries in black, displayed on lateral and medial views of the left and right hemisphere inflated cortical surfaces and on the corresponding flatmaps. The color choices below were inspired by the predominant colors in each region in Main Text Figure 3.

Area names and terminological styles

Supplemental Table 1 at the end of this document lists each area by parcellation index number, along with the area's brief name, full name, whether it was newly described, the primary (**Bold**) and secondary text section numbers that describe the features used to

distinguish the area from its neighbors, some synonyms for the area in the literature (or 'quasi-synonymns' for areas that are similar but not convincingly identical), and the primary reference(s) used in assigning these names. Supplemental Table 2 lists the studies used to identify the areas in this parcellation together with our area names and how they correspond to those mentioned in each study. In general, we used existing terminology whenever we could identify a reasonable match between an area in an existing parcellation and an area identified in the HCP data. Correspondence was based on similarity in location, using inferred local geographic landmarks (gyri and sulci) together with the spatial relationships with neighboring areas whose correspondence to our parcellation's areas was already established. Because we registered the data based on cortical areal features instead of folding patterns, only those folding features having consistent relationships with cortical areas were preserved in the group average data. Finally, we used specific areal features (e.g., degree of myelination, type of functional specialization, or topographic organization) when available in the prior studies (e.g. the comparison of myelin maps around 55b in Main Text Figure 2). In many instances, alternative names could have reasonably been selected. We strove for names that reflected the 'best fit', and secondarily to use similar terminology when feasible to describe the areas in a given region. However, in several regions we either introduced completely new terminology because we did not find appropriate correspondences in the literature, or we modified existing names to reflect a finer grained parcellation than was found in earlier studies.

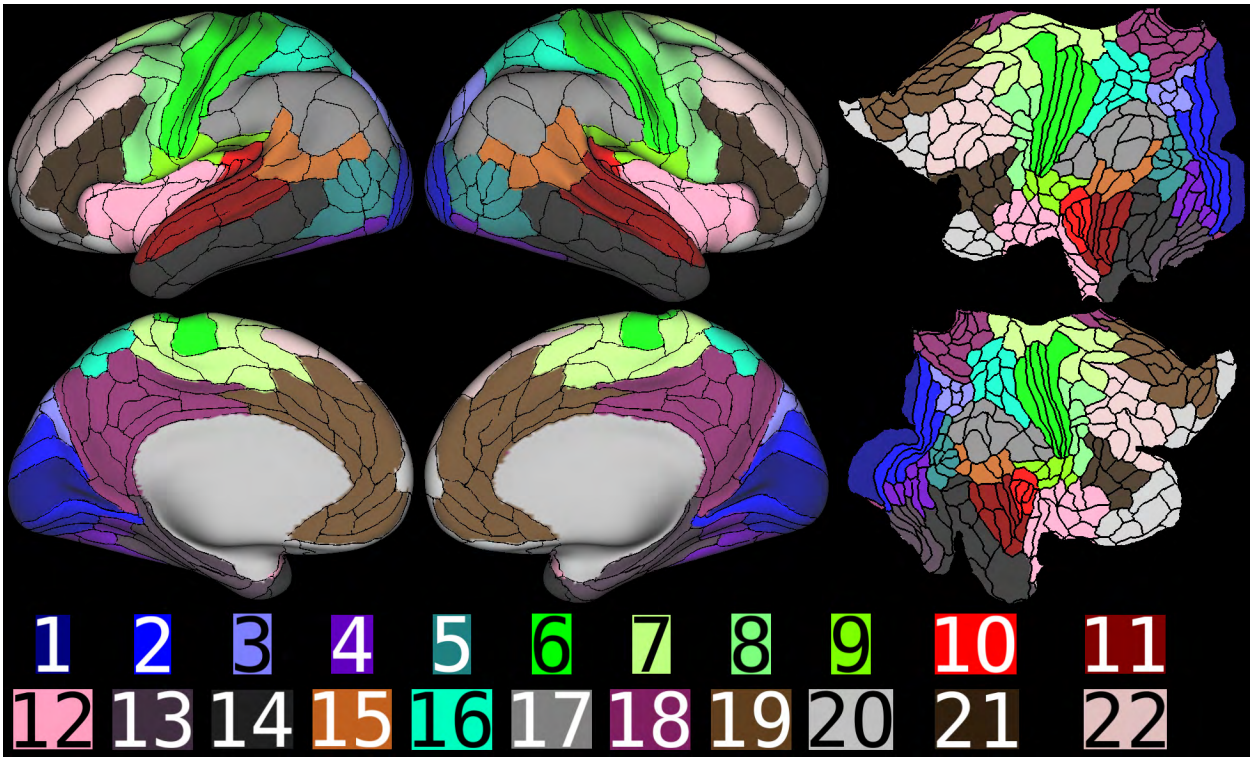

Figure 1 shows the 22 numbered results sections to be covered below. Data at http://balsa.wustl.edu/QnXj.

Given the diverse terminological styles used over the past century of parcellation work, our parcellation contains a mixture of these styles. Some areas are described by numerals (e.g., areas 1, 2, 4), others by all-caps letters (e.g., MT, PF), and others by

combinations of letters and numbers (e.g. V1, V2, OP1). Lower case letters typically represent subdivisions of a once-larger parcel, and they signify relative position within the brain. Some of these use the anterior/posterior convention (e.g., 6mp and 6ma), whereas others use the rostral/caudal convention (e.g., 47r). Some use the dorsal/ventral convention (e.g., LIPd, LIPv) whereas others use the superior/inferior convention (e.g., PGi, PGs). Others use numerals or letters for finer-grained parcellation that is not readily described using cardinal axes (e.g., TPOJ1, TPOJ2, TPOJ3). In some cases we adopted an existing name except for a format change. (i) We used capital 'L' instead of lower-case 'l' to avoid confusion with numeral '1' (e.g., area 7AL instead of 7Al). (ii) We converted the forward-slash '/' to a hyphen '-'(e.g., area 6-8 instead of published area 6/8), because '/' is a reserved character in many programming languages. (iii) We converted ['] to [pr] ('prime') for a similar reason.

Multi-modal Areal Differences

Nearly all areas identified in our parcellation had borders with their neighbors that reflected significant differences by at least two areal feature measures. The semi-automated border delineation tool provided estimates of statistical significance and effect size for each areal feature used to delineate each areal boundary. Most p values were very small (with a substantial fraction having p values too small to represent in float32), with a maximum pvalue of $p<0.001$ for all reported areal features across all boundaries. Additionally, most effect sizes were Cohen's $d>1$, with a minimum Cohen's $d>0.5$ for all reported areal features across all boundaries (0.5 is a 'medium' effect size). These statistical significance and effect size measures were used mainly to screen areal feature gradients to ensure they were likely to be statistically significantly and robustly different and thus strong candidates for true areal boundaries. However, because the tests were performed on the same data as were used to make the parcellation, the parcellation was additionally evaluated with non-circular statistical tests across all areal features using the 210V dataset (see Supplementary Figure 6 and #1.2 in the Supplementary Results and Discussion).

Some parcels are internally heterogeneous in single modalities that might hint at finer grained parcellation. Other parcels may have previously been parcellated more finely in published parcellations. However, we strove to include areal boundaries only when they are strongly supported by multiple modalities in our own data. Hence, our number of 180 cortical areas per hemisphere likely reflects a lower bound. Some areas may be further parcellated using new datasets and/or analysis methods, and some areas are explicitly identified as 'area complexes' (e.g., the Fusiform Face Complex, FFC). Additionally, there are some areas that are impossible to parcellate accurately with the current HCP data due to signal loss in the fMRI modalities from susceptibility artifacts or venous shadows. Higher resolution data with fewer artifacts, different task batteries, or other novel information will likely lead to refinements to this parcellation, which is why it is described as version 1.0.

Organization of subsequent sections

The primary purpose of the 22 sections that follow is to describe and illustrate much of the evidence that was used to delineate borders between each cortical area and each of its neighbors, using the gradient-based semi-automated border optimization method described in the Supplementary Methods. For these border delineations, only a subset of the possible feature contrasts were used. Hence, the descriptions of distinguishing areal features often do not include every feature that was significantly different, but they nonetheless provide a useful tabulation of many of the features that distinguish each area from its neighbors. For many/most area pairs, there are many more statistically significant areal-feature differences than are described in the sections below. The complete multi-modal signatures for each area and their differences relative to neighboring areas can be more systematically and robustly analyzed using the same approach that was used in the statistical cross-validation analysis (Supplementary Figure 6 in the Supplementary Results and Discussion).

In describing the positions of one area relative to its neighbors, we generally use superior/inferior instead of dorsal/ventral, and anterior/posterior instead of rostral/caudal, based on their locations on the HCP group average midthickness surface. To aid in reading the admittedly dense prose, we highlight the 'reference' area name in bold when making a between-area comparison (e.g., "Relative to its dorsal neighbor XX, **area YY** has more myelin, etc."

Most of the figures have a similar format: The first panel shows the borders of the region's constituent areas overlaid on a map showing the group average cortical folding pattern (based on FreeSurfer's mean curvature maps) on inflated or flattened surfaces, along with Connectome Workbench brain annotations naming all of the areas and many of their neighbors. The remaining panels use the same viewing perspective as the first panel together with the areal borders to illustrate much of the information that was used in delineating the areal borders with the semi-automated border optimization method in Connectome Workbench. These are typically ordered as (i) myelin maps, (ii) thickness maps, (iii) functional connectivity gradients, and (iv) various task-fMRI contrasts that are particularly informative about the region being discussed. Aside from the first section, we generally do not show gradients of many of the modalities, thereby reducing by ~half the number of panels in each figure. Each of the figures is available as a Connectome Workbench 'scene' that can be accessed via the BALSA database using the scene-specific URLs in each figure legend (http://balsa.wustl.edu/BALSA_Scene_ID). All scenes in this document are included in a single scene file that can be downloaded along with all associated data files for interactive visualization (with annotations included) in the 'wb_view' software (Connectome Workbench v1.2.0 and higher).

Caveats and comments on specific modalities:

Myelin. We use the expression that an area "has more myelin" or "has less myelin" than a neighbor to refer to cross-border differences in which a statistically significant and robust difference was found when comparing the two areas for the values of T1w/T2w mapped to the cortical surface as described in the Supplementary Methods (e.g., with bias correction). Strictly speaking, the T1w/T2w ratio is not a 'pure' measure of myelin content, as it may be influenced by other characteristics within each voxel (see Supplementary Figure 1 legend

in the Supplementary Results and Discussion, and also (Glasser et al., 2014; Glasser and Van Essen, 2011).

Cortical Thickness. Thickness measures were compensated for systematic folding-related biases (relative to neutral sulcal banks, gyral cortex is thicker and fundal cortex is thinner). Such variation will mask the area-specific differences in cortical thickness that are useful for parcellation. We compensated thickness for folding biases by regressing out FreeSurfer's mean curvature map (see Supplementary Methods #1.5), but refer to the resulting measure simply as 'cortical thickness' below.

Functional Connectivity. Functional connectivity in most cases is described only as demonstrating robust and statistically significant across-border 'connectivity differences', which are also generally evident in the mean functional connectivity gradient map. Some differences are larger than others. For example, there are prominent differences in local connectivity across a boundary, whereas most other brain regions have similar connectivity with the two areas, resulting in a mean gradient that appears weaker (from being "washed out" in the averaging) than the quantitative statistics and the functional connectivity maps would suggest. The functional connectivity maps associated with each area are often very informative with regard to specific spatial patterns (e.g., association with particular modalities or networks), but it was outside the scope of this document to illustrate these routinely. The dense connectomes from 210P and 210V used in this parcellation study can be viewed using this BALSA link (http://balsa.wustl.edu/WrwG).

Task fMRI Contrasts. Task contrasts were very useful for confirming the delineation of many borders, and also for providing some hints at the functional specialization of many areas. From the seven HCP tasks, the pipelines generate 86 task contrasts, 47 of which are unique (the other 39 are sign-reversed versions). In the text descriptions, we generally label task contrasts by the name assigned to each task contrast map in the tfMRI CIFTI files (https://wiki.humanconnectome.org/display/PublicData/Task+fMRI+Contrasts). Some of these map names are self-explanatory, whereas others (e.g., 'TOM – RANDOM' in the SOCIAL task) are less transparent. Supplemental Table 3, based on (Barch et al., 2013) provides brief additional descriptions of each task contrast.

We generally use terms 'more activated', 'less activated', 'more deactivated' and 'less deactivated' to refer to the magnitude of the BOLD signal deviation relative to the baseline across an areal boundary for a specified task contrast (i.e. the difference in beta values across the boundary). This avoids making assumptions about the absolute magnitude of the BOLD signal in one condition or contrast or on the complex relationship between BOLD signals and neural activity (impulses and synaptic activity) in a given grayordinate.

Primary vs secondary (task-specific) contrasts.

Many (31 of 47) of the unique task activations reported are 'primary' contrasts (BOLD responses to a complex task vs a fixation-only baseline condition for all but the Emotion and Language tasks; for the latter two, the baseline was the intercept of the GLM, i.e., the mean across the scan). The activations and deactivations associated with these primary contrasts are often stronger than those for the various differential activations

between two task conditions (e.g., STORY – MATH) and include changes related to the information provided to carry out the task (e.g., auditory for the two categories of LANGUAGE task; visual images for the four stimulus categories of the Working Memory task). There were 16 of the differential or 'secondary' contrasts. For our purposes, we consider any differential activity that distinguishes one area from another as a valid basis for identifying areal boundaries. We also avoid using information related to topographic activations in sensori-motor and visual cortices (e.g. right upper limb cortex in the left hemisphere from right handed button box pressing, or gradients along the eccentricity axis from visual task stimulation). Finally, because the primary task contrasts often show similar information (aside from the MOTOR and LANGAUGE tasks), we sometimes state that a border was present in multiple primary task contrasts without naming them all.

Information on the slopes.

Each task contrast shows a complex spatial profile in which typically only a few regions have BOLD signals approaching the peak magnitude. In contrast to common practice in many task-fMRI studies, we made use of the entire spatial pattern of BOLD responses, including information on the slopes of the profiles, rather than just focusing on the peak responses. This was feasible because of the high quality of the task-fMRI data, the improvements in intersubject alignment, and the large number of subjects included in the group analysis (see Supplementary Figures 2 and 3 in the Supplementary Results and Discussion). In general, we consider a strong spatial gradient in task-fMRI responses that correlates with other measures to be relevant evidence for identifying areal boundaries regardless of whether the underlying values represent a peak, a valley, or lie on the slopes in between. Thus, we presume that differences based on gradients at low activation or deactivation may still be neuroanatomically significant.

Additional Notes on the Strategy Used and Presentation.

In order to define the areal boundaries based on multiple modalities, we first looked at the intrinsic modalities (i.e. those not dependent on a task design) to identify candidate areal borders, i.e. gradients in myelin, thickness, resting state connectivity, and resting state visuotopy, which constituted a relatively minimal set of maps to look at. In many cases this set of putative areal borders already showed cross-modal correspondences as noted below. We then searched through the task fMRI data for boundaries that agreed with one or more of the intrinsic modalities (usually finding several task contrasts that agreed). Boundaries that relied solely on task fMRI gradients were rare (and those boundaries show agreement across many task contrasts). As a result, there are some areas in our parcellation where one or more tasks have gradients that cut across the area. Future studies may choose to subparcellate these areas into additional areas based on more multi-modal evidence not yet available.

Also, though there may be continuous gradual gradients in a modality within an area (e.g. the eccentricity gradient in the visual areas) we chose to focus on sharp transitions that allowed the semi-automated border-drawing tool to follow along a gradient ridge. There were some examples of gradients that cut across known cortical areas for known or strongly hypothesized reasons (e.g. the somatotopic subdivisions of sensory and motor

cortex or a strong gradient across early visual cortex that may reflect foveal stimulation from the eyes open resting state fixation cross). In the case of the somatotopic subdivisions, we characterized these separately (see Figure 8) as subareas of the known cortical areas. In the case of the visual cortex gradient, we ignored it because it is a likely "task-induced" artifact. In brain regions were we do not have such extensive and well-established priors, we did not ignore multi-modally present gradients. For this reason, it is possible that some areas that we describe here may be reclassified as subareas as the topographic organization of higher cognitive areas becomes better understood. We are hopeful that this parcellation, together with the methods that make it possible, will provide a framework for advancing such understanding.

The general parcellation strategy involved MG making an initial manual draft parcellation of parcel boundaries and names for areas within one of the regions shown in Figure 1 using the semi-automated border optimization algorithm, documenting the parcellation, and generating draft scene files similar to those illustrated in this document for visualization in Connectome Workbench. DVE then reviewed the documentation and scene file together with the data, boundaries, area names, and statistical outputs from the semi-automated border optimization algorithm for each areal border and suggested changes as appropriate for that region. These revisions were then discussed by the two neuroanatomists, region-by-region, and the parcellation presented here represents their consensus interpretation, and the borders represent the output of the semi-automated border drawing algorithm.

Finally, to keep the presentation of the data below manageable, we only show the resting state functional connectivity gradients, which represent a summary of the connectivity differences, rather than the functional connectivity maps in most cases. However, we did routinely inspect these maps to confirm that the functional connectivity patterns were indeed different on either side of a gradient. The functional connectivity data are part of the public data release, however, so that others may examine the connectivity differences themselves.

The following 22 sections, covering the multi-modal parcellation of 180 areas and areal complexes spanning the entire cerebral neocortex, are grouped by geographic proximity and functional similarities. As already noted, Figure 1 illustrates the regions to be covered (each in a different color) and numbered by the order in which they are presented. The first five regions cover early and intermediate visual cortex, including sections on V1 (1), early visual cortex (2), the dorsal stream (3), the ventral stream (4), and the MT+ Complex (5) and its neighbors. The next four regions cover the early somatosensory and motor cortex (6), the sensori-motor associated paracentral lobular and mid cingulate cortex (7), the premotor cortex (8), and the posterior opercular cortex (9). Next are three regions covering the early auditory (10) and association auditory cortex (11) and the insular and frontal opercular cortex (12). Then are two regions covering the rest of the temporal cortex including medial (13) and lateral temporal cortex (14). Then there are four regions covering the rest of the posterior cortex including the sensory "bridge" regions of the temporal-parietal-occipital junction (15) and the superior parietal and IPS cortex (16), along with the inferior parietal cortex (17), and the posterior cingulate cortex (18). The final four regions cover the rest of anterior cortex including the anterior cingulate and medial prefrontal cortex (19), orbital and polar frontal cortex (20), inferior frontal cortex (21), and the dorsolateral prefrontal cortex (22).

The Multi-modal Cortical Parcellation Region by Region

1. Primary Visual Cortex (V1)

We begin with area V1, given its importance to the subsequent visuotopic analyses and its status as arguably the most intensively studied cortical area in primates. We also use V1 to demonstrate the semi-automated border definition method and the initial statistical checks and to describe our "neuroanatomist's" approach to interpreting the data in more detail than is feasible for subsequent areas. V1 is the only cortical area that can be recognized in unstained brain slices, without the aid of microscopy, thanks to the heavily myelinated stria of Gennari in layer 4B (Gennari, 1782). In the HCP 0.7mm T1w/T2w myelin maps, the stria is discernible in some parts of the calcarine sulcus in many individuals, but the resolution is inadequate for delineating it reliably throughout V1. Although all modalities used in this study can provide useful information for delineating at least part of V1's borders with neighboring areas V2 and pro-striate cortex (ProS), we focus on myelin maps, LGN functional connectivity, and cortical thickness, as these were the modalities used by the semi-automated border optimizer to define the boundaries of V1. In a pattern to be emulated in subsequent sections, we will mention the areas adjacent to the region being discussed but cover them in more detail in their own region's section. We will also reference the figure panel that illustrates a given areal property if it is shown in the figure, otherwise such a reference will not appear for data that is not shown.

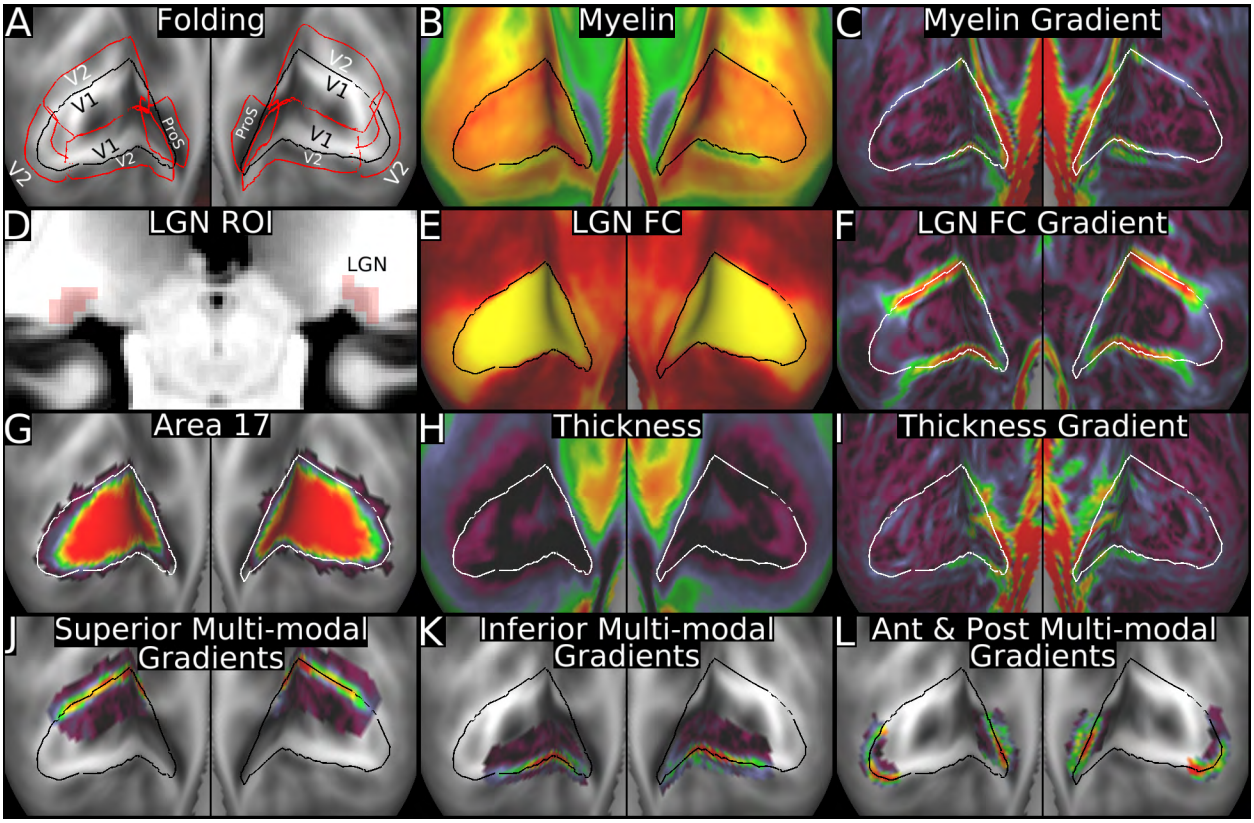

Figure 2, above, shows how the semi-automated border optimizer method was used to define V1, including the modalities used for areal delineation. The black or white outline in all panels is the V1 border. Panel A shows V1 on a group average cortical folding map (FreeSurfer mean curvature) together with the ROIs used for semi automated border drawing and the names of V1's neighbors. Panels B and C show the group average myelin map and gradients. Panels D, E, and F, show the LGN ROI (translucent red) displayed on the group average T1w image, the group average LGN functional connectivity map, and its gradient. Panel G shows the area 17 probabilistic maps (Fischl et al., 2008). Panels H and I show the group average cortical thickness maps and gradients. Panels J, K, and L show the effective combined gradients used by the algorithm for final border placement. Data at http://balsa.wustl.edu/Jg5v.

Figure 2, Panel A shows the borders of area **V1** as a black line on a group average map of the folding pattern (FreeSurfer mean curvature map). V1 occupies the entire calcarine sulcus, which is well defined despite areal feature-based registration, indicating that V1's location is tightly correlated with cortical folding patterns, as previously demonstrated (Fischl et al., 2008). Because there were some regional differences in which modalities best defined the border between V1 and V2 along its extent, the borders were automatically refined and the cross-border statistics were assessed separately for the anterior, superior, inferior, and posterior borders of V1, as indicated by the optimization ROIs (red outlines) in Panel A. Panels B and C respectively illustrate the group-average myelin maps and myelin map gradients. A gradient ridge runs along the margin of **V1**, but its magnitude varies, being strongest anteriorly (including the boundary with the lightly myelinated prostriate area ProS) and weakest posteriorly (in foveal V1). A striking delineation of the full extent of **V1** comes from seed-based functional connectivity (FC), using the left and right LGNs as seed ROIs. The LGNs are identifiable in the high resolution T1w and T2w volumes (Panel D ROI is translucent red, LGN is darker grey). The group-average LGN-seeded functional connectivity is high throughout **V1** (Panel E), and the LGN FC gradients (Panel F) have prominent ridges superiorly and inferiorly in mid-eccentricity ranges. The myelin (Panel C) and FC gradients (Panel F) were precisely colocalized along the superior and inferior borders of **V1**, and the semi-automated border optimizer easily followed their combined gradients. Along the anterior boundary with the prostriate area, the myelin and LGN FC gradient ridges overlap one another, but the myelin gradient ridge is broader and centered more anteriorly. The semi-automated gradient delineator identified a consensus border between the two gradient peaks. Along the superior boundary, the cross-border modality differences were largest for LGN-seeded FC (Cohen's d=7.06 (L) and d=6.46 (R)) and substantial for myelin (d=1.63 (L) and d=2.09 (R)). Differences were comparable along the inferior boundary for LGN-seeded FC (d=5.08 (L) and d=4.35 (R)) and for myelin (d=1.68 (L) and d=1.09 (R)). Panels J and K show the effective gradients used by the algorithm for these boundaries. Along the anterior border (adjoining the prostriate area) the differences were larger in magnitude for myelin (d=4.93 (L) and d=4.54 (R)) and smaller for LGN-seeded FC (d=3.73 (L) and d=2.36 (R)). Panel L shows the effective gradient used by the algorithm for this boundary. For all of the above comparisons, p values were less than $7 * 10^{-17}$ (p<floating point precision for all tests except right inferior myelin). Note that cortical thickness could also have been used to help define the anterior boundary of V1 with the Prostriate cortex (ProS) (Panels H and I).

The posterior (foveal) border of **V1** was more difficult to define because the gradients were less prominent for each modality and were less well aligned (and so more pre-gradient smoothing was used, sigma=2mm). In this region, we used myelin (Panels B

and C), cortical thickness (Panels H and I), and LGN connectivity (Panels E and F). The semi-automated border optimizer identified a trajectory based on all three gradients but closest to the thickness gradient ridge. The cross-border modality differences were substantial (Cohen's d=1.66 (L) and d=0.71 (R) for myelin, d=-0.83 (L) and d=-1.11 (R) for thickness, and d=2.56 (L) and 3.12 (R) for LGN connectivity), and all trans-border p values were less than 0.0003 in this region. Panel L shows the effective gradient used by the algorithm for this boundary.

As is well known (Abdollahi et al., 2014; Amunts et al., 2000; Fischl et al., 2008), the V1 border runs along the margins of the calcarine sulcus, just outside the gyral crown on the superior and inferior banks of the sulcus. This is evident in Panel A, where the V1 border is displayed over maps of folding patterns. Interestingly, in foveal cortex we identified a previously unappreciated correlation with cortical folding around the occipital pole posterior and lateral to the calcarine sulcus, in which the V1 boundary runs along a gyral ridge in the average midthickness surface. To enable direct comparison with a previous surface-based analyses of cytoarchitectonically defined V1/area 17, Panel G shows our V1 border overlaid on probabilistic architectonic maps of area 17 generated from 10 postmortem subjects (Amunts et al., 2000). The cytoarchitectonic definitions were mapped onto individual subject surfaces, registered to the fsaverage surface (Fischl et al., 2008), and then to the fs_LR atlas (Van Essen et al., 2012b), which has vertex correspondence with our HCP average surface. In general there is good agreement between the two studies, insofar as the (Fischl et al., 2008) 50% probability level (green) runs close to our V1 group average boundary, especially along the superior and inferior margins of the calcarine sulcus. There are modest discrepancies in foveal V1, where our border is modestly lateral to that of (Fischl et al., 2008), especially in the left hemisphere. In the far peripheral representation in the anterior calcarine sulcus, our V1 extends slightly farther anterior. These differences may be attributable in part to biases that arise in registering the (Fischl et al., 2008) dataset without the opportunity to incorporate the de-drifting process (see Supplementary Methods #2.5) because the individual postmortem surface reconstructions from that study were not available to us. Another technical consideration that might selectively impact analyses of foveal cortex is that the spacing of standard-mesh surface vertices near the occipital pole is larger than for most other regions, owing to how the elongated hemisphere is mapped to the sphere used for registration and resampling. This reduces the spatial resolution and sensitivity in a region that also contains early visual cortical areas that are notably narrow strips in this region.

2. Early Visual Cortex

Human area V1 is surrounded mainly by areas V2 and V3. Though they are concentrically arranged, V2 and V3 do not encircle V1 completely, as the far anterior extent of V1 is adjoined by an architectonically distinct prostriate area in humans (Sanides, 1970; Sanides and Vitzthum, 1965), similar to that found in the macaque (Morecraft et al., 2000; Van Essen et al., 1982). Many studies have mapped much of V2 and V3 using retinotopic fMRI (Abdollahi et al., 2014; Schira et al., 2009; Wandell and Winawer, 2011; Wang et al., 2015); however, this approach fails to capture the representation of the far periphery because it is difficult to stimulate the peripheral retina within the confines of an MRI scanner. Cytoarchitecture has also been used to map extrastriate occipital cortex, including

area 18 (Amunts et al., 2000), and subdivisions of classical area 19, or area OC, including hOC3v, hOC4v (Rottschy et al., 2007), hOC3d, hOC4d (Kujovic et al., 2013), hOC4lp, hOC4la (Malikovic et al., 2015), hOC5d, and hOC5v (Malikovic et al., 2007). Using functional connectivity to map the borders of early visual areas has proven challenging in previous studies, mainly because the central and peripheral parts of the visual field have very distinct patterns of functional connectivity, (Power et al., 2011; Van Essen et al., 2014; Yeo et al., 2011) and topographically corresponding regions of neighboring visual areas are highly functionally correlated (Heinzle et al., 2011). Here, we used a novel approach to delineate the full extent of areas V2, V3, and V4, based on topographically organized resting state functional connectivity with V1 (see Supplementary Methods #4.4). Figure 3 Panel A shows the arrangement of these areas overlaid on the group-average cortical folding map, along with the approximate locations of their 15 neighboring areas: V3A, V6, the Dorsal Visual Transitional area (DVT), the prostriate area (ProS), the presubiculum (PreS), parahippocampal area 1 (PHA1), the ventromedial visual areas (VMV1-3), V8, the PIT complex, LO1, LO2, V3CD, and V3B. We discuss areas V2 and V3 first, followed by area V4, whose analysis is more complex.

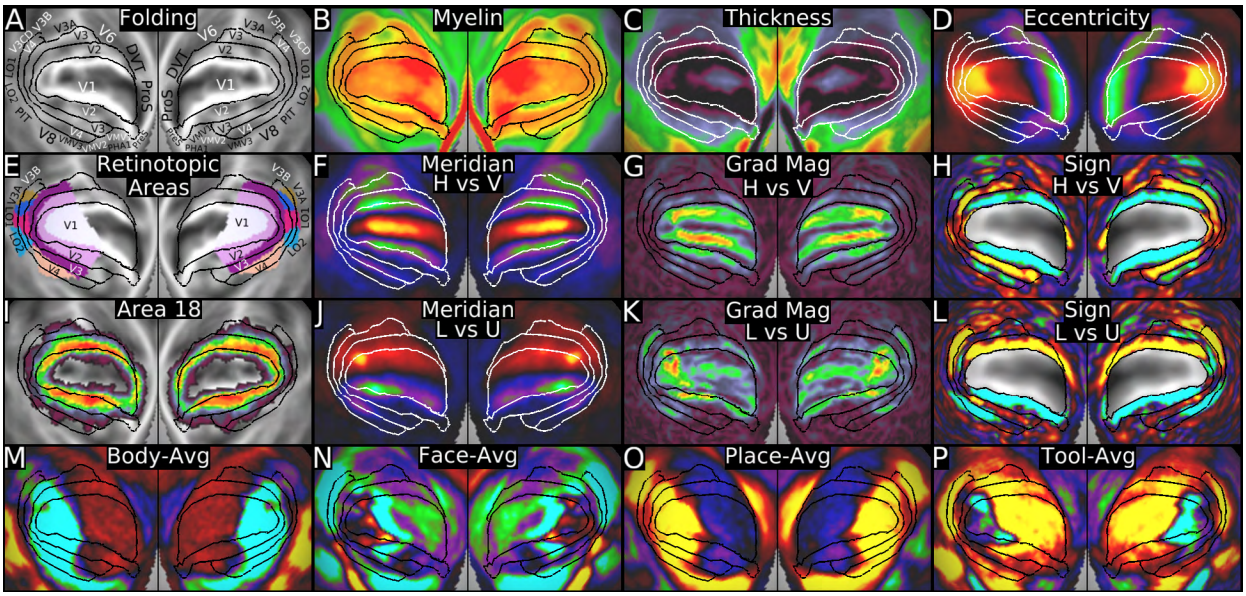

Figure 3 shows the delineation of early visual cortical areas. Panel A shows areas V1, V2, V3, and V4 overlaid on a folding map. Panels B and C show myelin and cortical thickness maps. Panel D shows the foveal vs peripheral eccentricity contrast. Panel E shows retinotopic parcels from (Abdollahi et al., 2014). There is notable agreement between these definitions in mid-eccentricity regions, but better coverage of peripheral regions in the present study and there are some differences in foveal regions and V4. Panels F, G, and H show the horizontal vs vertical meridian contrast, the gradient magnitude of the contrast, and the visuotopic sign produced by taking the dot product of the gradient vector with a vector that points towards V1 (see Supplementary Methods #4.4). Panel I shows area 18 (V2) from post-mortem cytoarchitecture registered across subjects on the surface (Fischl et al., 2008). Panels J, K, and L show the visuotopic maps for the lower vs upper vertical meridian contrast. Note that unlike the horizontal vs vertical meridian contrast, in the lower vs upper field contrast, the visuotopic signs are opposite for superior and inferior portions of each area. Panels M, N, O, and P show the working memory BODY-AVG, FACE-AVG, PLACE-AVG, and TOOL-AVG contrasts. Data at http://balsa.wustl.edu/WM22.

V2 was distinguished from V1 using mainly myelin (Panel B) and LGN connectivity (see section #1 V1 Results and Figure 2). To define the borders between V2 and V3 and between V3 and V4, we used visuotopic connectivity information. As described in the Supplementary Methods (#4.4; see Figure 8), spatial contrasts of horizontal vs vertical meridians and of lower vs upper vertical meridians (both restricted to V1) were used in a multiple regression to derive whole brain maps of the associated resting state functional connectivity, as in Panel F for horizontal meridian (more positive) vs vertical meridian (more negative). Spatial gradients of these maps were used to identify reversals in polar angle, which occur at local *minima* of the gradient magnitude (Panel G). In addition, Panel H shows a map of the dot product between the gradient vector and a reference vector that always points towards V1 (along the cortical surface). This serves as a 'visuotopic sign' that is analogous to the field sign maps developed by (Sereno et al., 1995; Sereno et al., 1994). Panels J, K, and L show analogous maps for the lower field (yellow, red) vs upper field (green, blue, indigo) contrast. Panel D shows the foveal (yellow, red) vs peripheral (green, blue, indigo) eccentricity contrast. The borders between V2 and V3 and between V3 and V4 are represented by both gradient magnitude minima (Panel G) and a horizontal vs vertical meridian visuotopic sign change from negative (V2, cyan/indigo) to positive (V3, yellow-red), and back to negative (V4) (Panel H).

In this parcellation, the inferior half of **V2** adjoins the entire inferior border of V1, extending to the anterior tip of the calcarine sulcus, where the lightly myelinated prostriate area ProS (Panel B) adjoins it as well as V1. **V2** also does not share V1's visuotopic pattern (Panel H). Relative to VMV1 inferiorly, inferior **V2** is substantially thinner (Panel C), has more myelin (Panel B), and has a clear visutopic pattern that VMV1 does not share (Panels H and L). Relative to area PHA1 inferiorly, **V2** has more myelin (Panel B) and is thinner (Panel C). Superior **V2**, in contrast, extends only to the fundus of the parieto-occipital sulcus (POS), where it adjoins a more lightly myelinated dorsal visual transitional area (DVT) (Panel B). Relative to DVT, superior **V2** also has a different task activity profile, being activated vs deactivated in the BODY-AVG (Panel M) and TOOL-AVG (Panel P) contrasts and deactivated vs activated in the PLACE-AVG (Panel O) and TOM-RANDOM contrasts. The large difference in myelin between heavily myelinated **V2** and lightly myelinated DVT was primarily used to define the boundary (Panel B). Superior **V2** also borders V6, where there is a visuotopic sign change in the horizontal vs vertical meridian contrast (Panel H) from negative in **V2** to positive in the inferior portion of V6.

Area **V3** surrounds most of V2, except in the far peripheral representation. Inferiorly, **V3** is bordered by areas VMV1 and VMV2, which do not share its visuotopic map (Panel H, weaker visuotopic signs) and have less myelin (Panel B, VMV2) or are thicker (Panel C, VMV1). The border between superior **V3** and V3A is primarily demarcated by a visuotopic sign change in both the horizontal vs vertical and the lower vs upper vertical meridian contrasts (Panels H and L). Also **V3** locally has less myelin than V3A and V6 (Panel B), and it has a different pattern of functional connectivity with higher visual areas in the MT+ complex.

In our parcellation, area V4 surrounds most of V3 and contains a full hemifield representation, with the upper quadrant represented inferiorly and the lower quadrant superiorly. This is similar to the arrangement reported in the macaque (Felleman and Van Essen, 1991) and to a previous parcellation of human V4 (Hansen et al., 2007) but contrary to several other human retinotopic parcellations (e.g., (Abdollahi et al., 2014; Goddard et

al., 2011; Wade et al., 2002; Winawer et al., 2010). Two lines of evidence suggest that this parcellation is the best fit for our data (though we acknowledge we do not definitively resolve the above controversy): 1) Visuotopic organization is evident in both superior and inferior portions of V4 in both the horizontal vs vertical and lower vs upper vertical meridian contrasts without strong evidence for finer-grained subdivisions (areas) of either region (Panels H and L). 2) In our parcellation the anterior border of V4 coincides with a decrease in myelin content (Panel B, superior V4) and an increase in cortical thickness (Panel C, inferior V4). In contrast, alternative published parcellations that involve multiple areas adjacent to V3 include not only the thin, heavily myelinated portion (part of our superior V4) but also the more lightly myelinated, thicker cortex outside of this area (e.g. areas LO1, LO2, V3A, and V3B (Abdollahi et al., 2014) (Panel E).

The superior boundaries of **V4** with V3B, V3CD, and LO1 were defined using visuotopic sign changes (reduced magnitude and/or sign reversal outside **V4**) in the horizontal vs vertical and lower vs upper vertical meridian contrasts (Panels H and L), decreases in myelin content (higher in **V4**, Panel B), and increases in cortical thickness (thinner in **V4**, Panel C). The boundary of **V4** with LO2 was defined by changes in myelin content (higher in **V4**, Panel B), cortical thickness (thinner in **V4**, Panel C), and activation vs deactivation in the PLACE-AVG task fMRI contrast (Panel O). Relative to the neighboring PIT complex, **V4** has more myelin (Panel B), is thinner (Panel C), is deactivated vs activated in the FACE-AVG task fMRI contrast (Panel N), and activated vs deactivated the PLACE-AVG contrast (Panel O). The boundary of **V4** with both V8 and VMV3 was defined primarily using visuotopic sign changes in the horizontal vs vertical meridian contrast (negative to positive in Panel H), but also **V4** is thinner (Panel C), and in the FACES-SHAPES contrast **V4** was less deactivated/activated vs more deactivated in VMV3. Relative to area VMV2, inferior **V4** has a greater magnitude of the visuotopic sign in the horizontal vs vertical meridian contrast (Panel H), more myelin (Panel B), and is deactivated vs activated in the TOM-RANDOM contrast.

Our maps of areas V1, V2, and V3 overlap extensively with the population-average retinotopic maps reported by (Abdollahi et al., 2014) (Panel E) and with the probabilistic architectonic map of area 18 (Fischl et al., 2008) (Panel I). There is agreement that V2 and V3 are narrower in the foveal region but continuous between superior and inferior portions, an interpretation supported by high-resolution retinotopic mapping of the foveal confluence (Schira et al., 2009). The discrepancies near the center of the foveal representation may reflect methodological limitations in one or both studies, as it is difficult to accurately map very low eccentricities in retinotopic studies (e.g., (Abdollahi et al., 2014)), and there are spatial sampling limitations near the occipital pole in our own analyses (see preceding Section #1 Primary Visual Cortex (V1)). In the visual periphery, retinotopic studies are limited by the range of eccentricities explored (maximum 7.75 degrees (Abdollahi et al., 2014)). Also the architectonic maps of area 18 (Amunts et al., 2000; Fischl et al., 2008) report complete encircling of area V1 (Panel I) despite published evidence for at least one architectonically distinct region (prostriate area ProS) adjoining V1 in anterior calcarine cortex (see above and also Section #1 Primary Visual Cortex (V1)). The inferior portion of our V4 overlaps extensively with that in (Abdollahi et al., 2014), but as noted above the superior portion overlaps with their V3A, V3B, LO1, and LO2 (Panel E). Published surface renderings of volume-based maximum probability postmortem cytoarchitectonic maps suggest that our V3 corresponds to hOC3d (Kujovic et al., 2013)

plus hOC3v (Rottschy et al., 2007). Our inferior V4 may correspond to hOC4v (Rottschy et al., 2007) and superior V4 may correspond to some or all of hOC4lp (Malikovic et al., 2015). More accurate comparisons would be made possible by reconstructing the postmortem individual subject surfaces and registering them to a surface template so that the cytoarchitectonic definitions could be compared directly with our HCP surface data as areas 17 and 18 were above.

3. Dorsal Stream Visual Cortex

The dorsal visual stream includes higher visual areas generally implicated in perceiving where visual stimuli are located and in planning visually guided actions (Goodale and Milner, 1992; Mishkin and Ungerleider, 1982) rather than object identification ('what it is'). In this section we discuss six dorsal stream areas (areas V3A, V3B, V6, V6A, V7, and IPS1) that are well visualized in Figure 4, as shown by the border outlines and labels in Panel A, overlaid on a map of the group-average folding pattern. These areas are bordered by three areas already discussed (V2, V3, V4) plus areas V3CD, IP0, MIP, and DVT. We start with area V3A, the largest area within this region, followed by V3B and V7, V6 and V6A, and IPS1. Figure 4 shows architectural, functional, connectivity, and topographic differences between these areas.

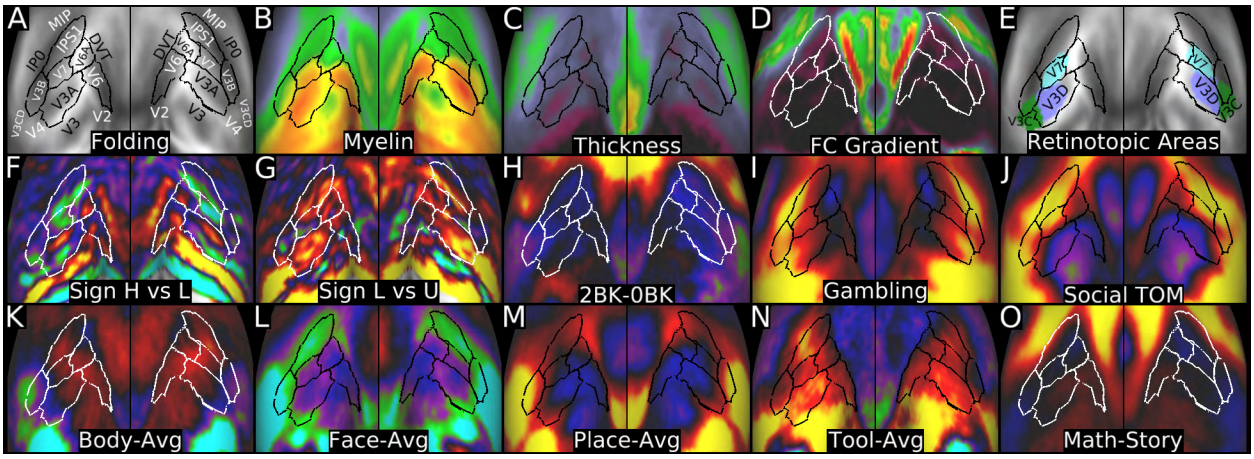

Figure 4 shows some of the architectonic, functional, connectivity, and topographic information that enabled delineation of areas V3A, V3B, V7, V6, V6A, and IPS1 in the dorsal visual stream. Panel A shows the folding pattern together with the areas discussed in this section. Panel B shows the areas together with the myelin map. Panel C shows the areas with the cortical thickness map. Panel D shows the functional connectivity gradient (note how there is a gradient above IPS1). Panel E shows some retinotopic areas (Abdollahi et al., 2014) that correspond to our areas. Panel F shows the horizontal vs vertical meridians' visuotopic sign and Panel G shows the lower vs upper vertical meridians' visuotopic sign. Panels H, I, and J show the working memory 2BK-0BK contrast, a GAMBLING primary contrast, and the SOCIAL TOM contrast. Panels K, L, M, and N show the BODY-AVG, FACE-AVG, PLACE-AVG, and TOOL-AVG category task fMRI contrasts. Panel O shows the MATH-STORY contrast. Data at http://balsa.wustl.edu/RB2m.

The border of **V3A** with V3 is based on a change in the visuotopic sign of the vertical vs horizontal meridian contrast (Panel F) and the lower vs upper vertical meridian contrast (Panel G), as discussed in Section #2 Early Visual Cortex. Unlike earlier visual areas, area **V3A** contains upper fields (red/yellow, superiorly) and lower fields (cyan, inferiorly)

(Larsson and Heeger, 2006; Swisher et al., 2007; Tootell et al., 1997), and thus contains both positive and negative visuotopic signs in the horizontal vs vertical meridian contrast (Panel F). In contrast, the visuotopic sign in the lower vs upper vertical meridian contrast is all positive (yellow/red) in **V3A**, reflecting a continuous gradient from lower to upper visual field from **V3A's** border with V3 to **V3A's** border with V7 (Panel G). **V3A** also has more myelin than many of its neighbors (Panel B, V3B, V6A, and locally more so than V4, V7, and V3). The border of **V3A** with V7 (adjoining antero-superiorly) is based primarily on visuotopic sign changes in the vertical vs horizontal meridian and in the lower vs upper vertical meridian contrasts (Panels F and G). **V3A** also has substantially lower functional connectivity with IPS1 than does V7. Relative to its medial neighbor V6, area **V3A** has a different visuotopic sign pattern (stronger +/- pair) in the horizontal vs vertical meridian contrast (Panel F), a stronger visuotopic sign in the lower vs upper vertical meridian contrast (Panel G), locally less myelin (Panel B), and is more activated in the GAMBLING (Panel I) and EMOTION primary contrasts. Relative to its antero-medial neighbor V6A, area **V3A** has more myelin (Panel B), is activated vs deactivated in the GAMBLING primary contrasts (e.g., Panel I), and is deactivated vs activated in the SOCIAL primary contrasts (e.g., Panel J). Relative to its latero-inferior neighbor V4, area **V3A** differs in having an upper-plus lower-field representation instead of lower-field only (Panel F), and is deactivated vs activated in the working memory and SOCIAL primary contrasts (e.g. panel J). Relative to its lateral neighbor V3B, area **V3A** has more myelin (Panel B), is thinner (Panel C), is more activated in the TOOL-AVG (Panel N) and RANDOM-TOM contrasts, and has stronger visuotopic sign changes in the horizontal vs vertical meridian and the lower vs upper vertical meridian contrasts (Panels F and G). Our V3A overlaps extensively with area V3D of (Abdollahi et al., 2014), but extends further medially, presumably because our multimodal map includes the peripheral representation, whereas their retinotopic map did not. It also likely corresponds to architectonic area hOC4d (Kujovic et al., 2013). We use the more common name of V3A (Larsson and Heeger, 2006; Swisher et al., 2007; Tootell et al., 1997; Wandell and Winawer, 2011; Wang et al., 2015) for broader consistency with the literature.

Areas **V7** (Tootell et al., 1998) and **V3B** (Smith et al., 1998) lie superior to V3A along the superior margin of heavily myelinated visual cortex. They differ from areas V6A, IPS1, IP0, and V3CD in having more myelin (Panel B). Relative to its antero-superior neighbor IPS1, area **V7** also differs in functional connectivity and is also less activated in the working memory primary contrasts and less deactivated in the FACE-AVG contrast (Panel L). The visuotopic patterns in group average data are not as clear in these areas; however, they both have a negative (or less positive) visuotopic sign throughout much of their extents in the lower vs upper vertical meridian contrast (Panel G). **V7** and also IPS1 differ from V6A in several task vs baseline primary contrasts, especially their stronger activation in the SOCIAL TOM task (Panel J) and also the GAMBLING primary contrasts (e.g. Panel I). **V7** and also V6A differ from IPS1 in being less deactivated in the FACE-AVG category task contrast (Panel L). Relative to its lateral neighbor V3B, area **V7** has more myelin (Panel B), is activated vs deactivated in the BODY-AVG contrast (Panel K), less deactivated in the FACE-AVG contrast (Panel L), and less activated in the MOTOR CUE contrast. Relative to its superior neighbor IP0, area **V3B** has more myelin (Panel B), is thinner (Panel C), is locally less activated in the PLACE-AVG contrast (Panel M), locally activated vs deactivated in the TOOL-AVG contrast (Panel N), and less activated in the TOM-RANDOM contrast. Relative to

its lateral neighbor area V3CD, area **V3B** has more myelin and is less deactivated in the FACE-AVG contrast (Panel L) and less activated in the TOOL-AVG contrast (Panel N). Relative to its superior neighbor IPS1, area **V3B** has more myelin (Panel B), is deactivated vs activated in the BODY-AVG contrast (Panel K), and activated vs deactivated in the FACES-SHAPES contrast. Our V7 corresponds closely to that from (Abdollahi et al., 2014) (Panel E), and our V3B shows a similar topological relationship to V3A and V7 as is reported in other studies (Larsson and Heeger, 2006; Swisher et al., 2007; Wang et al., 2015) and some overlap with area V3C from (Abdollahi et al., 2014).

Areas **V6** and **V6A** lie mainly medial and anterior to areas V2, V3, V3A, and V7 along the posterior bank of the partieto-occipital sulcus and have been studied extensively (Pitzalis et al., 2006; Pitzalis et al., 2013). V6 is heavily myelinated relative to most of its neighbors (particularly V6A and DVT, the dorsal transitional visual area, Panel B). Relative to its superior neighbor V6A, area **V6** is weakly activated vs weakly deactivated in the Working Memory contrast (2BK-0BK, Panel H), and less deactivated in the MOTOR AVG contrast. Areas **V6** and **V6A** have more myelin than DVT, are deactivated vs activated in the PLACE-AVG contrast (Panel M), and are activated vs deactivated in the TOOL-AVG contrast (Panel N). Finally, **V6** and **V6A** differ in functional connectivity compared to DVT, as **V6** and **V6A** are more strongly correlated with earlier visual cortex, whereas DVT is more strongly correlated with higher association areas. Areas V6 and V6A may correspond largely to myeloarchitectonic area 112 from the Vogt school (Nieuwenhuys et al., 2015), and V6 has also been recognized via its myelin content signature (Sereno et al., 2013).

We identified **IPS1** (Hagler et al., 2007; Swisher et al., 2007; Wang et al., 2015) on the basis of its strong functional connectivity with other visual areas, its position superior to area V7, and some visuotopic organization (e.g. all positive visuotopic sign in the lower vs upper vertical meridian contrast, Panel G). Like V6A, area **IPS1** has less myelin than V7 and V3B (Panel B). **IPS1** also has notably lower functional connectivity with more posterior visual areas than do its posterior neighbors (e.g. V7, V3B, V3A) and stronger connectivity with more anterior areas along the border between visual and cognitive regions. That being said, it is much more visually connected than its superior neighbor MIP, with a resting state functional connectivity gradient separating these areas (Panel D). **IPS1** differs strongly from adjoining MIP and IP0 in several task fMRI contrasts, including being much less activated in the LANGUAGE MATH-STORY contrast (Panel O), deactivated vs activated in the Working Memory contrast (Panel H), and less activated in the MOTOR CUE and CUE-AVG contrasts. Additionally **IPS1** is thinner than IP0 (Panel C). **IPS1** has more myelin than DVT (Panel B) and differs from DVT and V6A in multiple task fMRI contrasts, including greater activation in the SOCIAL TOM (Panel J) and RELATIONAL vs baseline task contrasts.

4. Ventral Stream Visual Cortex

This section focuses on seven areas and complexes anterior to the early visual areas lying along the ventral aspect of each hemisphere: V8, the Ventral Visual Complex (VVC), the PIT Complex, the Fusiform Face Complex (FFC), and Ventro-Medial Visual areas 1, 2, and 3. They are surrounded by areas V2, V3, V4, LO2, PH, TE2p, TF, parahippocampal areas PHA1, PHA2, and PHA3, which were discussed already or will be discussed later. The ventral visual areas are intermediate in myelination relative to more heavily myelinated

earlier visual areas (posterior/superior) and neighboring lightly myelinated "cognitive" areas (anterior). Consistent with the areas being part of the ventral stream (Goodale and Milner, 1992), the categories task in the task fMRI battery was particularly useful in distinguishing between many of these areas. Some of these areas are dubbed "complexes" because they are likely to contain multiple subdivisions, based on published data and/or evidence in our data that was too weak or inconsistent in individuals to allow the areal classifier to reliably detect a finer-grained parcellation in individual subjects. Figure 5, shows architectural, connectivity, topographic, and functional information used to define the areal boundaries. Panel A shows the areas on a cortical folding map.

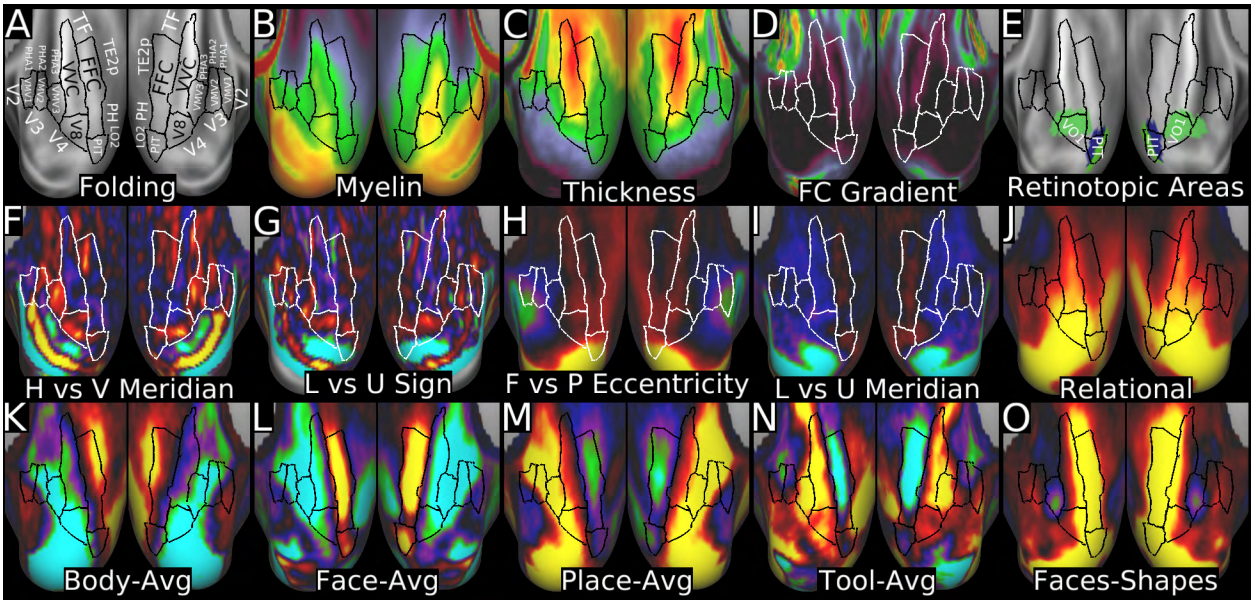

Figure 5 shows architectonic, connectivity, topographic and functional information that was used to parcellate the ventral stream visual cortex. Panel A shows the areas on a cortical folding map. Panels B and C show myelin and cortical thickness maps. Panel D shows the functional connectivity gradients. Panel E shows several retinotopic areas (Abdollahi et al., 2014) (areas PITd and PITv are shown separately but named PIT for space efficiency). Panels F and G show the horizontal vs vertical meridian contrast's visuotopic sign map and the lower vs upper vertical meridian contrast's visutopic sign map. Panels H and I show the foveal vs peripheral and lower vs upper vertical meridian whole brain contrast maps. Panel J shows a RELATIONAL primary contrast. Panels K, L, M, and N show the BODY-AVG, FACE-AVG, PLACE-AVG, and TOOL-AVG contrasts. Panel O shows the FACES-SHAPES contrast. Data at http://balsa.wustl.edu/Jlz0.

V8 and the VVC form a heavily myelinated core of the ventral stream visual region (Panel B). V8 is so named because of multiple similarities with area V8 of (Hadjikhani et al., 1998): It adjoins the horizontal meridian representation of inferior V4 (Panels F and G, the vertical-vs-horizontal and lower-vs-upper field visuotopic sign maps); it includes an upper field representation mainly on the medial side and a lower-field representation mainly on the lateral side (respectively blue and red in Panel I, the whole brain map of lower- vs upper-field contrast); and its eccentricity representation includes central fields mainly anterior and (somewhat) more peripheral fields mainly posterior (respectively red and black/blue in Panel H, the whole brain map of foveal vs peripheral contrast). Its border with the VVC was primarily defined by a transition in visuotopic sign in the lower vs upper vertical meridian contrast (Panel G), but there is also a statistically significant increase in

cortical thickness (Panel C). V8 overlaps substantially with VO1 from (Abdollahi et al., 2014) (Panel E).

Functionally, **V8** and the **VVC** are strongly de-activated in the FACE-AVG contrast (Panel L) and strongly activated in the PLACE-AVG contrast (Panel M, V8 more than VVC) and in the TOOL-AVG contrast (Panel N, VVC more than V8). These contrasts plus the difference in myelin (Panel B) robustly distinguish them from laterally adjoining areas PIT and FFC. Relative to its medial neighbor VMV3, the **VVC** has more myelin (Panel B), is thicker (Panel C), is activated vs deactivated in the FACES-SHAPES task contrast (Panel O), and is less deactivated in the BODY-AVG contrast (Panel K). Thickness and the FACES-SHAPES contrast were primarily used to delineate the border. Relative to its medial neighbor parahippocampal area PHA3, the **VVC** has more myelin (Panel B), is thicker (Panel C), is separated by a resting state functional connectivity gradient (Panel D), and is more activated in primary task contrasts (e.g. Panel J, RELATIONAL). Finally, relative to its anterio-lateral neighbor TF, the **VVC** has more myelin (Panel B), differs in functional connectivity (Panel D), is activated vs deactivated in the TOOLS-AVG contrast (Panel N), and is deactivated vs activated in the FACE-AVG contrast (Panel L). We consider **VVC** an areal complex because other studies (Arcaro et al., 2009; Wandell and Winawer, 2011; Wang et al., 2015) have distinguished multiple visuotopic maps that overlap with this region (VO1, VO2, PHC1, PHC2), and there is weak evidence for multiple visuotopic maps in our data as well.

The Ventro-medial Visual Areas (**VMV1-3**) lie medially, between heavily myelinated inferior portions of V2, V3, and V4 and the more lightly myelinated parahippocampal areas PHA1, PHA2, and PHA3 (Panel B). The VMV areas show strong functional connectivity with early visual areas (in contrast to a very different pattern for PHA1-3) but they lack a clear visuotopic organization (Panel F and G). **VMV1** (the most medial) is much thinner and more heavily myelinated that PHA1, which borders it anteriorly (Panels B and C). The pattern is similar for **VMV3** and PHA3, though the thickness differences are not as great (Panels B and C). Relative to their anterior neighbor PHA2, areas **VMV1** and **VMV2** have more myelin (Panel B), differ in functional connectivity, (Panel D), and are locally more deactivated in the BODY-AVG contrast (Panel K). **VMV1** and **VMV3** are thicker than VMV2, and thickness also helps distinguish **VMV1** from areas V2 and V3 (Panel C). Among the three areas, **VMV1** is the most heavily myelinated (Panel B) and **VMV2** is the thinnest (Panel C). Relative to its medial neighbor VMV2, area **VMV3** is more activated in the TOOL-AVG (Panel N), the SOCAL and RELATIONAL primary contrasts (e.g. Panel J), and is more deactivated in the FACES-SHAPES contrast (Panel O). Relative to its anterior neighbor PHA3, area **VMV2** is thinner (Panel C), is locally deactivated vs activated in the TOOL-AVG contrast (Panel N), and is activated vs deactivated in the FACES-SHAPES contrast (Panel O). However, the areal classifier did not perform as well at reliably identifying these areas in individuals compared to other cortical regions (see Main Text Figure 5). Notably, this region has not been previously well parcellated in either the human or the macaque, usually either being left unparcellated or parts of it being included in other areas. In humans, this is partly due to its largely representing high eccentricities that are difficult to map with retinotopic studies. That being said, our VMV3 may overlap partly with area VO2, VMV2 with area PHC1, and VMV1 with area PHC2 (Arcaro et al., 2009; Wandell and Winawer, 2011; Wang et al., 2015).

The **PIT** complex ((Abdollahi et al., 2014; Kolster et al., 2010); see Panel E) and the fusiform face complex (FFC) (Kanwisher and Yovel, 2006; Rajimehr et al., 2009; Tsao et al., 2008) are both strongly activated by the FACE-AVG contrast (Panel L) and the FACE-SHAPES contrast (Panel O). Compared to posterior neighbor V4 and inferior neighbor V8, the **PIT** complex has less myelin (Panel B) and does not have as organized visuotopy (Panels F and G). Relative to area V8, the **PIT** complex is activated vs deactivated in the FACE-AVG contrast (Panel L), deactivated vs activated in the PLACES-AVG contrast (Panel M), and more activated in the FACES-SHAPES contrasts (Panel O). Relative to its supero-lateral neighbor LO2, the **PIT** complex is more activated in the FACE-AVG (Panel L) and FACES-SHAPES contrasts (Panel O) and less activated in the TOOLS-AVG contrast (Panel N). Relative to its antero-superior neighbor PH, the **PIT** complex has more myelin (though the change is gradual, Panel B), is activated vs deactivated in the FACE-AVG (Panel L) and FACES-SHAPES (Panel O) contrasts, is less activated in the TOOL-AVG (Panel N) and TOM-RANDOM contrasts. Relative to anterior neighbor FFC, the **PIT** complex is thinner (Panel C) and there is a local reduction in the strength of the FACE-AVG activation at their boundary (Panel L). Overall the PIT/FFC border is only highly significant for the thickness modality (Panel C), so we relied also on published evidence (e.g., (Abdollahi et al., 2014; Kanwisher and Yovel, 2006; Rajimehr et al., 2009) supporting a boundary between this region and the rest of face selective cortex (Panel L). Our PIT is nearly co-extensive with areas phPITd and phPITv combined (Abdollahi et al., 2014), but we did not find strong evidence for these subdivisions and refer to our area as the PIT complex. It may overlap with the occipital face area (OFA) (Kanwisher and Yovel, 2006; Tsao et al., 2008) and part of hOC4la (Malikovic et al., 2015).

The Fusiform Face Complex (**FFC**) is called a complex because it has substantial intra-areal heterogeneity and thus may contain additional subparcels. Relative to its lateral neighbors PH and TE2p, the **FFC** has more myelin (Panel B), is more activated in the FACE-AVG (Panel L) and FACES-SHAPES contrasts (Panel O), is deactivated vs activated in the TOOL-AVG contrast (Panel N), and differs in resting state functional connectivity (Panel D). Finally, relative to its anterior neighbor TF, the **FFC** has more myelin (Panel B) and is more activated in the FACE-AVG (Panel L) and FACES-SHAPES contrasts (Panel O). There is some uncertainty about the anterior/posterior position of this border because the task activations may also decrease due to susceptibility dropout, and the myelin content changes relatively gradually. Some studies of the fusiform face area (FFA) have reported a patchy organization in individual subjects (e.g., (Kanwisher and Yovel, 2006; Tsao et al., 2008), but our results for the group average are more similar to the strip-like organization reported by (Rajimehr et al., 2009) in some individuals as well as their group average. The VVC and the FFC show substantial overlap with architecturally defined areas FG1 and FG2 (Caspers et al., 2013) including a boundary along the mid-fusiform sulcus (Weiner et al., 2014), which is visible in our group average data despite the use of areal feature-based registration, supporting the suggested areal/folding correlation in this region (Weiner et al., 2014).

5. MT+ Complex and Neighboring Visual Areas

This section covers nine visual areas in lateral occipital and posterior temporal cortex: V3CD, LO1, LO2, LO3, V4t, FST, MT, MST, and PH. These areas are surrounded by early visual cortex (V4) posteriorly, dorsal stream visual cortex (V3B) medially, ventral stream visual cortex (PIT and FFC) inferiorly, inferior parietal cortex (PGp, IP0) superiorly, and the temporal-parietal-occipital junction (TPOJ2 and TPOJ3) plus lateral temporal cortex (PHT and TE2p) anteriorly. These areas are generally more heavily myelinated than their neighbors in inferior parietal and lateral temporal association cortex, but less heavily myelinated than early visual areas. Exceptions are the very heavily myelinated areas MT and MST of the MT+ complex near the center of this region. Figure 6 shows architectural, functional, connectivity, and topographic information that was used to parcellate the MT+ region and neighboring cortex. Panel A shows the areas on a map of the group average folding pattern.

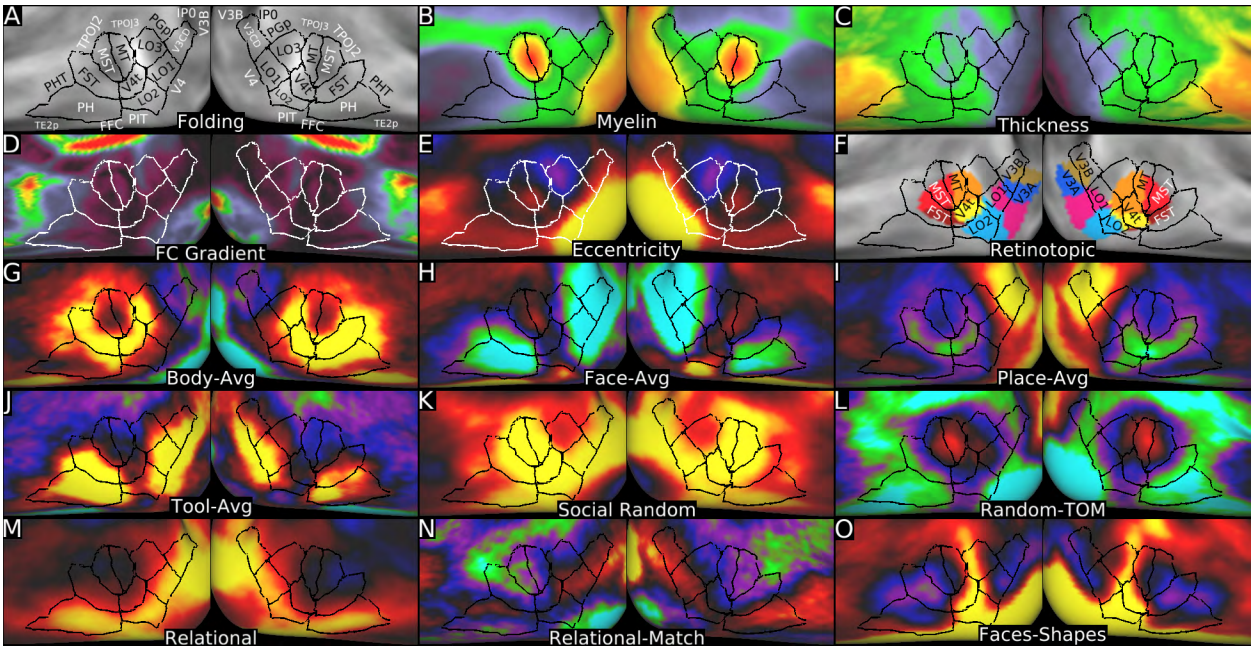

Figure 6 shows multi-modal information used to parcellate the MT+ complex and surrounding cortex. Panel A shows the areas on a group average cortical folding map. Panels B and C show myelin and cortical thickness maps. Panel D shows the resting state functional connectivity gradient. Panel E shows the foveal vs peripheral eccentricity contrast, highlighting the foveal confluence in the center of the MT+ complex. Panel F shows some retinotopic areas (Abdollahi et al., 2014). Panels G, H, I, and J show the BODY-AVG, FACE-AVG, PLACE-AVG, and TOOL-AVG contrasts. Panels K and L show the SOCIAL RANDOM primary contrast and RANDOM-TOM contrasts. Panels M, N and O show a RELATIONAL primary contrast, the RELATIONAL-MATCH contrast, and the FACES-SHAPES contrast. Data at http://balsa.wustl.edu/QqnB.

Areas **V3CD**, **LO1**, **LO2**, and **LO3** are moderately myelinated areas lying between the early visual cortex and the MT+ complex (Panel B). V3CD, LO1, and LO2 differ from adjacent area V4 because of myelin, thickness, and visuotopic transitions (see Panels B and C and Section #2 Early Visual Results). **V3CD's** medial border with V3B was described in Section #3 Dorsal Stream Visual Results. Relative to its supero-medial neighbor IP0, area **V3CD** differs in functional connectivity (Panel D), is activated vs deactivated in the TOOL-

AVG (Panel J) and RELATIONAL-MATCH (Panel N) contrasts, and is deactivated vs activated in the FACES-SHAPES (Panel O) contrast. Relative to its supero-anterior neighbor PGp, area **V3CD** has more myelin (Panel B), is much thinner (Panel C), differs more modestly in functional connectivity (Panel D), and is more activated in the working memory RELATIONAL and EMOTION primary contrasts, the TOOLS-AVG (Panel J), and RELATIONAL-MATCH contrast (Panel N). Relative to its infero-lateral neighbor LO1, area **V3CD** is less activated in the BODY-AVG (Panel G) and more activated in the PLACE-AVG (Panel I) task fMRI contrasts, and it is also slightly thicker (Panel C, more prominent in the right hemisphere). Relative to its superior neighbor LO1, area **LO2** is thicker (Panel C) and is strongly activated vs activated/deactivated in the FACES-SHAPES task contrast (Panel O). LO2's border with PIT was covered previously in Section #4 Ventral Visual Stream Results. Relative to its anterior neighbor V4t, area **LO2** is much less activated in the BODY-AVG contrast (Panel G), much more activated in the relational primary contrasts (e.g. Panel M), and differs modestly in functional connectivity (Panel D). Relative to its posterior neighbor LO1, area **LO3** is less activated in the TOOL-AVG contrast (Panel J) and in several primary task fMRI contrasts (e.g. Panels K and M) and is deactivated vs activated in the RELATIONAL-MATCH contrast (Panel N). On the other hand, LO1 and LO3 have similar architecture, and LO1 represents central visual fields whereas LO3 represents more peripheral visual fields (Panel E). A reasonable alternative would be to consider these areas to be a single area having significant internal heterogeneity. Relative to its superior neighbor PGp, area **LO3** has more myelin (Panel B), is strikingly thinner (Panel C), differs modestly in functional connectivity (Panel D), and is deactivated vs activated in the PLACE-AVG task contrast (Panel I). Relative to its inferior neighbor V4t, area **LO3** is thinner (Panel C), differs in functional connectivity (Panel D), is more deactivated in the FACE-AVG contrast (Panel H), and is less activated in the SOCIAL RANDOM primary contrast (Panel K). Relative to its anterior neighbor MT, area **LO3** has less myelin (Panel B), differs in functional connectivity (Panel D), and is less activated in the SOCIAL RANDOM task contrast (Panel K). Relative to its antero-superior neighbor TPOJ3, area **LO3** differs in functional connectivity (Panel D), is deactivated vs activated in the working memory 2BK-0BK contrast, and is less deactivated in the RELATIONAL-MATCH contrast (Panel N). Our LO1 and LO2 each overlap with anterior portions of published LO1 and LO2 maps (Panel F) (Abdollahi et al., 2014; Kolster et al., 2010), and for this reason we kept these names. Because we found that the Hansen et al parcellation of V4 best fit our data (Hansen et al., 2007), the posterior portion of LO1 and LO2 (Abdollahi et al., 2014) are a part of our area V4 and similarly our LO1 and LO2 areas do not match those of Larsson and Heeger (Larsson and Heeger, 2006) and their followers (their LO1 is part of our dorsal V4, and their LO1+LO2 have been subdivided into V4t, LO1, and LO2). Our area V3CD overlaps extensively with V3A and V3B (Abdollahi et al., 2014), but again parts of their areas overlap with our dorsal V4 (we reverse their V3A/V3B/V3C/V3D nomenclature to better match other studies, as noted above). Areas V3CD, LO1, LO2, and LO3 likely overlap with cytoarchitectonic hOC4la and perhaps parts of hOC4lp (Malikovic et al., 2015).

The MT+ complex contains four areas encircling a central foveal confluence (Panel E). The arrangement is similar to that reported for the motion-sensitive cluster mapped previously (Abdollahi et al., 2014; Kolster et al., 2010), so we use their terminology (Panel F). Areas **MT** and **MST** are both heavily myelinated, **V4t** is moderately myelinated, and **FST** is more lightly myelinated (Panel B). Relative to its anterior neighbor MST, area **MT** is

more activated in the RANDOM-TOM task contrast (Panel L; these task conditions differ in the pattern of moving objects); **MT** and MST also differ modestly in functional connectivity (Panel D). The MT/MST boundary is not as robust as most others reported here and additionally draws on visuotopic evidence (not shown) that MT and MST share an upper field representation as reported by others (Abdollahi et al., 2014; Kolster et al., 2010). **MT** and **MST** both differ from areas FST, V4t, and LO3 in being much less activated in the BODY-AVG task fMRI contrast (Panel G). Relative to its superior neighbor MT and anterior neighbor FST, area **V4t** is much more activated in the FACES-SHAPES contrast (Panel O). Relative to its inferior neighbor FST, area **MST** is activated vs deactivated in the FACE-AVG contrast (Panel H) and less activated in the TOOL-AVG contrast (Panel J). Relative to its posterior neighbor V4t, area **FST** is more activated in the TOOL-AVG contrast (Panel J) and is deactivated vs activated in the FACES-SHAPES task contrast (Panel O). Relative to their anterior neighbor TPOJ2 and superior neighbor TPOJ3, areas **MT** and **MST** have more myelin (Panel B), differ in functional connectivity (Panel D), and are less activated in the MOTOR CUE-AVG task contrast. Relative to its superior neighbor TPOJ2, area **FST** has less myelin (Panel B) and is more activated in the BODY-AVG contrast (Panel G), deactivated vs activated in the FACE-AVG contrast (Panel H), and activated vs deactivated in the TOOL-AVG contrast (Panel J). Relative to its inferior neighbor PH, area **FST** is thinner (Panel C) and is more deactivated in the PLACE-AVG contrast (Panel I) and less activated in the RELATIONAL primary contrast (Panel M). Relative to its anterior neighbor PHT, area **FST** is thinner (Panel C), differs in functional connectivity (Panel D), is more activated in the BODY-AVG contrast (Panel G), and more deactivated in the PLACES-AVG contrast (Panel I). Cytoarchitectonic areas hOC5v and hOC5d (Malikovic et al., 2007) likely correspond to areas MT and MST in our study, and our V4t may overlap with part of hOC4la (Malikovic et al., 2015).

Area **PH** lies between the MT+ complex and the ventral stream FFC. It has strong functional connectivity with other higher visual areas such as IPS1, V3CD, and the VVC, but has less myelin (Panel B) and is thicker (Panel C) than most other visual areas. The functional connectivity of **PH** differs from FFC and its anterior neighbors TE2p and PHT, (Panel D). Relative to its antero-superior neighbor PHT and supero-anterior neighbor TE2p, area **PH** has more myelin (Panel B) and is thinner (Panel C). Relative to PHT, area **PH** also is much more activated in the TOOL-AVG contrast (Panel J), much more deactivated in the FACE-AVG contrast (Panel H), and more activated in the RELATIONAL primary contrast (Panel M). PH in our parcellation corresponds to the superior part of PH in the Von Economo and Koskinas parcellation (Triarhou, 2007a, b; von Economo and Koskinas, 1925).

6. Somatosensory and Motor Cortex

The next four sections cover early and intermediate somatosensory and motor cortex, beginning with the core areas 4, 3a, 3b, 1, and 2. We previously (Glasser and Van Essen, 2011) used myelin mapping to identify boundaries between these areas and compared them to probabilistic surface-based cytoarchitectonic maps (Fischl et al., 2008), thereby providing a neuroanatomical validation of the T1w/T2w myelin mapping technique. Here we delineate these areas using multi-modal information that distinguishes them from surrounding areas (24dd, 6mp, 6d, FEF, 55b, 6v, 43, OP4, PFop, PFt, AIP, 7PC,

7AL, 5L, and 5m). We also present evidence for five somatotopic subregions within these early somatosensory and motor areas. Each subregion spans portions of multiple areas and the areas and subregions can be combined to be further subdivide this region of cortex into distinct subareas that represent topographic subdivisions of a single architectonic area. Figure 7 shows the multi-modal information used to define these areas (displayed on cortical flat maps because the entirety of the somatomotor strip cannot be seen from one perspective on inflated surfaces). The locations of the early sensory and motor areas are tightly correlated with cortical folding patterns, resulting in a sharp delineation of the fundus of the central sulcus and the crowns of the pre- and post-central gyri in the group average mean curvature map after MSMAll areal-feature-based registration (Panel A).

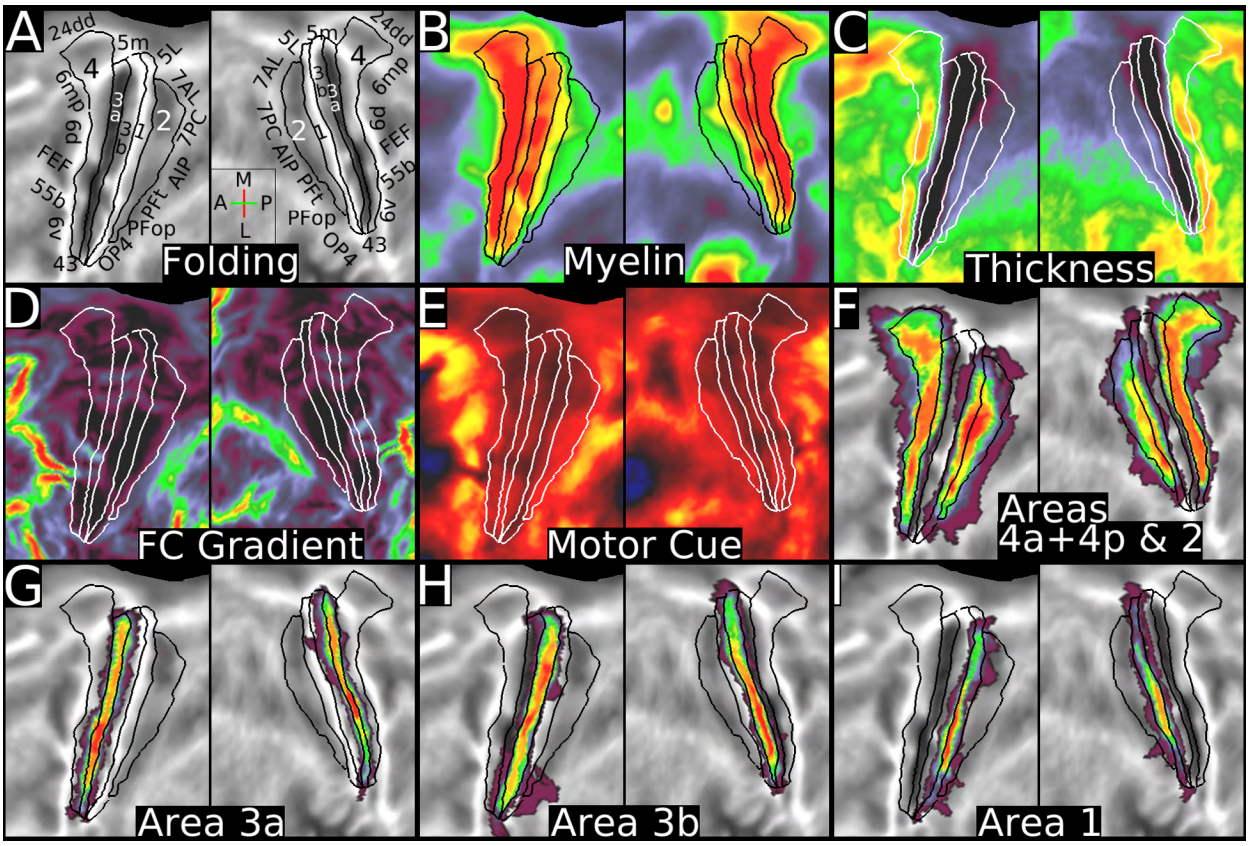

Figure 7 shows multi-modal information used to define early sensory and motor areas and surface-based probabilistic maps of these areas defined using post-mortem cytoarchitecture and the registered on the surface with FreeSurfer registration. The direction icon in Panel A shows Anterior (A), Posterior (P), Medial (M), and Lateral (L) directions (approximate orientation in 3D space) for the left surface (the A/P axis is reversed for the right surface). Panel A shows the areas on a mean curvature map, displayed on cortical flatmaps. Panels B and C show myelin and thickness maps. Panels D and E show the resting state functional connectivity gradient and the task fMRI MOTOR CUE contrast. Panels F, G, H, and I show probabilistic cytoarchitectonic areas. Panel F shows the sum of the probabilities of areas 4a and 4p and area 2. Panels G, H, and I show areas 3a, 3b and 1. Data at http://balsa.wustl.edu/Jjv2.

Area **4** (M1, or primary motor cortex) on the anterior bank of the central sulcus is perhaps the most architecturally distinct area in current non-invasive neuroimaging, as it is much more heavily myelinated than its anterior neighbors 6mp, 6d, FEF, 55b, and 6v (Panel B), and much thicker than its posterior neighbors 3a and 5m (Panel C). Additionally,

the body part task fMRI contrasts (T-AVG, ?H-AVG [? is a shorthand used here and below to mean both L and R for left and right hemispheres], ?F-AVG) each decrease in strength anterior to area **4**. Relative to its inferior neighbor 43, area **4** has more myelin (Panel B) and differs in functional connectivity (Panel D). Relative to its posterior neighbors 3a and 5m, area **4** has more myelin (Panel B), is thicker (Panel C), and (for 5m) differs in functional connectivity (Panel D). For the border with area 3a, the semiautomated border optimizer relied most on myelin because there is a narrow sharp gradient in myelin between areas 4 and 3a. Relative to its infero-medial neighbor 24dd (up on the flat map), area **4** has more myelin (Panel B) and differs in functional connectivity (Panel D). Our area 4 agrees well with the combined areas 4p and 4a from post-mortem cytoarchitecture registered on the surface (Fischl et al., 2008; Geyer et al., 1996)(Panel F).

Primary somatosensory cortex (S1) includes areas **3a** (in the fundus of the central sulcus) and **3b** (occupying the entire posterior bank of the sulcus). Relative to its posterior neighbor 3b, area **3a** has less myelin (Panel B) and is thicker (Panel C), and the semiautomated border optimizer relied most on myelin. Relative to its inferior neighbor OP4, area **3a** has more myelin (Panel B), is thinner (Panel C), and differs in functional connectivity (Panel D). Area **5m**, medial to 3a and 3b (up on the flatmap) has less myelin than either 3a or 3b (Panel B), differs modestly from 3a in functional connectivity (Panel D), and is much thicker than 3b (Panel C). Relative to its posterior neighbor area 1, area **3b** is much thinner (Panel C) and has more myelin (Panel B). Our areas 3a and 3b agree well with probabilistic areas 3a and 3b from post-mortem cytoarchitecture registered on the surface (Fischl et al., 2008; Geyer et al., 1999; Geyer et al., 2000) (Panels G and H).

Areas **1** and **2** are also part of the S1 primary somatosensory complex. Relative to its posterior neighbor area 2, area **1** has more myelin (Panel B), is less activated in the motor CUE task (Panel E) and in the LH and RH task fMRI contrasts (specifically in the ipsilateral hemisphere), and is more activated in the EMOTION FACES-SHAPES contrast. Relative to its inferior neighbors OP4 and PFop, area **1** has more myelin, is thinner, differs in functional connectivity (Panel D), and is less activated in the MOTOR CUE contrast (Panel E). Relative to their postero-medial neighbor 5L, both areas **1** and **2** have more myelin (Panel B) and are less activated in the MOTOR CUE task contrast (Panel E). Relative to the four areas (7AL, 7PC, AIP, and PFt) sharing a substantial common boundary along its posterior side, area **2**: (i) has more myelin than area 7AL, differs in functional connectivity, and is less activated in in the MOTOR CUE contrast (Panel E); (ii) has more myelin than area 7PC and is less activated in the MOTOR CUE contrast (Panel E); (iii) is thinner than area AIP, differs in functional connectivity, is less activated in the working memory 2BK-0BK, and more activated in the, FACE-AVG contrast (along with differences in at least four other contrasts); and (iv) has more myelin and is thinner than area PFt, differs in functional connectivity, is less activated in the BODY-AVG contrast and more activated in the ?H-AVG and FACES-SHAPES contrasts. Our areas 1 and 2 generally align well with the corresponding areas mapped using post-mortem cytoarchitecture and registered on the surface (Fischl et al., 2008; Geyer et al., 1999; Geyer et al., 2000; Grefkes et al., 2001), but there are some differences (Panel I, F). Our area 1 (Panel I) tends to be wider than the probabilistic map, especially in the left hemisphere, and area 2 (Panel F) extends more posteriorly in some regions (indeed, the maximum probabilities of areas 3b and 2 almost join in some locations). Also, our area 1 is symmetric in terms of its overall extent along the postcentral gyrus, whereas the probabilistic map is modestly asymmetric. The

differences in area 1 may be related to the strong distortion that occurs on the post-central gyral crown (Robinson et al., 2014) from the FreeSurfer registration used to register the post-mortem cytoarchitectonic maps. Our area 2's medial/superior extent also likely overlaps some with area 5L from Scheperjans, (Scheperjans et al., 2008a; Scheperjans et al., 2008b) though our border is placed at the maximum architectural and functional transition as for other areas.

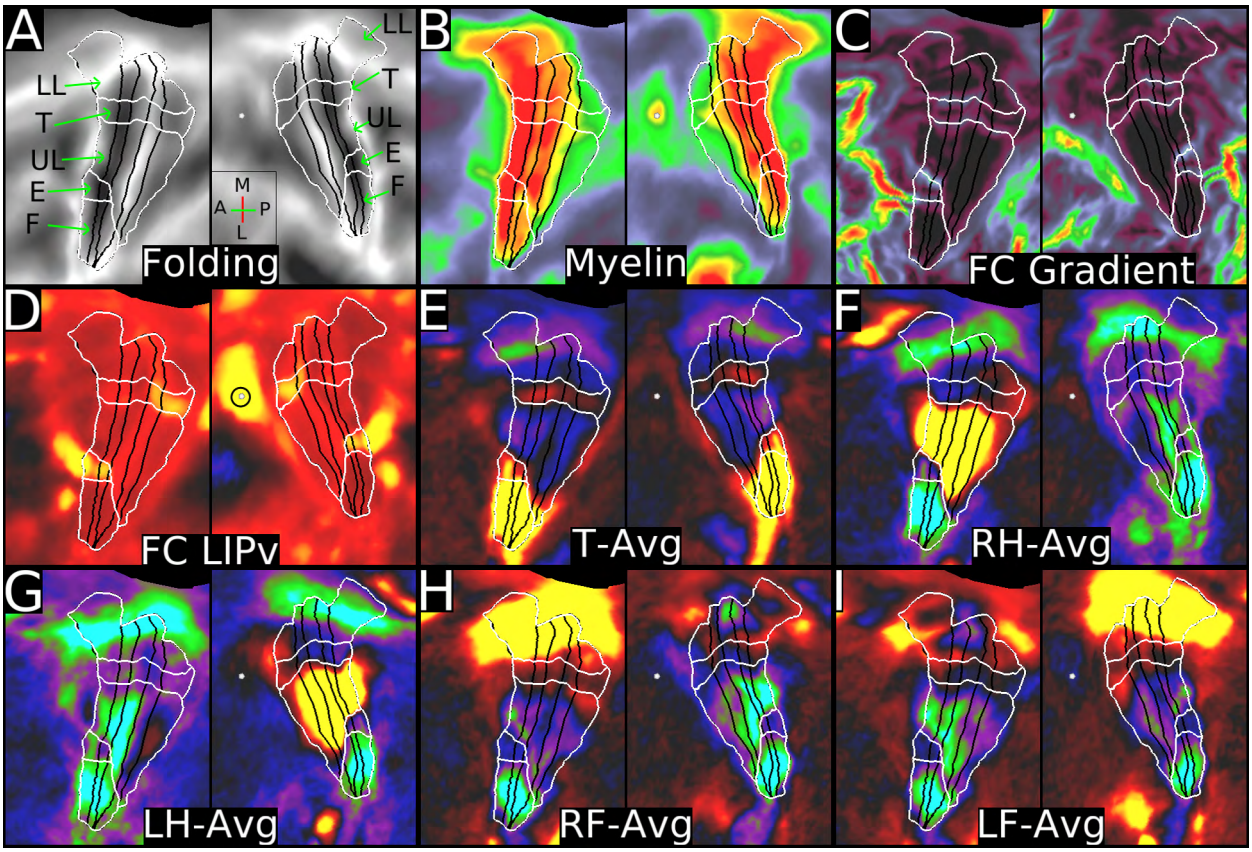

Figure 8 shows subregions and subareas of the sensorimotor strip, displayed on cortical flatmaps. Panel A shows folding maps. The direction icon in Panel A shows Anterior (A), Posterior (P), Medial (M), and Lateral (L) directions (approximate orientation in 3D space) for the left surface (the A/P axis is reversed for the right surface). Panel B shows myelin maps, which interestingly have some correspondence with the subareas (white). Areal boundaries remain black. Panel C shows the resting state functional connectivity gradients that were used to define the subregions using the semiautomated border drawing approach. Panel D shows functional connectivity from the heavily myelinated LIPv seed (black circle, which has functional connectivity with some parts of the sensori-motor strip. Panels E, F, G, H, and I show the task fMRI contrasts T-AVG, ?H-AVG (RH-AVG and LH-AVG), and ?F-AVG (RF-AVG and LF-AVG). Data at http://balsa.wustl.edu/QwnL.

Sensorimotor areas 4, 3a, 3b, 1, and 2 are largely architecturally defined. Previous fMRI studies have revealed highly inhomogeneous functional connectivity within the sensorimotor strip, but the heterogeneity is more related to somatotopic boundaries than areal boundaries, with distinct subregions related to representations of the face vs the rest of the body (Power et al., 2011; Van Essen et al., 2014; Yeo et al., 2011). Here, we provide evidence for a finer-grained somatotopic organization that includes 5 functional and connectional subdivisions within the sensorimotor strip (see Figure 8), based on resting state functional connectivity gradients (Panel C; see also Panel D of Figure 7) and

somatotopic task fMRI contrasts (Panels E, F, G, H, I). Each white-outlined region spans multiple architectonic areas but occupies a restricted portion of the somatotopic map and a small portion of each architectonic area. We label these five somatomotor subregions based on the known or presumed portion of the body involved: the F (face), E (eye), UL (upper limb), T (trunk), and LL (lower limb). The intersection of the somatomotor subregions with the architectonic areas can be used to define distinct 'subareas' (four or five subareas for each of the five architectonic areas), but our analysis here focuses mainly at the level of somatomotor subregions.

The most infero-lateral subregion, F (face) is activated in the T-AVG contrast (Panel E). Subregion E (eye) lies just posterior to the frontal eye fields (FEF, a heavily myelinated hotspot just anterior to area 4) and is clearly evident only in areas 4 and 3a. This approximate region was previously shown to be activated by squeezing (squinting) the muscles around the eyes (Meier et al., 2008). This was not explicitly tested in the HCP motor task fMRI paradigm, but subregion E has strong functional connectivity with the LIP/VIP complex (heavily myelinated hotspot posterior to area 2 marked by small white sphere), similar to that found in areas FEF and PEF (Panel D, hotspots of myelin and functional connectivity anterior to area 4). It is also activated in the T-AVG contrast (Panel E). The middle subregion UL is activated in the ?H-AVG task contrasts (Panels F and G). Interestingly, its proportional representation across the sensorimotor strip changes markedly: subarea 4_UL (upper limb) occupies about one-fourth of area 4, whereas subarea 2_UL occupies more than half of area 2. Subregion T (trunk) was not explicitly tested for in the motor task paradigm but its somatotopic assignment seems highly likely given its position between the upper and lower limb representations (Penfield and Rasmussen, 1950). It is intriguing but puzzling that subareas 1_T and 2_T show strong functional connectivity with the LIP/VIP complex (Panel D; same seed as correlates with subregion E). Subregion LL (lower limb) is strongly activated contralaterally in the ?F-AVG task contrasts but only moderately activated in subarea 2_LL (Panels H and I). In adjoining area 5L, the foot activation is strong, but bilateral – see Section #7 Paracentral Lobular and Mid Cingulate Cortex). Interestingly, some reproducible (see Supplementary Figure 1 in the Supplementary Results and Discussion and Main Text Figure 1) variations in myelin content within area 3b (see Panel B) align with the subareas described above, particularly the trunk subarea (3b_T) and the boundary between subareas 3b_F and 3b_UL. Somatotopic variations in myelin content have previously been reported in area 3b using histological methods, including a similar face/hand boundary myelin content decrease in the macaque (Krubitzer et al., 2004) and marmoset (Krubitzer and Kaas, 1990), and further variations in more superior regions (Krubitzer and Kaas, 1990).

7. Paracentral Lobular and Mid Cingulate Cortex

This section discusses areas in and around the paracentral lobule and mid-cingulate cortex. These are higher sensory and motor regions that include cingulate motor areas (24dd and 24dv), supplementary motor areas (6mp, 6ma, SCEF), and subdivisions of area 5 (5m, 5L and 5mv). They are surrounded by areas 4, 3a, 3b, 1, 2, 7AL, 7Am, PCV, 23c, p24pr, p32pr, 8BM, SFL, s6-8, 6a, and 6d. Figure 9 shows much of the multi-modal information used to parcellate this region, displayed on inflated maps that are viewed from a medio-superior perspective (lateral is up, medio-inferior is down, anterior is towards the center of

the panel, posterior is towards the outside of the panel). Area 4 extends medially, onto the anterior portion of the paracentral lobule (Fischl et al., 2008; Geyer et al., 1996; Rademacher et al., 1993), Panel A), whereas areas 3a, 3b, and 1 do not in our or previous studies (Fischl et al., 2008; Geyer et al., 1999; Geyer et al., 2000; Rademacher et al., 1993), Panel A). We first discuss subdivisions of Brodmann's area 5, then the cingulate motor areas, and finally some supplementary motor areas.

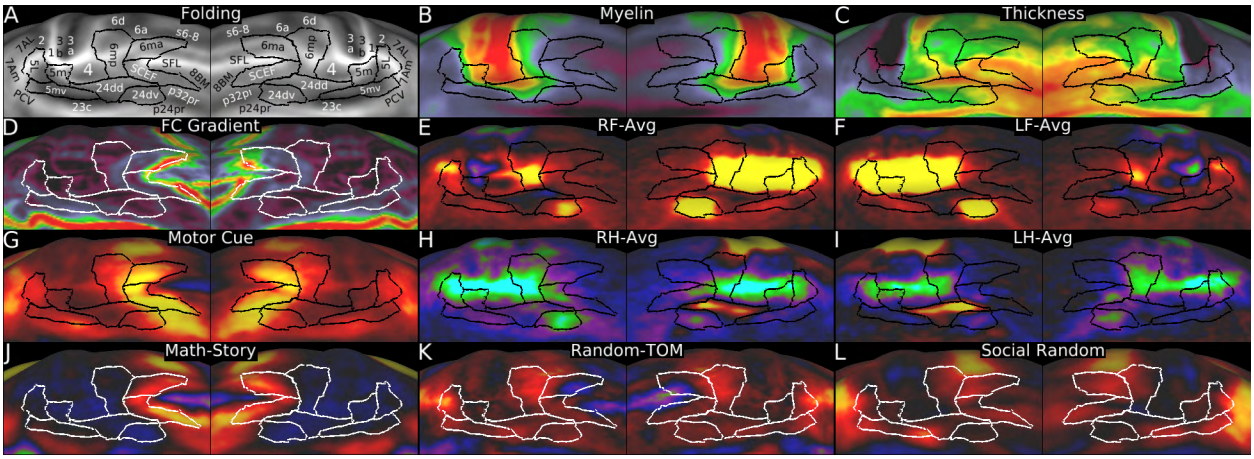

Figure 9 shows some of the multi-modal information used to delineate cortical areas in the paracentral lobular and mid cingulate cortical region. Panel A shows the areas delineated in this section overlaid on a folding map. Panels B and C show myelin and thickness maps. Panel D shows the resting state functional connectivity gradient. Panels E and F show the MOTOR RF-AVG and LF-AVG task fMRI contrasts (referred to as ?F-AVG in the text). Panel G shows the MOTOR CUE task contrast. Panels H and I show the RH-AVG and LH-AVG task contrasts (referred to as ?H-AVG in the text). Panels J, K and L show the MATH-STORY, RANDOM-TOM, and SOCIAL RANDOM task contrasts. Data at http://balsa.wustl.edu/J49j.

We identified 3 subdivisions of area 5. Area **5L** occupies a similar location to that reported previously, though our area 2 may overlap with its most lateral extent (Scheperjans et al., 2008a; Scheperjans et al., 2008b). Area **5m** occupies a similar location to that reported previously on the paracentral lobule (Scheperjans et al., 2008a; Scheperjans et al., 2008b), though the group definition does not extend past the fundus of the posterior cingulate sulcus (some individuals likely do, however). Area **5mv** overlaps with area 5ci reported previously and the most posterior extent of area 5m (Scheperjans et al., 2008a; Scheperjans et al., 2008b). Area 5L is a lightly myelinated area (Panel B) whose borders with areas 1 and 2 were described above in Section #6 Somatosensory and Motor Cortex. Relative to its posterior neighbors 7AL and 7Am, area **5L** differs in functional connectivity (Panel D) and is less activated in the CUE-AVG task contrast. **5L** is also much more strongly activated than 7Am in the ?F-AVG foot motor task contrasts (Panels E and F). Relative to its anterior neighbor 5m, area **5L** has much less myelin (Panel B) and is more activated in the MOTOR CUE task (Panel G), the ipsilateral hemisphere's ?F-AVG foot motor contrast (Panels E and F), and the RANDOM-TOM contrast (Panel K). Area **5L**'s inferior border with **5mv** is marked by a change in functional connectivity (Panel D) and decreased activation in the ?F-AVG foot motor contrasts (Panels E and F) and the MOTOR AVG contrast. Area 5m's borders with areas 3b, 3a, and 4 were covered previously in Section #6 Somatosensory and Motor Cortex. Relative to its anterior neighbor 24dd, area **5m** is thinner (Panel C) and differs in functional connectivity (Panel D). Relative to its inferior

neighbor 5mv, area **5m** has much more myelin (Panel B), differs in functional connectivity (Panel D) and is less activated in the SOCIAL RANDOM-TOM (Panel K) contrast. Relative to its anterior neighbor 24dd, area **5mv** has less myelin (Panel B), is thinner (Panel C), differs in functional connectivity (Panel D), is more strongly activated in the ?F-AVG foot motor contrast (Panels E and F), and is deactivated instead of strongly activated in the ?H-AVG contralateral hand motor contrast (Panels H and I). Relative to its inferior neighbor 23c, area **5mv** is thinner (Panel C), differs in functional connectivity (Panel D), and is more activated in the RANDOM-TOM task contrast (Panel K). Relative to its postero-inferior neighbor PCV, area **5mv** is thinner (Panel C), is deactivated vs activated in the working memory 2BK-0BK contrast, the GAMBLING primary contrasts, and less activated in the SOCIAL primary contrasts in the right hemisphere (Panel L). Relative to its posterior neighbor 7Am, area **5mv** differs in functional connectivity (Panel D) and is less activated in the working memory 2BK-0BK contrast, the MOTOR CUE contrast (Panel G), and the SOCIAL primary contrasts (Panel L).

Areas **24dd** and **24dv** constitute most of the cingulate motor cortex (Palomero-Gallagher et al., 2009; Vogt and Vogt, 2003). The borders of area 24dd with areas 4 and 5mv were already described above and in Section #6 Somatosensory and Motor Cortex. Relative to its inferior neighbor 23c, area **24dd** has more myelin (Panel B) and differs in functional connectivity (Panel D). Relative to its antero-inferior neighbor 24dv, area **24dd** has more myelin, differs in functional connectivity (Panel D), is strongly activated vs deactivated in the contralateral ?H-AVG hand motor contrast (Panels H and I) and is minimally activated vs strongly activated in the ?F-AVG contrast (Panels E and F). Relative to its antero-superior neighbor 6mp, area **24dd** differs in functional connectivity (Panel D), is strongly activated vs deactivated in the contralateral ?H-AVG hand motor contrast (Panels H and I) and less activated in the ?F-AVG foot motor contrasts (Panels E and F). Relative to the anteriorly neighboring supplementary and cingulate eye fields (SCEF), area **24dd** has more myelin (Panel B), differs in functional connectivity (Panel D), is strongly activated vs deactivated in the contralateral ?H-AVG hand motor contrast (Panels H and I), and is less activated in the T-AVG, MOTOR AVG contrast, CUE contrast (Panel G) and other task primary contrasts. Relative to its anterior neighbor p32pr, area **24dv** differs in functional connectivity (Panel D), is less activated in the CUE contrast (Panel G), more activated in the ?F-AVG foot motor contrast (Panels E and F), and deactivated instead of activated in the MATH-STORY contrast (Panel J). Relative to its inferior neighbor p24pr and posterior neighbor 23c, area **24dv** has more myelin (Panel B), differs modestly in functional connectivity (Panel D), and is more activated in the ?F-AVG foot motor contrasts (Panels E and F). The cingulate motor cortex is particularly active in the motor tasks and shows somatotopic organization, with 24dd more related to the upper limb and 24dv more related to the lower limb. It is in the expected location inferior and anterior to motor cortex as reported previously (Vogt et al., 1995; Vogt et al., 2005). Based only on topography, the foot (24dv) and hand (24dd) representations could be considered subareas within a single cingulate motor area (CMA) having a more complete body representation (perhaps even including the face representation in adjoining SCEF). However, the prominent architectural and other differences already noted above argue against combining these regions, as does the precedent set by other studies cited above.

The supplementary motor cortex was divided into three areas, **6mp**, **6ma**, and the supplementary and cingulate eye fields (**SCEF**). Area 6mp overlaps with SMAc of (Vorobiev

et al., 1998) on the medial surface, but extends supero-laterally into a region they did not map. Area 6ma overlaps partially with SMAr of (Vorobiev et al., 1998) but extends farther anteriorly and laterally and not as far inferiorly on the mesial surface. Collectively these areas overlap extensively with the region previously identified as the supplementary motor cortex (Roland and Zilles, 1996). The boundaries of 6mp with areas 4 posteriorly and 24dd inferiorly were already described in Section #6 Somatosensory and Motor Cortex and above. Relative to its anterior neighbor 6ma, area **6mp** has more myelin, differs in functional connectivity (Panel D), is less activated in the MOTOR CUE contrast (Panel G) and more activated in the FOOT-AVG contrast (Panels E and F). Relative to its anterior neighbor SCEF, area **6mp** has more myelin (Panel B), differs in functional connectivity (Panel D), is less activated in the MOTOR AVG and MATH-STORY contrasts (Panel J), and differs in a number of the primary contrasts including the RELATIONAL MATCH contrast. Relative to its lateral neighbor 6d, area **6mp** differs in functional connectivity (Panel D), and is deactivated vs activated in the contralateral ?H-AVG hand motor contrast (Panels H and I). Additionally, **6mp** is more deactivated than 6d in the LANGUAGE MATH, and STORY contrasts and less activated in the RANDOM-TOM contrast. Relative to area 6a anteriorly, **6mp** is slightly thinner (Panel C) and less activated in the working memory 2BK-0BK, MATH-STORY (Panel J), and many primary task contrasts, e.g. the SOCIAL RANDOM (Panel L) contrast. Relative to its latero-inferior neighbor 6a, area **6ma** has less myelin (Panel B), differs in functional connectivity (Panel D), and is less activated in the SOCIAL RANDOM (Panel L) and TOM contrasts. Relative to its anterior neighbor s6-8, area **6ma** differs dramatically in functional connectivity (Panel D), is more activated in the MOTOR CUE contrast and is deactivated vs activated in the RELATIONAL MATCH contrast. Relative to its anterior neighbor SFL, area **6ma** differs dramatically in functional connectivity (Panel D), is more activated in the MOTOR CUE contrast (Panel G), is deactivated vs activated in the LANGUAGE STORY contrast and activated vs deactivated in the MATH-STORY contrast (Panel J). Relative to its medial neighbor SCEF, area **6ma** is thinner (Panel C), has less myelin (Panel B), and is much less activated in the MOTOR AVG contrast. Areas 6ma and 6mp are parts of probabilistic cytoarchitectonic area 6 (Fischl et al., 2008; Geyer, 2004). The supplementary and cingulate eye fields (SCEF) are named because of their functional connectivity with the frontal and premotor eye fields (areas FEF and PEF) together with other visual regions. They also have a their similar location to that described in (Amiez and Petrides, 2009), but they also overlap with SMAr from (Vorobiev et al., 1998). Relative to its superior neighbor SFL, area **SCEF** differs in functional connectivity (Panel D), has more myelin (Panel B), is activated vs deactivated in the LANGUAGE MATH-STORY contrast, is deactivated vs activated in the LANGAUGE STORY contrast, and is activated vs deactivated in the RELATIONAL-MATCH contrast in the left hemisphere only (as will be highlighted in later sections, area SFL is one of several areas with substantial lateralization of functional activation). Relative to its anterior neighbor 8BM, **SCEF** has more myelin (Panel B), is thinner, differs substantially in functional connectivity (Panel D), is locally more activated in the primary gambling contrasts and the MOTOR CUE contrast (Panel G), and less activated in the RELATIONAL-MATCH contrast. Finally, relative to its inferior neighbor p32pr, area **SCEF** is more activated in multiple primary contrasts in the working memory and gambling tasks, the LANGUAGE MATH contrast, the SOCIAL RANDOM contrast (Panel L), RELATIONAL, and EMOTION-SHAPES and MATH-STORY task contrasts (Panel J). Area SCEF is part of probabilistic cytoarchitectonic area 6 (Fischl et al., 2008; Geyer, 2004)

8. Premotor Cortex

This section includes six areas that occupy what is typically called the premotor region anterior to area 4 (Roland and Zilles, 1996). Area 55b lies immediately anterior to area 4, splitting premotor cortex into superior and inferior subdivisions, but it is very different from all other areas within classical architectonic area 6 (Fischl et al., 2008; Geyer, 2004). The superior premotor subdivisions include areas 6d, 6a, and the frontal eye field (FEF), whereas the inferior premotor subdivisions include 6v, 6r, and the premotor eye field (PEF). These areas are surrounded by areas 4, 6mp 6ma, s6-8, i6-8, 8Av, 8C, IFJp, 44, FOP4, FOP1, and 43. Figure 10 shows some of the multi-modal information that we used to parcellate the premotor cortex, with Panel A showing the areas and their neighbors labeled on an inflated surface with an underlay of cortical folding.

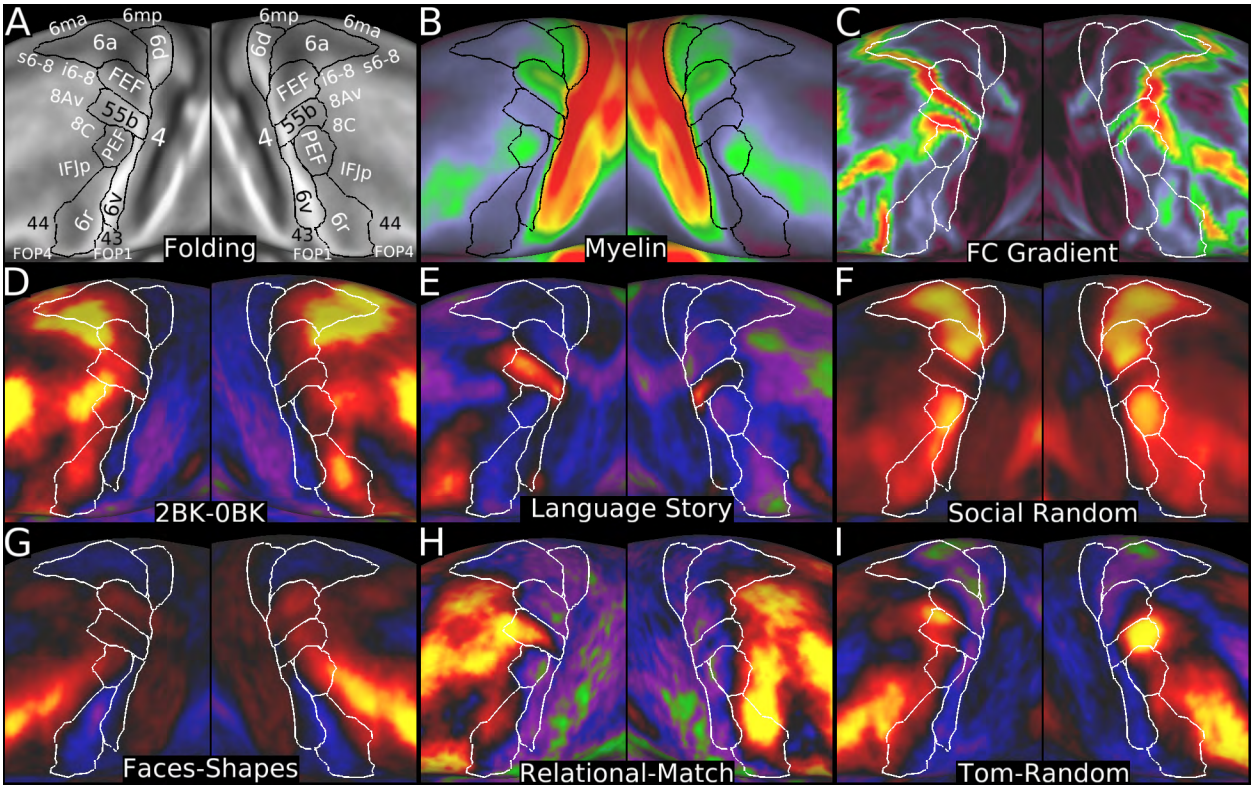

Figure 10 shows multi-modal information used to parcellate the premotor cortex. Panel A shows the 6 premotor areas plus 55b on a folding map. Panel B shows them on the myelin map. Panel C shows the functional connectivity gradient. Panels D, E, and F show the working memory 2BK-0BK contrast, the LANGUAGE STORY contrast, and the SOCIAL RANDOM contrast. Panels G, H, and I show the EMOTION FACES-SHAPES contrast, the RELATIONAL-MATCH contrast, and the SOCIAL TOM-RANDOM contrast. Data at http://balsa.wustl.edu/Qm5v.

The superior borders of **6a** and **6d** and the posterior border of area 6d were covered in the preceding two Sections (#6 Somatosensory and Motor Cortex and #7 Paracentral Lobular and Mid Cingulate Cortex). Relative to its anterior neighbor 6a, area **6d** differs in functional connectivity (Panel C), is less activated in the working memory 2BK-0BK (Panel D), MATH-STORY, and SOCIAL RANDOM (Panel F) contrasts, and is more activated in the ?H-AVG hand motor contrasts. Relative to its inferior neighbor FEF, area

6d has less myelin (Panel B), differs in functional connectivity (Panel C), and is less activated in many of the primary task contrasts, including the GAMBLING, SOCIAL (Panel F), RELATIONAL, and EMOTION contrasts. Relative to its antero-medial neighbor s6-8, area **6a** differs strongly in functional connectivity (Panel C), is more activated in the LANGUAGE MATH, SOCIAL (Panel F), and RELATIONAL primary contrasts, and is less deactivated in the STORY contrast (Panel E). Relative to its anterior neighbor area i6-8, area **6a** differs markedly in functional connectivity (Panel C), is more activated in the SOCIAL primary contrasts (Panel F), and is deactivated vs activated in the FACES-SHAPES (Panel G) and RELATIONAL REL-MATCH contrasts (Panel H). For this border, the semiautomated border optimizer relied most on functional connectivity. Relative to its latero-inferior neighbor FEF, area **6a** has less myelin (Panel B) and differs in several task contrasts including less activation in the GAMBLING and RELATIONAL primary contrasts, and the EMOTION SHAPES primary contrast. These superior subdivisions of area 6 are within the territory of probabilistic surface-registered cytoarchitectonic area 6 (Fischl et al., 2008; Geyer, 2004). The border between 6a and 6d may correspond to the border between 6aβ and 6aα (Geyer et al., 2000).

The premotor cortex contains two moderately myelinated eye fields, the Frontal Eye Field (**FEF**) and the Premotor Eye Field (**PEF**), separated by a lightly myelinated isthmus, area **55b** (Panel B). The eye fields share similar patterns of functional connectivity, which differs markedly from that of area 55b (Panel C). Also, they have similar patterns of task activation (being particularly activated during the primary contrasts of many tasks (e.g. Panel F), as distinct from 55b's lesser activation). The borders of FEF with 6a and 6d superiorly and with area 4 posteriorly were covered above and in Section #6 Somatosensory and Motor Cortex. Relative to its anterior neighbors i6-8, and 8Av, area **FEF** is deactivated vs activated in the RELATIONAL REL-MATCH contrast (Panel H). Relative to 8Av, **FEF** is also more activated in the MATH-STORY contrast and the CUE-AVG contrast. Relative to its inferior neighbor 55b, area **FEF** has more myelin (Panel B), differs markedly in functional connectivity (Panel C), and in primary task contrasts (e.g. Panel F), and is less activated in the STORY contrast (Panel E). Area **55b** (Hopf, 1956) was already covered in the Main Results (see Figure 2), and 55b's border with 8Av and 8C is covered below in Section #22 DorsoLateral Prefrontal Cortex. The Main Text and the Supplementary Results and Discussion sections #1.3-1.4 and Supplementary Figures 7-10 describe the distinct topologies that area 55b and the eye fields have in atypical individuals. Here, we focus on the typical relationships revealed in the group average analyses.

Relative to its superior neighbor 55b, area **PEF** has more myelin (Panel B), differs in functional connectivity (Panel C), is less activated in the LANGUAGE STORY contrast (Panel E), and is more activated in a number of primary task contrasts (e.g. SOCIAL RANDOM in Panel F). Relative to its anterior neighbor 8C, area **PEF** has more myelin (Panel B), differs in functional connectivity (Panel C), and is more activated in primary task contrasts (e.g. SOCIAL RANDOM in Panel F). Relative to its antero-inferior neighbor IFJp, area **PEF** differs in functional connectivity (Panel C), is more activated in the SOCIAL primary contrasts (Panel F), and is deactivated vs activated in the RELATIONAL-MATCH contrast (Panel H). Relative to its inferior neighbor 6r and infero-posterior neighbor 6v, area **PEF** has more myelin (Panel B), differs in functional connectivity (Panel C), and is more activated in the primary task contrasts (e.g. Panel F). **PEF** is also less activated than 6r in the BODY-AVG contrast and more activated in the PLACE-AVG contrast. The eye fields PEF and FEF

correspond closely to those identified in (Amiez and Petrides, 2009). PEF is also similar in location to 6v2 from (Amunts et al., 2010).

Premotor areas **6v** and **6r** appear in similar locations to those described in (Amunts et al., 2010), with their 6v1 matching our 6v. The borders of 6v with areas 4 posteriorly and PEF anteriorly have already been described (in Section #6 Somatosensory and Motor Cortex and above). Relative to its superior neighbor 55b, area **6v** differs in functional connectivity, is less activated in the STORY contrast and more activated in the MOTOR CUE contrast. Relative to its anterior neighbor 6r, area **6v** differs in functional connectivity, having particularly strong connectivity with areas 6d, 2, 24dd, and SII, along with the upper limb representation of the sensori-motor cortex, which is distinct from area 6r (gradient in Panel C). Area **6v** is also deactivated vs activated relative to 6r in the WORKING MEMORY 2BK-0BK (Panel D), RELATIONAL-MATCH (Panel H), and TOM-RANDOM (Panel I) contrasts, and less activated in the BODY-AVG and MATH-STORY contrasts. Relative to its inferior neighbor 43, area **6v** differs in functional connectivity (Panel C) and is activated vs deactivated in primary task contrasts (e.g. Panel F). Relative to its antero-inferior neighbor IFJp, area **6r** has less myelin (Panel B), is more activated in the BODY-AVG contrast, and is less activated or deactivated in the PLACE-AVG, FACES-SHAPES (Panel G) and several primary task contrasts. Relative to its anterior neighbor area 44, area **6r** differs in functional connectivity (Panel C), is more activated in the MOTOR AVG contrast, is deactivated vs activated in the LANGUAGE STORY contrast (Panel E) and STORY-MATH contrast, and activated vs deactivated in the FACES-SHAPES contrast (Panel G). Also relative to area 44, area 6r is less activated in the right hemisphere in the TOM-RANDOM contrast (Panel I), and less activated in the left hemisphere in the RELATIONAL-MATCH contrast (Panel H). Relative to its inferior neighbors FOP4 and FOP1, area **6r** differs in functional connectivity (Panel C), has more myelin (Panel B), and is thinner than FOP4. Relative to its posterior neighbor 43, area **6r** has less myelin (Panel B), differs in functional connectivity (Panel C), is more activated in primary task contrasts (e.g. Panel F), has differential activity in the T-AVG and ?H-AVG contrasts (more prominent in the ipsilateral hemisphere), and is more activated in the working memory 2BK-0BK contrast (Panel D).

9. Posterior Opercular Cortex

The posterior operculum of the Sylvian fissure, including the second somatosensory area, SII, is the fourth and final region of our parcellation that is related mainly to sensori-motor function, based on functional connectivity and task-fMRI activations. This region includes six areas, 43, FOP1 (Frontal Opercular area 1), OP4, OP1, OP2-3, and PFcm, which are surrounded by areas 1, 3b, 3a, 4, 6v, 6r, FOP4, FOP2, Ig, 52, RI, PSL, PF, PFop. Figure 11 shows multi-modal information that was used to parcellate this region of cortex on a very inflated view of the posterior operculum inside the Sylvian fissure, together with the six areas overlaid on a folding map (Panel A).

The superior borders of area **43** and **FOP1** with areas 4, 3a, 6v and 6r were covered earlier (Sections #6 Somatosensory and Motor Cortex, #8 Premotor Cortex). Relative to its anterior neighbor FOP4, area **FOP1** has more myelin (Panel B), differs in functional connectivity (Panel D) and is more activated in many MOTOR primary contrasts (exemplified by the MOTOR AVG contrast, Panel G). Relative to its infero-medial neighbor FOP2, area **FOP1** differs in functional connectivity (Panel D), is more activated in the ?F-

AVG foot (Panels H and I) contrasts, and is deactivated vs activated in the contralateral ?H-AVG hand (Panels K and L) and TOM-RANDOM contrasts. Relative to its posterior neighbor 43, area **FOP1** differs in functional connectivity and is much more activated in the MOTOR AVG contrast (Panel G). Relative to its inferior neighbor FOP2, area **43** has more myelin (Panel B), differs in functional connectivity (Panel D), and is deactivated vs activated in the SOCIAL TOM contrast. Relative to its posterior neighbor OP4, area **43** differs in functional connectivity (Panel D), and is deactivated or less activated in many primary task contrasts including LANGAGE MATH (Panel E) and GAMBLING, and is much less activated in the T-AVG motor contrast (Panel J). Area 43 is assigned this name for its similarity in location to area 43 as described by Brodmann (Brodmann, 1909; Brodmann, 2007) directly inferior to sensorimotor cortex (though OP4 may also correspond to the posterior part of Brodmann's 43, (Eickhoff et al., 2006a; Eickhoff et al., 2006b)). Our area 43 may correspond to area 41 from the Vogt-Vogt school (Nieuwenhuys et al., 2015).

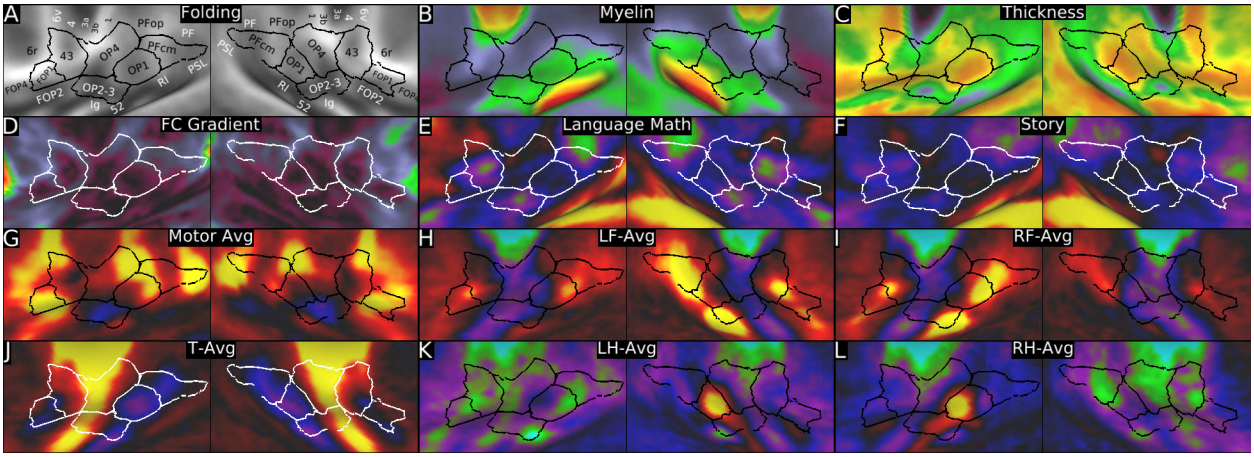

Figure 11 shows multi-modal information that was used to define the boundaries of the areas in the posterior opercular cortex. Panel A shows these areas on a folding map. Panels B and C show the myelin and thickness maps. Panel D shows the resting state functional connectivity gradients. Panels E and F show the LANGUAGE MATH and STORY task contrasts. Panels G, H, I, J, K, and L show the MOTOR AVG, LF-AVG, RF-AVG, T-AVG, LH-AVG, and RH-AVG task contrasts. Data at http://balsa.wustl.edu/JZ31.

Relative to its infero-medial neighbor OP2-3 (on the opercular surface; down in the figure), area **OP4** has less myelin, is activated vs deactivated in the MOTOR AVG task contrast (Panel G) and is more activated in the LANGUAGE MATH contrast (Panel E). Relative to its posterior neighbor OP1, area **OP4** is has less myelin, differs in functional connectivity (Panel D), is deactivated vs strongly and focally activated in the contralateral ?H-AVG hand motor contrasts (Panels K and L) and is strongly activated vs deactivated in the T-AVG contrast (Panel J). **OP4's** boundary with area 1 was covered previously in Section #6 Somatosensory and Motor Cortex. Relative to its supero-posterior neighbor PFop, area **OP4** differs in functional connectivity (Panel D) and is modestly activated vs strongly deactivated in the LANGUAGE STORY contrast (Panel F). Our area OP4 may correspond to area 68 from the Vogt-Vogt school (Nieuwenhuys et al., 2015).

Relative to its anterior neighbor FOP2, area **OP2-3** has more myelin (Panel B), differs in functional connectivity (Panel D), is deactivated vs activated in the MOTOR AVG contrast (Panel G) and in many primary contrasts including RELATIONAL and EMOTION

contrasts. Relative to its medio-inferior neighbor Ig (down in the figure; on the insula instead of the operculum), area **OP2-3** is thinner (Panel C), is deactivated vs activated in the MOTOR AVG contrast (Panel G), and is more deactivated in the working memory 2BK-0BK contrast. OP2-3 (and also Ig, covered in Section #12 Insular and Frontal Opercular Cortex) has an orderly somatotopic representation revealed in the MOTOR task contrasts (T-AVG, ?H-AVG, and ?F-AVG, Panels H, I, J, K, L) that involves contralateral activation for the foot and hand and bilateral activation for the tongue. Relative to its posterior neighbor retroinsular area RI, area **OP2-3** has less myelin (Panel B), is locally thicker (Panel C), differs in functional connectivity (Panel D), and is more deactivated in the working memory 2BK-0BK and LANGUAGE STORY contrasts (Panel F). Relative to its lateral neighbor OP1, area **OP2-3** has slightly less myelin (Panel B), differs in functional connectivity (Panel D), is more deactivated in the working memory 2BK-0BK task contrast, less activated in the ?H-AVG hand motor contrasts (Panels K and L), and more deactivated in the LANGUAGE MATH contrast (Panel E). Area OP2-3 is so named because it overlaps extensively with the locations of areas OP2 and OP3 (Eickhoff et al., 2006a; Eickhoff et al., 2006b), which we were unable to clearly distinguish in our data. Cortex activated by vestibular stimulation (sometimes called parieto-insular vestibular cortex, or PIVC) appears to include OP2 (Eickhoff et al., 2006c).

Area **OP1** has more myelin than all of its neighbors except area RI (Panel B), and likely corresponds to area SII (Burton et al., 2008; Eickhoff et al., 2006a; Eickhoff et al., 2006b). Relative to its medial neighbor RI, area **OP1** has less myelin (Panel B), is thicker (Panel C), differs in functional connectivity (Panel D), and is much more activated in the contralateral ?H-AVG hand motor contrasts (Panels K and L). Relative to its posterior neighbor PFcm, area **OP1** differs in functional connectivity (Panel D) and is much more activated in the contralateral ?H-AVG hand motor contrasts (Panels K and L). Our OP1 matches the location of OP1 previously reported (Eickhoff et al., 2006a; Eickhoff et al., 2006b) and is consistent with our previous report of it having more myelin (Glasser and Van Essen, 2011).

Relative to its superior neighbors PFop and PF and its posterior neighbor PSL, area **PFcm** has more myelin (Panel B) and differs in functional connectivity (Panel D). Relative to PFop and PF, area **PFcm** is less activated in the BODY-AVG contrast (in the left hemisphere for PFop and in both hemispheres for PF) and less deactivated in the LANGUAGE STORY contrast (Panel F). Relative to its lateral neighbor PSL, area **PFcm** is more activated in the contralateral ?F-AVG foot motor contrasts, (Panel H and I) and is deactivated vs activated in the STORY contrast (left hemisphere only, Panel F) and in the MATH contrast (Panel E). Relative to its inferior neighbor RI, area **PFcm** has less myelin (Panel B), differs in functional connectivity (Panel D), is more deactivated in the working memory 2BK-0BK contrast, and is more activated the MOTOR CUE contrast and in the ?F-AVG foot motor contrasts (Panels H and I). We previously identified **PFcm** as being more heavily myelinated (Glasser and Van Essen, 2011), having compared its location (Caspers et al., 2008; Caspers et al., 2006) with myelin maps.

10. Early Auditory Cortex

We now discuss auditory cortex, the last of the three large sensory domains in human neocortex. We divide the auditory cortex into the heavily myelinated early auditory

cortex and the more moderately myelinated auditory association cortex (Section #11). The early auditory areas include A1, LBelt (Lateral Belt), MBelt (Medial Belt), PBelt (Para-Belt), and the retro-insular cortex (RI). These areas are surrounded by areas, OP2-3, OP1, PFcm, PSL, A4, Ig, and TA2. The multi-modal information used to parcellate the auditory cortex is shown on flattened surfaces in Figure 12, with the areas identified shown in Panel A on a folding map.

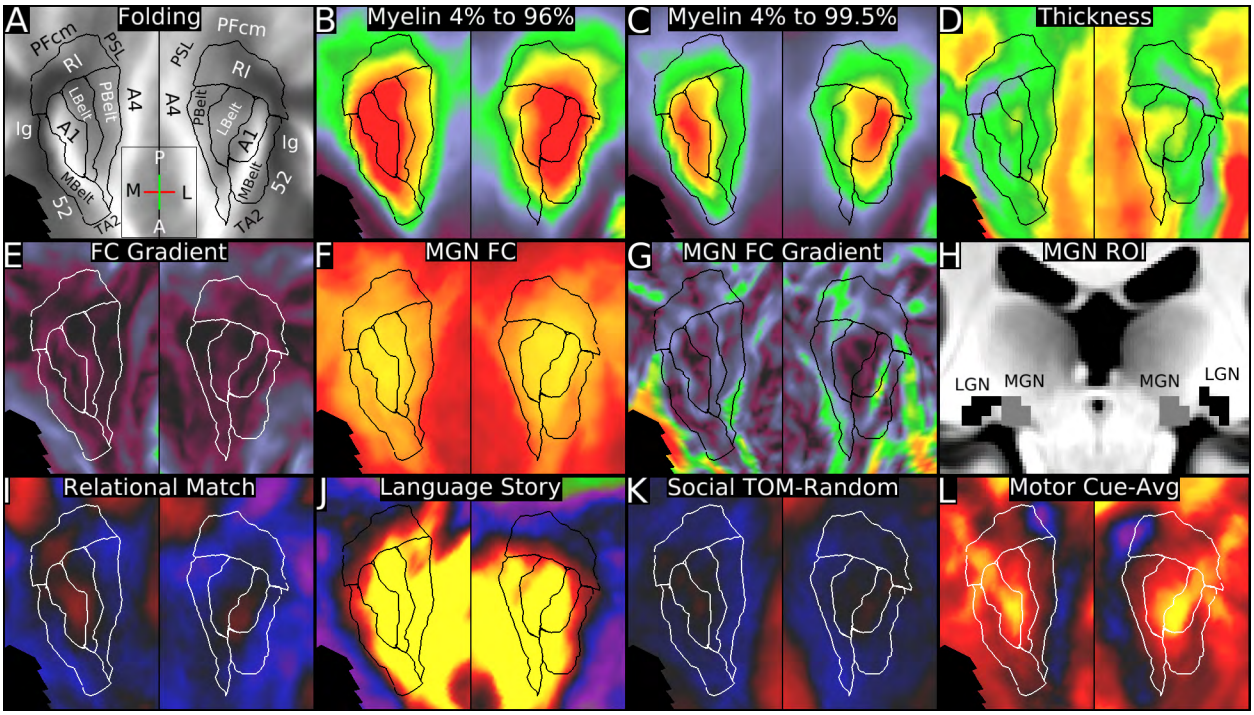

Figure 12 shows the multi-modal information used to parcellate the early auditory areas on flattened surfaces. The direction icon in Panel A shows Anterior (A), Posterior (P), Medial (M), and Lateral (L) directions (approximate orientation in 3D space) for the left surface (the M/L axis is reversed for the right surface). Panel A shows the early auditory areas on a folding map. Panels B and C show myelin maps with different scaling, 4% to 96% and 4% to 99.5% to highlight differences in myelin content of the very heavily myelinated auditory cortex. Panel D shows cortical thickness and Panel E shows functional connectivity gradients. Panel F shows the connectivity map from the MGN seed (Panel H) scaled from 2% to 99.5% to highlight differences in functional connectivity in the early auditory cortex, and Panel G shows the gradient of this map. Panels I, J, K, and L show the RELATIONAL MATCH, LANGUAGE STORY, SOCIAL TOM-RANDOM, and MOTOR CUE-AVG task contrasts. Data at http://balsa.wustl.edu/RV3p.

In contrast to early visual and somatomotor cortex, parcellation of the early auditory cortex has proven much more challenging in both macaques and humans (Baumann et al., 2013; Hackett et al., 2001; Kaas and Hackett, 2000; Moerel et al., 2014). In macaques there is evidence for a core auditory strip containing a primary area A1 plus one or two additional tonotopic areas. These areas are surrounded by medial and lateral belt complexes, each containing multiple tonotopic areas, plus a lateral parabelt complex that also contains multiple subdivisions (Hackett, 2007). Human architectonic and fMRI studies provide evidence for a similar overall arrangement, but a consensus is lacking on the number and precise locations of these areas (Baumann et al., 2013; Moerel et al., 2014). In our parcellation, we identify a very heavily myelinated core on medial and posterior

aspects of Heschl's gyrus (Panels A and C), which we consider likely to be primary auditory cortex, or A1. We identified three complexes surrounding our A1. Two are heavily myelinated (Panels B and C), (as are human and macaque belt areas – (Hackett et al., 2001). We identify them as MBelt (medial belt), LBelt (lateral belt) because they are similar but not identical to previous parcellations and hence warrant modified names (Moerel et al., 2014). The retro-insular area, RI, adjoining A1 postero-superiorly, is moderately-to-heavily myelinated (Panel B), corresponds to the retroinsular region identified by (Kurth et al., 2010; Pandya and Sanides, 1973), which we previously noted was heavily myelinated (Glasser and Van Essen, 2011), and overlaps with the postero-superior portion of the belt as delineated by (Moerel et al., 2014). We also identify PBelt as a lateral parabelt complex and area 52 medial to our MBelt complex. (Architectonic area 52 has been suggested to correspond to the medial belt (Moerel et al., 2014), but we consider this unlikely based on its location and degree of myelination, as discussed below.) Our arrangement of areas is also similar to that of Von Economo and Koskinas, with their TC corresponding to our A1, their TB corresponding to our MBelt and LBelt, their TA1 corresponding to our PBelt, and their TD corresponding to our RI (Triarhou, 2007a, b; von Economo and Koskinas, 1925). All of these areas are likely complexes of smaller fields (Moerel et al., 2014) that were not readily discernible in our data.

A1 (or the auditory core) is bordered by areas MBelt antero-medially, LBelt posteriorly, and RI supero-postero-medially. **A1** is very heavily myelinated, even relative to its heavily myelinated surrounding neighbors, as shown in Panel B (using our standard palette scale that saturates at a maximum of 96%) and in Panel C (using a saturation level of 99.5% to reveal the heavier myelination of A1 relative to its neighbors). **A1** is also moderate in thickness (Panel D), in contrast to the much thinner primary visual (area V1) and somatosensory (area 3b) cortex illustrated in previous sections (#1 Primary Visual Cortex (V1) and #6 Somatosensory and Motor Cortex). Using a different dataset acquired at 1mm isotropic resolution, we previously reported that A1 appeared notably thinner than its neighbors and speculated that this might reflect a bias in which FreeSurfer's segmentation of the gray/white boundary extended into deep cortical layers in heavily myelinated regions (Glasser and Van Essen, 2011). This speculation is confirmed insofar as the higher resolution (0.7mm) T1w and T2w images plus additional processing pipeline improvements for the HCP data (Glasser et al., 2013) indicate that A1 is indeed as thick as its neighbors (Panel D). The region of heaviest myelination is situated on the medial half of Heschl's gyrus, mostly on the posterior bank but extending over the crown of the gyrus. This overlaps with both areas TE1.0 and TE1.1 of (Morosan et al., 2001) (their Fig. 11, also see (Glasser and Van Essen, 2011)). Additionally, many primary task contrasts show modest differences in activation in **A1** relative to its neighbors (e.g., the RELATIONAL MATCH contrast, Panel I). Specifically, relative to its postero-lateral neighbor LBelt, **A1** has more myelin (Panel C), differs in functional connectivity (Panel E) and is more activated in the RELATIONAL MATCH contrast (Panel I). Relative to its antero-medial neighbor MBelt, area **A1** has more myelin (Panel C), differs in functional connectivity with a Medial Geniculate Nucleus (MGN) thalamic seed ROI (Panels F, G, and H), and is more activated in the RELATIONAL MATCH contrast (Panel I). Relative to its posterior neighbor RI, area **A1** has more myelin (Panels B and C), differs in functional connectivity both overall (Panel E) and when seeded from the MGN (Panels F, G), and is more activated in the LANGUAGE MATH and STORY contrasts (Panel J).

Relative to its antero-medial neighbor area 52, the **MBelt** complex has more myelin (Panel B), is thicker (Panel D), and is activated vs deactivated in the LANGUAGE MATH and STORY contrasts (Panel J). Relative to its antero-lateral neighbor area TA2, **MBelt** has more myelin (Panel B), is thinner (Panel D), and is more activated in the LANGUAGE MATH and STORY contrasts (Panel J). Relative to its lateral neighbor PBelt, the **MBelt** complex has more myelin (Panel C) and is less activated in the language MATH and STORY contrasts (Panel J) and more activated in the EMOTION FACES-SHAPES contrast. The antero-lateral portion of the MBelt complex likely overlaps with area TE1.0 of (Morosan et al., 2001) (Glasser and Van Essen, 2011). Relative to its lateral neighbor PBelt, the **LBelt** complex has more myelin (Panel C), has stronger functional connectivity with the MGN nucleus (Panels F and G), and is modestly activated vs deactivated in the TOM-RANDOM contrast (Panel K). Relative to its postero-superior neighbor RI, the **LBelt** complex has more myelin (Panel C), has stronger functional connectivity with the MGN (Panels F and G), and is more activated by the MATH and STORY contrasts (Panel J). Relative to its lateral neighbor A4, the **PBelt** complex has more myelin (Panel B and C), is thinner (Panel D), has greater functional connectivity with the MGN (Panels F and G), and is more activated in the CUE-AVG contrast (Panel L). Relative to its supero-medio-posterior (up on the map) neighbor RI, the **PBelt** complex has more myelin (Panels B and C; the myelin gradient is strong where **PBelt** and RI adjoin), and greater functional connectivity with the MGN (Panels F and G). Finally, relative to area PSL postero-laterally, area **RI** has more myelin (Panels B and C), is thinner (Panel D, more prominently in the right hemisphere), differs in functional connectivity (Panel E), is deactivated vs activated in primary contrasts (e.g. the GAMBLING primary contrasts), and is less activated in the MATH-STORY contrast. The anterior (OP2-3) and superior (OP1 and PFcm) borders of **RI** were covered in the Section #9 Posterior Opercular Cortex, and the inferior borders were covered above.

11. Auditory Association Cortex

We identified auditory association cortex as a region mainly on the superior temporal gyrus and within the superior temporal sulcus that is activated in the LANGUAGE STORY, MATH, and STORY-MATH contrasts. It is strongly functionally connected with the inferior frontal gyrus, including areas 44, 45, and 47l. This auditory region likely becomes progressively less purely auditory and more multi-modal as one progresses inferiorly, anteriorly, and posteriorly (away from early auditory cortex, e.g. Main Text Figure 3). Indeed, functional connectivity with early auditory cortex progressively decreases along those directions. This region includes eight areas that we identify as A4, A5, STSdp, STSda, STSvp, STSva, STGa, and TA2. Because our parcellation is finer grained than most previously attempted parcellations of the superior temporal gyrus and sulcus, we have introduced largely novel terminology here, except that TA2 is based on the Von Economo and Koskinas parcellation (Triarhou, 2007a, b; von Economo and Koskinas, 1925). These areas are surrounded by PBelt, MBelt, PI, TGd, TE1a, TE1m, TE1p, PHT, TPOJ1, STV, and PSL. Figure 13 shows multi-modal information used to parcellate this region's cortex into the areas displayed on a folding map in Panel A.

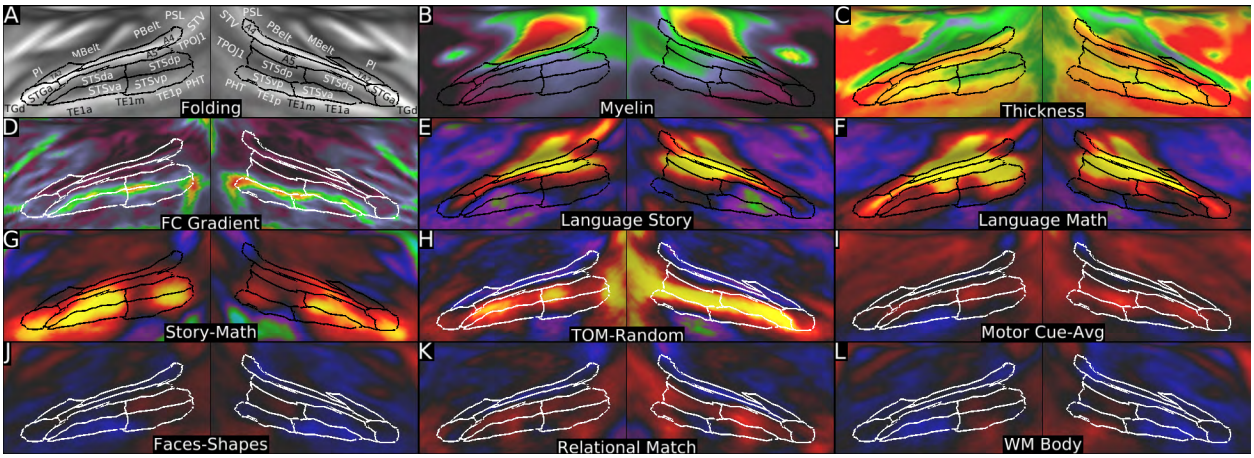

Figure 13 shows multi-modal information used to parcellate the auditory association cortex. Panel A shows the cortical areas overlaid on a folding map. Panels B and C show myelin and cortical thickness maps. Panel D shows the resting state functional connectivity gradient. Panels E, F, and G show the LANGUAGE STORY, MATH, and STORY-MATH contrasts. Panels H, I, and J show the TOM-RANDOM, MOTOR CUE-AVG, and FACES-SHAPES contrasts. Panels K and L show the RELATIONAL MATCH and WM BODY primary task contrasts. Data at http://balsa.wustl.edu/W3v5.

A4's supero-medial border with PBelt was covered in Section #10 Early Auditory Cortex. Relative to its inferior neighbor A5, area **A4** differs in functional connectivity, and this gradient was primarily used to define the boundary (Panel D). **A4** also has more myelin than **A5** assessed statistically (Panel B), though the myelin gradient peak does not align with the functional connectivity gradient peak. Relative to its antero-medial neighbor TA2, area **A4** has more myelin (Panel B), differs in functional connectivity (Panel D), is more activated in the LANGUAGE MATH and STORY contrasts (Panels E and F), and is less activated in the CUE-AVG contrast (Panel I). Based on its position on the crown of the superior temporal gyrus, area **A4** may correspond to cytoarchitectonic area Te3 (Morosan et al., 2005). The borders of A4, A5, and STSdp with areas PSL, STV, and TPOJ1 posteriorly will be covered in Section #15 Temporal-Parietal-Occipital Junction. Relative to its antero-medial neighbor TA2, area **A5** differs in functional connectivity (Panel D), and is more activated in the LANGAUGE STORY-MATH (Panel G) and TOM-RANDOM (Panel H) contrasts. Relative to its inferior neighbor STSdp, area **A5** differs in many primary and non-primary task contrasts including more activation in the LANGAUGE MATH (Panel E) and STORY (Panel F) contrasts and less activation in the working memory (e.g Panel L) and RELATIONAL (e.g. Panel J) primary contrasts, and the FACE-AVG, TOM-RANDOM (Panel H), and FACES-SHAPES (Panel K) contrasts. Relative to its inferior neighbor STSda, area **A5** again shows differences in a variety of task contrasts including markedly more activation in the LANGAUGE MATH contrast (Panel E), more activation in the TOOL-AVG contrast, markedly less activation in the TOM-RANDOM contrast (Panel H), and less activation in the CUE-AVG (Panel I) and FACES-SHAPES (Panel K) contrasts. Relative to its anterior neighbor STGa, area **A5** has more myelin (Panel B) and differs in functional connectivity (Panel D).

Relative to area STSvp on the inferior bank of the STS, area **STSdp** on the superior banks is has more myelin (Panel B), differs markedly in functional connectivity (Panel D), is more activated in the LANGUAGE MATH (Panel E), TOM-RANDOM (Panel H, especially in the right hemisphere), and MOTOR CUE-AVG (Panel I) contrasts. Relative to its anterior

neighbor STSda in the superior bank of the STS, area **STSdp** has more myelin (Panel B), and differs markedly in its functional activation profile, being more activated in the CUE-AVG contrast (Panel I) and the RELATIONAL MATCH (Panel J), working memory (e.g. Panel L), SOCIAL TOM and other primary contrasts, and less active in the STORY-MATH contrast (Panel G). Relative to its inferior neighbor STSva on the inferior bank of the STS, area **STSda** differs greatly in functional connectivity (Panel D) and is more activated in the in the MOTOR CUE-AVG contrast (Panel I) and less deactivated in the GAMBLING primary contrasts (more on the left than on the right). Relative to its anterior neighbor STGa, area **STSda** is has more myelin, is thinner, is less activated in the LANGUAGE MATH and STORY contrasts, and is more activated in the TOM-RANDOM contrast.

Relative to PHT anteriorly, area **STSvp** differs strongly in functional connectivity and is activated instead of deactivated in the LANGUAGE STORY contrast and the STORY-MATH contrast. Relative to its postero-inferior neighbor TE1p on the inferior temporal gyrus (MTG), area **STSvp** differs in functional connectivity (Panel D), is more activated in the STORY (Panel F) and STORY-MATH contrasts (Panel G), and is less activated in the FACES-SHAPES contrast (Panel K). Relative to its inferior neighbor TE1m, further anterior on the MTG, area **STSvp** differs in functional connectivity (Panel D) and is activated vs deactivated in the STORY (Panel F), STORY-MATH (Panel G), and TOM-RANDOM (Panel H) contrasts. Relative to its anterior neighbor STSva, area **STSvp** has more myelin (Panel B), differs in functional connectivity (Panel D), is more activated in working memory (e.g Panel L), GAMBLING, EMOTION, and other primary task contrasts, and differs in the STORY-MATH contrast (Panel G, especially in the right hemisphere). Relative to its infero-lateral neighbor area TE1a on the anterior MTG, area **STSva** has more myelin (Panel B), is thinner (Panel C), is more activated in the STORY-MATH contrast (Panel G), and differs in some primary contrasts including more deactivation in the RELATIONAL (Panel K), working memory (e.g. Panel L), GAMBLING, and EMOTION contrasts.

The final two auditory association areas, **TA2** and **STGa,** lie on the planum polare and STG anterior to Heschl's gyrus. **TA2**'s medial border with MBelt was covered in Section #10 Early Auditory Cortex and its borders with A4 and A5 were covered above. Relative to its antero-medial neighbor area PI, area **TA2** has more myelin (Panel B), is thicker (Panel C), and is activated vs deactivated in the LANGAUGE MATH (Panel E) and STORY (Panel F) contrasts. Relative to its lateral neighbor STGa, area **TA2** has more myelin (Panel B), differs in functional connectivity (Panel D), and is less activated in the STORY-MATH task contrast (Panel G) and deactivated vs activated in the TOM-RANDOM contrast (Panel H). Relative to its medio-inferior neighbor PI, area **STGa** is substantially thicker (Panel C) and is more activated in the LANGAUGE STORY-MATH (Panel G) and TOM-RANDOM task contrasts (Panel H). Relative to its anterior neighbor TGd (including the temporal pole), area **STGa** differs in functional connectivity (Panel D) and is more activated in the STORY (Panel F) and CUE-AVG (Panel I) contrasts. Area TA2 may overlap with TE1.2 from (Morosan et al., 2001).

12. Insular and Frontal Opercular Cortex

This section covers the insular and frontal opercular cortex. Previous architectonic studies have subdivided the insula into a superior and posterior granular region, an

anterior, inferior agranular region, and a dysgranular region lying in between (Kurth et al., 2010; Morel et al., 2013). We identified 13 areas in the insula and frontal operculum, including areas 52, PI (ParaInsular cortex), Ig (Insula granular), Posterior Insular areas PoI1 and PoI2, Frontal Opercular areas FOP2 and FOP3, a Middle Insular area MI, an Anterior Ventral Insular area AVI, an Anterior Agranular Insular Complex AAIC, the Piriform cortex Pir, and Frontal Opercular areas FOP4 and FOP5. These areas are surrounded by areas TGd, STGa, TA2, MBelt, OP2-3, 43, FOP1, 6r, 44, 45, 47l, 47s, and pOFC. Figure 14 shows multi-modal information used to define the cortical areas in the insular and frontal opercular cortex (areas on a folding map, Panel A).

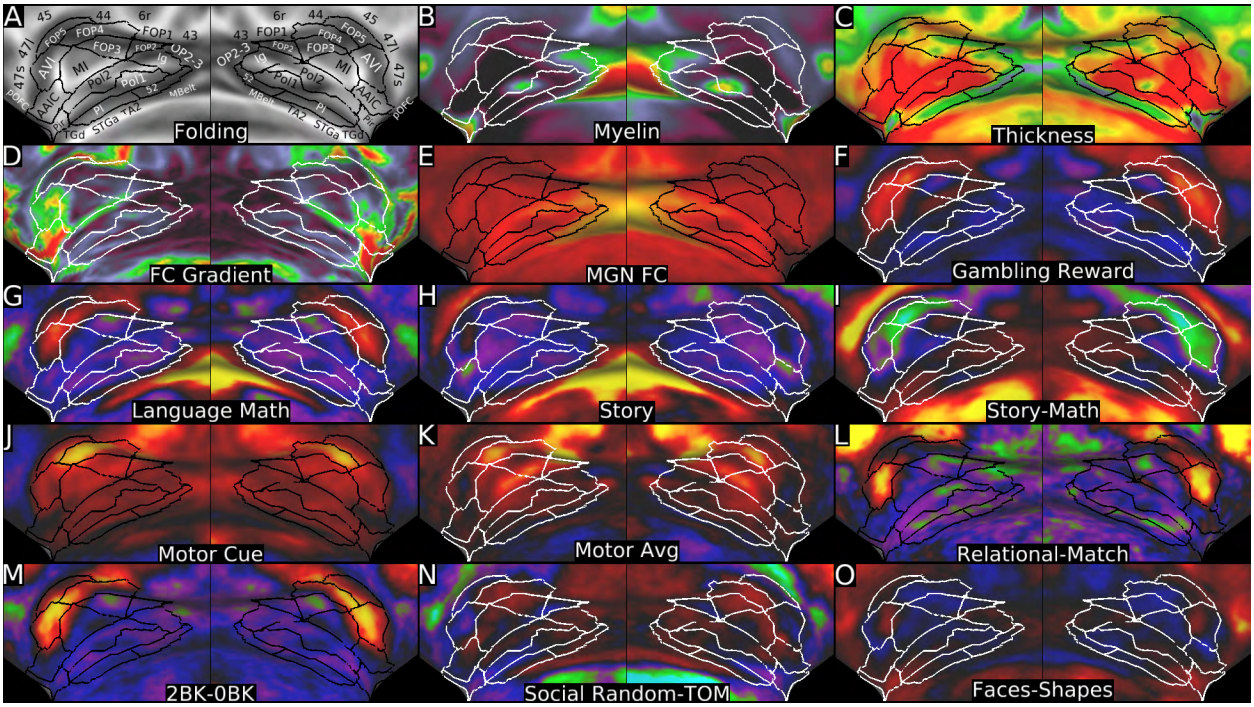

Figure 14 shows multi-modal information used to define cortical areas in the insula and frontal operculum. Panel A shows the areas on a folding map. Panels B and C show myelin and cortical thickness maps. Panels D and E show the resting state functional connectivity gradient and the map of functional connectivity with the MGN. Panel F shows an example primary task contrast (GAMBLING Reward). Panels G, H, and I show the LANGUAGE MATH, STORY, and STORY-MATH contrasts. Panels J, K, and L show the MOTOR CUE, MOTOR AVG, and RELATIONAL-MATCH contrasts. Panels M, N, and O show the working memory 2BK-0BK, SOCIAL RANDOM-TOM, and EMOTION FACES-SHAPES contrasts. Data at http://balsa.wustl.edu/Wznm.

Area **52** is a transitional region lying between an early auditory sensory area (MBelt) and a very different type of cortex (insular area PoI1, and granular insular area Ig). In this respect it is analogous to the Dorsal Visual Transitional area DVT described below (Section #18 Posterior Cingulate Cortex), which is transitional between early visual areas and very different cortex. Area **52** shares some properties with MBelt, including functional connectivity with the MGN (Panel E) and being relatively thin (Panel C), but it has important differences, including having much less myelin (Panel B) and net deactivation in the LANGUAGE STORY and MATH task contrasts (Panels G and H), features that it shares with its more anterior insular neighbors. Thus, it seems reasonable to consider area **52** as a transitional auditory area. We identify it as area **52** based on its similarity in location to

Brodmann's area **52** (Brodmann, 1909; Brodmann, 2007) (Figure 89) within the inferior portion of the circular sulcus, between early auditory cortex (his area 41) and the posterior insula. It appears to also correspond to the posterior portion of area IBT in von Economo and Koskinas's parcellation, as there is room for an MBelt-like set of areas between their auditory core and area IBT (Triarhou, 2007a, b; von Economo and Koskinas, 1925). The posterior granular insular cortex identified by (Morel et al., 2013) may include area **52**. The posterior border of area **52** with MBelt was described already (Section #10 Early Auditory Cortex). Relative to its anterior neighbor Ig, area **52** is thinner (Panel C), has stronger functional connectivity with the MGN (Panel E), and is more activated in the BODY-AVG task contrast and less deactivated in the LANGUAGE MATH and STORY contrasts (Panels G and H). Similarly, relative to area PoI1, area **52** is substantially thinner (Panel C) and has stronger functional connectivity with the MGN (Panel E). Area **52** is also statistically more activated than Pol1 in the LANGUAGE MATH contrast (Panel G). Relative to area PI (the anterior extension of Von Economo and Koskinas area IBT (Triarhou, 2007a, b; von Economo and Koskinas, 1925), area **52** has many similarities, but has more myelin (Panel B), is thinner (Panel C), and has stronger functional connectivity with the MGN (Panel E). Area **PI's** posterior borders with area TA2 and area STGa were previously covered (Section #11 Auditory Association Cortex). Relative to its antero-inferior neighbor TGd, area **PI** is thinner (Panel C), differs in functional connectivity (Panel D), is more activated in the LANGUAGE MATH contrast (Panel G) and less activated (or deactivated) in the STORY-MATH (Panel I), and the RANDOM-TOM contrasts. Relative to area PoI1 medially, area **PI** is substantially thinner (Panel C) and is less deactivated in the working memory 2BK-0BK contrast (Panel M). **PI** is also statistically less deactivated than Pol1 in the LANGUAGE MATH (Panel G) contrast. Area PI corresponds approximately to area PI in (Ding et al., 2009) lying in the inferior circular sulcus.

We identified area **Ig** as a region that appears to overlap extensively with area **Ig** of (Morel et al., 2013) and with areas Ig1 and Ig2 of (Kurth et al., 2010). As defined, **Ig** has some internal heterogeneity, but insufficient for us to unambiguously make a finer parcellation based on our data. The superior and posterior borders of **Ig** were already described (Section #9 Posterior Opercular Cortex, and above). As noted previously, area **Ig** contains a somatotopic representation of the body (see Figure 11). Relative to antero-inferior neighbors PoI1 and PoI2, area **Ig** has more myelin (Panel B), is thinner (Panel C), and is more activated in the FACES-SHAPES contrast (Panel O). Relative to its supero-medial neighbor FOP2, **Ig** has more myelin (Panel B), differs in functional connectivity (Panel D), and in a large number of task contrasts, including less activation in many primary contrasts (e.g. Panel F) and the MOTOR AVG contrast (Panel K) and more activation in the RANDOM-TOM (Panel N) and FACES-SHAPES (Panel O) contrasts.

We identified two areas, **PoI1** and **PoI2** overlapping the posterior portion of dysgranular areas Id1, Id2, and Id3 by (Morel et al., 2013) and (Kurth et al., 2010), and possibly the posterior portion of the agranular cortex. Unfortunately, parcellation of this region is confounded by a relatively consistent surface reconstruction artifact caused by the FreeSurfer white matter surface and the putamen subcortical segmentation encroaching into the claustrum, leading to artifactual peaks in the myelin maps (Panel B). In addition, because of the very deep white matter surface placement and overlap between the white matter surface and putamen segmentation, the reconstructed pial surface does not extend all the way out to the real pial surface, leading to an artifactual dip in estimated

cortical thickness, more prominent in the right hemisphere (Panel C). The parcellation of this region should be revisited when this artifact is removed in a future FreeSurfer version. Aside from these focal artifacts, both **PoI1** and **PoI2** are very thick (Panel C) and very lightly myelinated (Panel B). Relative to its supero-medial neighbor PoI2, area **PoI1** differs in functional connectivity (Panel D) and is deactivated or weakly activated vs strong activation of **PoI2** in the T-AVG tongue MOTOR contrast. Relative to their anterior-inferior neighbor Pir, areas **PoI1** and **PoI2** have much less myelin (Panel B) and are thicker (Panel C). Relative to anterior neighbor AAIC, area **PoI2** differs in functional connectivity (Panel D), is more deactivated in the working memory 2BK-0BK (Panel M) and RELATIONAL-MATCH (Panel L) contrasts and more activated in the MOTOR CUE contrast (Panel J). Relative to its superior neighbor MI (the middle insular area), area **PoI2** differs in functional connectivity, is deactivated vs activated in the GAMBLING primary contrast (Panel F) and activated vs deactivated the STORY-MATH contrast (Panel I). For area **FOP2**, its borders superiorly (FOP1 and 43) and posteriorly (OP2-3) were covered previously (Section #9 Posterior Opercular Cortex), and its inferior border with Ig was covered above. Relative to its anterior neighbors FOP3 and FOP4, **FOP2** has more myelin, but less than posteriorly adjoining granular cortex Ig (Panel B). Relative to FOP3, **FOP2** also differs in functional connectivity (Panel D) and is less deactivated in the LANGUAGE MATH and STORY contrasts (Panels G and H).

Along the antero-inferior margin of the insula, at the juncture of the frontal and temporal lobes (limen insula), the cortex is substantially more heavily myelinated and thinner (Panels B and C) than nearby AAIC antero-superiorly and TGd antero-inferiorly, and previously discussed borders with PoI1 and PoI2. This area likely corresponds to the piriform olfactory cortex (**Pir**) (Ding et al., 2009; Morel et al., 2013), as we noted previously (Glasser and Van Essen, 2011). Relative to its neighbors, area **Pir** shows apparent differences in functional connectivity and in a number of task contrasts. However, we do not consider these differences to be convincing because strong vascular artifacts were commonly identified in this region in the resting state data (i.e., as structured noise components in FIX+ICA denoising), and there is relatively little signal in the Pir in the denoised resting state connectivity data. The task data are thus suspect because they were not processed using ICA+FIX denoising. Medially, area Pir adjoins non-cortical gray matter that is outside of the grayordinates space (Glasser et al., 2013).

We identified two areas in the anterior insula, the anterior agranular insular complex (**AAIC**) and the Middle Insular area (**MI**). AAIC is called a complex because it includes inferior portions of the architectonic subdivisions Iai and Ial of (Ongur et al., 2003) and because it has considerable functional heterogeneity in our data that could potentially reveal subdivisions using higher resolution data. The agranular insula is among the most lightly myelinated and thickest cortical regions (Panels B and C; see also (Glasser and Van Essen, 2011). Relative to its neighbors 47s antero-laterally and AVI superiorly, area **AAIC** has less myelin (Panel B) and is thicker (Panel C). Additionally, area AAIC differs from area 47s in functional connectivity and being slightly activated vs deactivated in the MOTOR CUE-AVG contrast and less activated in the STORY-MATH (Panel I) and SOCIAL TOM contrasts. Area AAIC differs from AVI in being deactivated vs activated in many primary task fMRI contrasts (e.g. Panel F), the LANGUAGE MATH contrast (Panel G), the RELATIONAL-MATCH contrast (Panel L), and the working memory 2BK-0BK contrast (Panel M). Relative to superior neighbor MI, area **AAIC** differs in functional connectivity

(Panel D), is less activated in the MOTOR CUE (Panel J) and MOTOR AVG (Panel K) contrasts, and is deactivated vs activated in the EMOTION SHAPES contrast. Relative to anterior neighbor AVI, area **MI** has less myelin (Panel B), differs in functional connectivity (Panel D), is deactivated vs activated in the LANGUAGE MATH and STORY primary contrasts (Panels G and H) and in the RELATIONAL REL-MATCH (Panel L) and working memory 2BK-0BK (panel M) contrasts, and is more activated in the MOTOR AVG (Panel K) and RANDOM-TOM (Panel N) contrasts. Relative to superior neighbor FOP3, area **MI** has less myelin (Panel B), is thinner (Panel C), is less deactivated in the LANGUAGE MATH contrast (Panel G), deactivated vs activated in the LANGUAGE STORY-MATH contrast (Panel I), and less activated in the RANDOM-TOM contrast (Panel N). Architectonically, **MI** is likely a dysgranular area (Morel et al., 2013). The anterior portion of **MI** overlaps with superior portions of the architectonic subdivision Ial of (Ongur et al., 2003).

Cortex superior to the anterior insula includes areas **FOP3** (along the superior peri-insular sulcus) and **FOP4**. **FOP3** and **FOP4** are more lightly myelinated than their anterior, superior, and posterior neighbors (Panel B). The borders of **FOP3** with MI inferiorly and FOP2 posteriorly have already been described. Relative to its supero-lateral neighbor FOP4, area **FOP3** is thinner (Panel C), differs modestly in functional connectivity (Panel D), is deactivated vs activated in the primary task contrasts (e.g. Panel F) and the working memory 2BK-0BK (Panel M), MOTOR CUE (Panel J), and LANGUAGE MATH (Panel G) contrasts, is activated vs deactivated in the LANGUAGE STORY-MATH contrast (Panel I), and is more deactivated in the RELATIONAL-MATCH contrast. **FOP4's** posterior (FOP1) and superior (6r) borders have previously been described (Sections #8 Premotor Cortex and #9 Posterior Opercular Cortex). Relative to supero-lateral neighbor area 44, area **FOP4** has less myelin (Panel B), differs strongly in functional connectivity (Panel D), is more activated in the MOTOR CUE (Panel J) and MOTOR AVG contrasts (Panel K), and is deactivated vs activated in the RELATIONAL-MATCH contrast (Panel L). Relative to anterior neighbor FOP5, area **FOP4** has less myelin (Panel B), is more activated in the MOTOR AVG contrast (Panel K), is activated vs deactivated in the RANDOM-TOM contrast (Panel N), and is deactivated vs activated in the FACES-SHAPES contrast (Panel O). Relative to supero-anterior neighbor area AVI, area **FOP4** is more heavily myelinated, differs in functional connectivity, is more activated in the MOTOR CUE (Panel J) and MOTOR AVG (Panel K) contrasts, is activated vs deactivated in the RANDOM-TOM contrast (Panel N), and is less activated in the RELATIONAL-MATCH contrast (Panel L).

Areas **FOP5** and **AVI** are the most anterior pair of areas in this region. Relative to its postero-superior neighbor area 44, area **FOP5** differs in functional connectivity (Panel D, especially in the left hemisphere) and is more activated in the MOTOR CUE contrast (Panel J) and less activated in the RELATIONAL-MATCH contrast (in the left hemisphere, Panel K). Relative to its neighbors area 45 supero-laterally and area 47l antero-laterally, area **FOP5** differs in functional connectivity (Panel D) and is more activated in many primary task contrasts (e.g. Panel F), the MOTOR CUE-AVG contrast (greater difference in left than right), and is deactivated vs activated in the LANGUAGE STORY (Panel H) and the STORY-MATH (Panel I) contrasts. Relative to its inferior neighbor AVI, area **FOP5** differs in functional connectivity (Panel D), is less activated in the working memory 2BK-0BK contrast (Panel M), more activated in the MOTOR AVG contrast (Panel K), and less activated in the RELATIONAL-MATCH contrast (Panel L). Relative to its anterior neighbor 47l, area **AVI** differs in functional connectivity, and is more activated in many primary task contrasts (e.g.

Panel F), the working memory 2BK-0BK contrast (Panel M), and the MOTOR CUE-AVG contrast, and is deactivated vs activated in the LANGUAGE STORY (Panel H) and STORY-MATH (Panel I) contrasts. Finally, relative to its infero-lateral neighbor 47s, area **AVI** differs in functional connectivity (Panel D), is more activated in many primary task contrasts (Panel F), the MOTOR CUE-AVG contrast (greater difference in left than right), the LANGUAGE MATH contrast (Panel G), and the RELATIONAL-MATCH contrast (Panel L), and is deactivated vs activated in the STORY-MATH contrast (Panel I). Area FOP5 likely overlaps considerably with a locally more heavily myelinated region that we previously identified as area PrCO (Glasser and Van Essen, 2011). AVI overlaps with superior portions of the architectonic subdivision Iai of (Ongur et al., 2003).

13. Medial Temporal Cortex

The inferior medial temporal region contains a set of seven elongated areas, including the hippocampus (H), presubiculum (PreS), entorhinal cortex (EC), the peri-entorhinal and ectorhinal complex (PeEc), and peri-hippocampal areas 1, 2 and 3 (PHA1, PHA2, and PHA3). These areas are surrounded by the retrosplenial cortex (RSC), the prostriate cortex (ProS), V2, the ventromedial visual areas (VMV1-3), the ventral visual complex (VVC), and areas TF, TGv, and TGd. We include the hippocampus because the cortical grayordinates space includes a portion of the hippocampus (the full hippocampus is also segmented by FreeSurfer and is represented as a volume in the subcortical portion of the grayordinates space (Glasser et al., 2013)). Figure 15 shows multi-modal information that was used to parcellate the medial temporal cortex (on a folding map in Panel A).

The hippocampal complex (**H**), including the subiculum, includes the inferior bank of the hippocampal fissure extending laterally to its fundus, where it adjoins the non-cortical medial wall ROI of the grayordinates space. Relative to the presubiculum (**PreS**) medially, the hippocampal complex (**H**) has much less myelin (Panel B) and appears to be thicker in places (Panel C), though the latter likely reflects imperfect FreeSurfer segmentation of hippocampal subfields. The **PreS** contains the perforant path (Augustinack et al., 2010; Glasser and Van Essen, 2011) and is thus much more heavily myelinated than all of its neighbors except the retrosplenial cortex, RSC (Panel B). **PreS** is also thinner than V2 and the Prostriate area (ProS) posteriorly (Panel C). Relative to its supero-posterior neighbor retrosplenial cortex (RSC), **PreS** is also thinner (Panel C) and differs in functional connectivity (Panel D). Relative to its antero-lateral neighbor entorhinal cortex (EC), area **PreS** has much more myelin (Panel B) and is somewhat thinner (Panel C). Relative to its inferior neighbor area PHA1, the **PreS** has much more myelin (Panel B), is thinner (Panel C), is less activated in the PLACE-AVG (Panel K), LANGUAGE STORY-MATH (Panel G), and SOCIAL TOM-RANDOM (Panel H) contrasts, and is more activated in the BODY-AVG contrast (Panel I). Relative to its infero-medial neighbor PeEc, the **EC** has more myelin (Panel B), is much thinner (Panel C), differs in functional connectivity (Panel D), is less activated in the primary task contrasts (e.g. Panel F) and in the TOM-RANDOM (Panel H) and FACES-SHAPES (Panel M) contrasts, and is activated vs deactivated in the working memory 2BK-0BK contrast (Panel E). Relative to area PHA1 posteriorly, the **EC** has more myelin (Panel B), is thinner (Panel C), and is less activated in

the LANGUAGE STORY-MATH (Panel G) and SOCIAL TOM-RANDOM (Panel H) contrasts. Our area EC overlaps extensively with probabilistic EC from (Fischl et al., 2009) (Panel O).

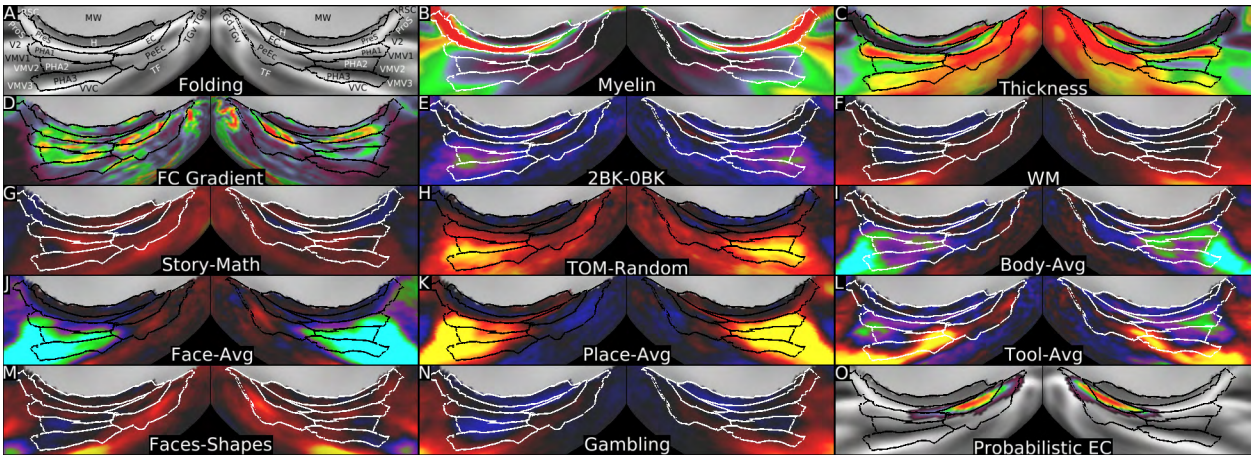

Figure 15 shows the multi-modal information used to parcellate the medial temporal cortex. Panel A shows the areas on a folding map. Panels B and C show the myelin and cortical thickness maps. Panel D shows the resting state functional connectivity gradient. Panels E and F show the working memory 2BK-0BK and an example working memory primary contrast. Panels G and H show the LANGAUGE STORY-MATH contrast and the SOCIAL TOM-RANDOM contrast. Panels I, J, K, and L show the categories contrasts, BODY-AVG, FACE-AVG, PLACE-AVG, and TOOL-AVG. Panels M and N show the EMOTION FACES-SHAPES contrast and the GAMBLING primary contrast. Panel O shows the probabilistic map of the entorhinal cortex (EC) from (Fischl et al., 2009). Data at http://balsa.wustl.edu/QXDP.

We were unable to reliably distinguish between the peri-entorhinal cortex (BA 35) and the ectorhinal cortex (BA 36), which together we identified as the **PeEc** complex, located outside of the entorhinal cortex (Augustinack et al., 2013; Ding et al., 2009). Relative to its anterior neighbor area TGd, **PeEc** is thicker (Panel C) and differs in functional connectivity (Panel D). Relative to its antero-inferior neighbor TGv, area **PeEc** has more myelin (Panel B) and is more activated in the working memory (Panel F) and relational primary task contrasts. Relative to its inferior neighbor TF, area **PeEc** has less myelin (Panel B), is thicker (Panel C), and has greater activation in the working memory primary contrasts (Panel F). Relative to its postero-inferior neighbor PHA3, area **PeEc** has less myelin (Panel B), is thicker (Panel C), is modestly less deactivated in the working memory 2BK-0BK contrast (Panel E), less deactivated in the BODY-AVG contrast (Panel I), activated vs deactivated in the FACE-AVG contrast (Panel J), deactivated vs activated in the PLACE-AVG contrast (Panel K), less activated in the TOM-RANDOM contrast (Panel H), and more activated in the FACES-SHAPES contrast (Panel M). Relative to its posterior neighbor PHA2, area **PeEc** is much thicker (Panel C) and differs in task activations similar to those just described for PHA3. Relative to its postero-medial neighbor PHA1, area **PeEc** is slightly thicker (Panel C) and is deactivated vs activated in the PLACES-AVG contrast (Panel K) and more activated in the GAMBLING primary contrasts (Panel N). The PeEc may be the site of the anterior temporal face patch (ATFP, AFP1) (Rajimehr et al., 2009; Tsao et al., 2008), given its activation in the FACE-AVG and FACES-SHAPES contrasts.

Relative to its medio-inferior neighbor PHA2, area **PHA1** is dramatically thicker (Panel C) and is less deactivated in the FACE-AVG contrast (Panel J). Relative to its inferior neighbor PHA3, area **PHA2** has less myelin (Panel B), is thinner (Panel C), and differs in

functional connectivity (Panel D). Relative to its antero-medial neighbor TF, area **PHA3** differs in functional connectivity (Panel D), is deactivated vs activated in the BODY-AVG (Panel I) and FACE-AVG (Panel J) contrasts, and is activated vs deactivated in the PLACE-AVG (Panel K) and TOOL-AVG (Panel L) contrasts. The borders of the PHA 1-3 areas with areas VMV1-3 and the VVC were covered in Section #4 Ventral Stream Visual Cortex.

14. Lateral Temporal Cortex

Lateral temporal cortex has expanded dramatically over the course of human evolution (Glasser et al., 2014; Hill et al., 2010). We identified nine areas in lateral temporal cortex and the temporal pole that are architecturally lightly myelinated, thick, and functionally multi-modal, and many are involved in the task negative network. The nine areas include PHT, TE1p, TE1m, TE1a, TE2p, TE2a, TGv, TGd, and TF. They are surrounded mainly by auditory and visual association areas, including STGa, STSda, STSva, STSvp, TPOJ1, TPOJ2, FST, PH, FFC, VVC, PHA3, PeEc, Pir, and PI. Figure 16 shows multi-modal information used to parcellate the lateral temporal cortex, and the areas on a folding map (Panel A). The area names in this region generally reflect correspondences with the Von Economo and Koskinas temporal lobe parcellation (Triarhou, 2007a, b; von Economo and Koskinas, 1925), but for several of their areas, we identified subdivisions along the anterior-posterior axis.

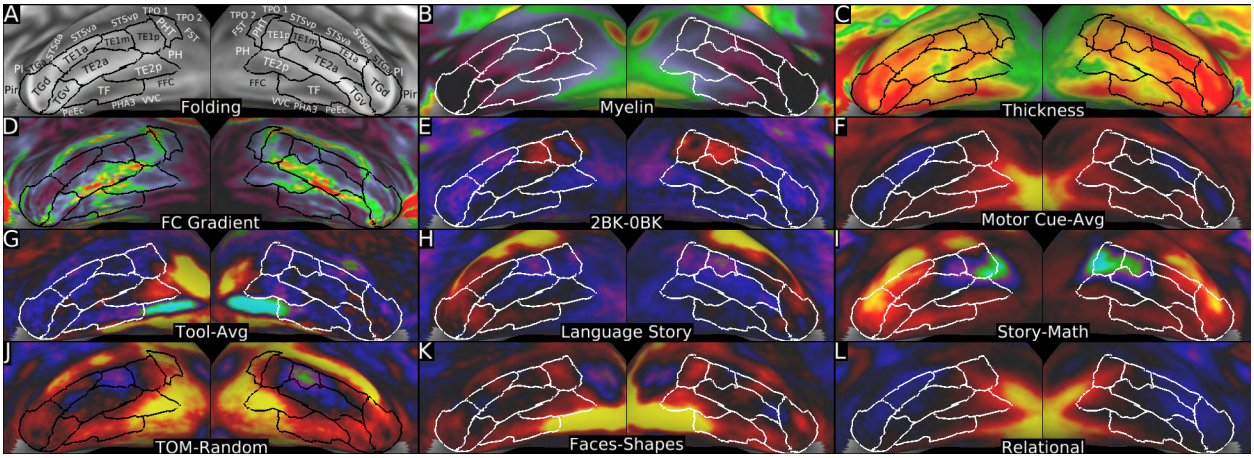

Figure 16 shows multimodal information used to parcellate the lateral and polar temporal cortex. Panel A shows the areas on a folding map. Panels B and C show the myelin map and cortical thickness map. Panel D shows the functional connectivity gradient. Panels E, F, and G show the working memory 2BK-0BK contrast, the MOTOR CUE-AVG contrast, and the categories TOOL-AVG contrast. Panels H and I show the LANGUAGE STORY and STORY-MATH contrasts. Panels J, K, and L show the SOCIAL TOM-RANDOM contrast, the EMOTION FACE-SHAPES contrast, and a RELATIONAL primary contrast. Data at http://balsa.wustl.edu/W8rz.

The temporal polar cortex was divided into two areas, **TGd** and **TGv**. Both are very lightly myelinated (Panel B) and thick (Panel C) relative to their neighbors. The superior (Pir, PI, STGa) and inferior borders (PeEc) of these areas were described already (Sections #12 Insular and Frontal Opercular Cortex insular, #11 Auditory Association Cortex, and #13 Medial Temporal Cortex). Relative to its inferior neighbor TGv, area **TGd** differs in functional connectivity (Panel D) and is deactivated vs activated in the MOTOR CUE-AVG

contrast (Panel F) and the RELATIONAL primary contrasts (Panel L). Relative to its posterior neighbor TE1a, area **TGd** differs modestly in functional connectivity (Panel D) and is more activated in the TOM-RANDOM contrast (Panel J). There is also a gradual decrease in myelin content progressing from the back of TE1a to **TGd** (Panel B). Relative to its infero-posterior neighbor TE2a, area **TGd** has less myelin (Panel B), is thicker (Panel C), differs in functional connectivity (Panel D), is deactivated vs weakly activated in the working memory 2BK-0BK (Panel E) and MOTOR CUE-AVG (Panel F) contrasts, and is more activated in the STORY-MATH contrast (Panel I). Relative to its posterior neighbor TE2a, area **TGv** is thicker (Panel C), differs in functional connectivity (Panel D), and is more activated in the MOTOR CUE-AVG (Panel F), LANGUAGE STORY (Panel H), and TOM-RANDOM (Panel J) contrasts. Relative to its infero-posterior neighbor TF, area **TGv** has less myelin (Panel B), is thicker (Panel C), and is less deactivated in the LANGUAGE MATH contrast.

Posterior to temporal polar cortex are three areas in the inferior temporal sulcus and gyrus, **TF**, **TE2a**, and **TE2p**. **TF's** anterior, medial (PeEc and PHA3), and posterior boundaries (FFC and VVC) have already been covered (above and Sections #4 Ventral Stream Visual Cortex and #13 Medial Temporal Cortex). Relative to its lateral-superior neighbor TE2a, area **TF** has more myelin (Panel B), differs in functional connectivity (Panel D), and is more activated in the MOTOR CUE-AVG (Panel F), LANGUAGE STORY (Panel H), and the TOM-RANDOM (Panel J) contrasts. Relative to its posterior neighbor TE2p, area **TF** differs in functional connectivity (Panel D) and is more activated in the LANGUAGE STORY (Panel H) and FACE-AVG contrasts (both more prominent on the left than the right). Relative to its antero-lateral neighbor TE2a, area **TE2p** has more myelin, differs in functional connectivity (Panel D), and is more activated in the CUE-AVG (Panel F) and the TOM-RANDOM (Panel J) contrasts. Because of noisier gradients in this region (near the temporal lobe susceptibility artifact), the automated border optimizer's penalty for taking circuitous paths was increased for this border. Relative to supero-lateral neighbor TE1a, area **TE2a** has more myelin (Panel B), is thinner (Panel C), differs in functional connectivity (Panel D), is weakly activated vs strongly deactivated in the working memory 2BK-0BK (Panel E) and MOTOR CUE-AVG (Panel F) contrasts, deactivated vs activated in the LANGUAGE STORY contrast (Panel H), and less activated in the LANGUAGE STORY-MATH contrast (Panel I). Relative to supero-lateral neighbor TE1m, area **TE2a** has less myelin (Panel B), is less activated in the working memory 2BK-0BK contrast (Panel E), less deactivated the LANGUAGE STORY contrast (Panel H), and less deactivated in the TOM-RANDOM contrast (Panel J). Relative to postero-superior neighbor TE1p, **TE2a** has less myelin (Panel B), differs in functional connectivity (Panel D), is less activated in the CUE-AVG (Panel F) and RELATIONAL-MATCH contrasts, less deactivated in the LANGUAGE STORY-MATH contrast (Panel I), and more activated in the FACES-SHAPES contrast (Panel K). Relative to medial neighbor TE1p, area **TE2p** differs in functional connectivity (Panel D), is deactivated vs activated in the working memory 2BK-0BK contrast (Panel E), activated vs strongly deactivated in the LANGUAGE STORY-MATH contrast (Panel I), and more activated in the TOM-RANDOM contrast (Panel J). Notably, area **TE2p** is activated in the TOOL-AVG contrast in the left hemisphere but deactivated in the right hemisphere (Panel G).

The middle temporal gyrus includes four areas, **TE1a**, **TE1m**, **TE1p**, and **PHT**. The first three are strongly associated with the task negative network, whereas PHT is strongly

associated with the task positive network. The inferior and anterior borders of these areas were covered above, and their posterior borders (FST and PH) and superior (STSva and STSvp) were covered previously (Sections #5 MT+ Complex and Neighboring Visual Areas and #11 Auditory Association Cortex). Relative to posterior neighbor TE1m, area **TE1a** has less myelin (Panel B), is thicker (Panel C), differs in functional connectivity (Panel D), is deactivated vs activated in many primary task contrasts (e.g. RELATIONAL Panel L) and in the working memory 2BK-0BK (Panel E) and the MOTOR CUE contrasts, and is more activated in the LANGUAGE STORY-MATH contrast (Panel I). Relative to posterior neighbor TE1p, area **TE1m** differs in functional connectivity (Panel D), is less activated in the MOTOR CUE-AVG (Panel F) and FACES-SHAPES (Panel K) contrasts, and is more deactivated in the TOM-RANDOM contrast (Panel J). Relative to posterior neighbor PHT, area **TE1p** differs markedly in functional connectivity (Panel D), is less activated in the BODY-AVG and SOCIAL TOM contrasts, deactivated vs activated in the MOTOR AVG contrast, and activated vs deactivated in the FACES-SHAPES contrast (Panel K). Relative to areas TPOJ1 and TPOJ2 supro-medially, area **PHT** has less myelin (Panel B), differs in functional connectivity (Panel D), is deactivated vs activated in the FACE-AVG contrast, and is less activated in the MOTOR AVG contrast.

15. Temporo-Parieto-Occipital Junction

We identified the temporo-parieto-occipital junction as a strip of cortex bounded by auditory, lateral temporal, inferior parietal and occipital (visual MT+ complex) regions. This region contains five multimodal areas, TPOJ1, TPOJ2, TPOJ3, STV, and PSL, that are surrounded by areas PGp, PGi, PFm, PF, PFcm, RI, A4, A5, STSdp, STSvp, PHT, FST, MST, MT, and LO3. Areas TPOJ1-3 are moderately myelinated and show strong functional connectivity among themselves and with STV. They form a bridge between higher auditory and higher visual areas, as they are correlated with both. Figure 17 shows the multi-modal information used to parcellate these areas, along with the areas on a folding map (Panel A). All five areas have novel names, as these areas to do not clearly correspond with previous parcellations of this region.

The anterior and inferior borders of areas **TPOJ2** and **TPOJ3** have previously been described previously (Sections #5 MT+ Complex and Neighboring Visual Areas, #11 Auditory Association Cortex, and #14 Lateral Temporal Cortex). Relative to its posterior neighbor PGp, area **TPOJ3** has more myelin (Panel B), is thinner (Panel C, especially on the left), differs in functional connectivity (Panel D), is activated vs deactivated in the working memory 2BK-0BK and BODY-AVG (Panel M) contrasts, weakly activated vs strongly deactivated in the FACE-AVG contrast, weakly deactivated vs strongly activated in the PLACE-AVG contrast, and strongly activated vs weakly activated or deactivated in the FACES-SHAPES contrast (Panel O). Relative to its superior neighbor PGi, area **TPOJ3** has more myelin (Panel B), is thinner (Panel C), differs strongly in functional connectivity (Panel D), is more activated in primary task contrasts (e.g., Panel J), the BODY-AVG contrast (Panel M), the MOTOR CUE contrast (Panel K), and is less activated in the LANGUAGE STORY (Panel H) and STORY-MATH (Panel I) contrasts. Relative to its anterior neighbor TPOJ2, area **TPOJ3** is thinner (Panel C), more activated in the working memory 2BK-0BK contrast, less activated in the RELATIONAL primary contrast (Panel J), MOTOR AVG (Panel L), and FACES-SHAPES (Panel O) contrasts. Relative to its superior neighbor PGi, area

TPOJ2 has more myelin (Panel B), differs strongly in functional connectivity (Panel D), and is more activated in primary task contrasts (e.g., Panel J), the BODY-AVG contrast (Panel M), the MOTOR CUE contrast (Panel K), and is less activated in the LANGUAGE STORY (Panel H) and STORY-MATH (Panel I) contrasts. Relative to its anterior neighbor TPOJ1, area **TPOJ2** is thinner (Panel C), differs in functional connectivity (Panel D), is more activated in the BODY-AVG contrast (Panel M), is deactivated in the PLACE-AVG contrast, and is deactivated vs activated in the LANGUAGE STORY contrast (Panel H).

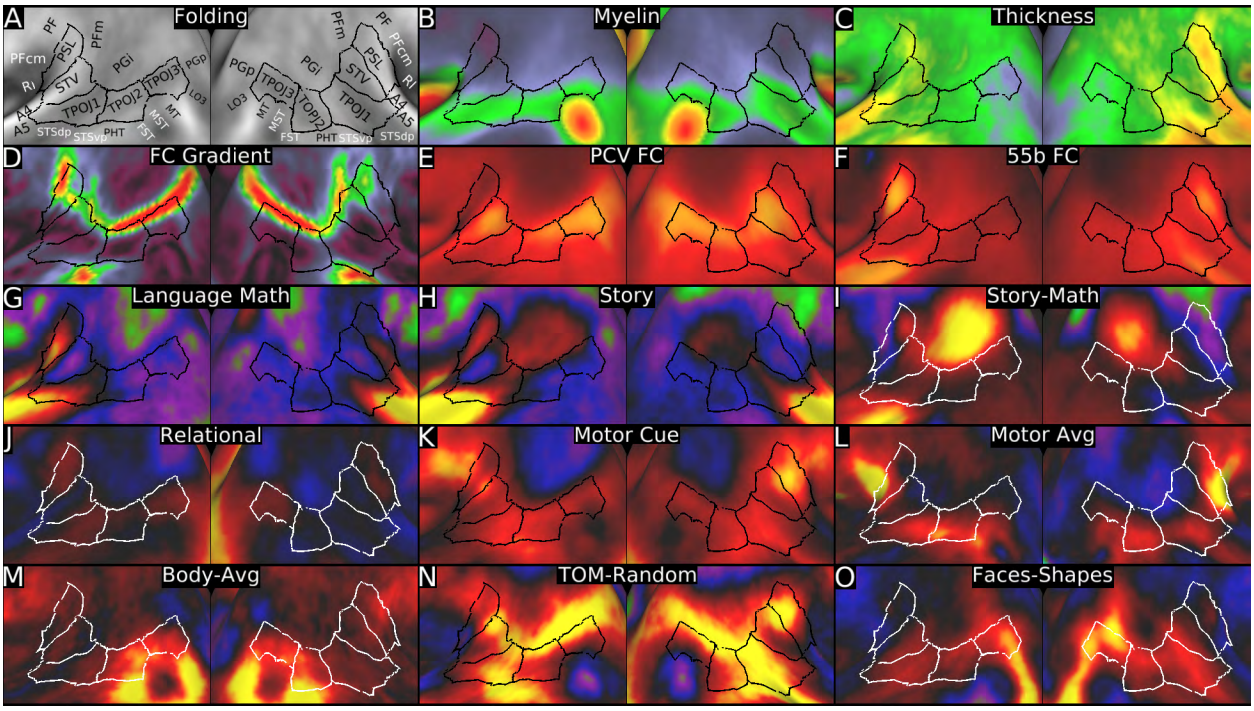

Figure 17 shows multi-modal information used to parcellate the cortex of the temporo-parieto-occipital junction. Panel A shows the five areas on a group average folding map. Panels B and C show the myelin and thickness maps. Panel D shows the overall resting state functional connectivity gradient. Panel E shows the functional connectivity map from seeding area PCV bilaterally. Panel F shows the functional connectivity map from seeding area 55b unilaterally (seeding left 55b shown on the left and seeding right 55b shown on the right). Panels G, H, and I show the LANGUAGE MATH, STORY, and STORY-MATH task fMRI contrasts. Panels J, K, and L show a RELATIONAL primary contrast, the MOTOR CUE contrast, and the MOTOR AVG contrast. Panels M, N, and O show the BODY-AVG contrast, the TOM-RANDOM contrast, and the FACES-SHAPES contrast. Data at http://balsa.wustl.edu/WKkq.

Relative to its postero-superior neighbor PGi, **TPOJ1** has more myelin (Panel B), differs in functional connectivity (Panel D), and is more activated in primary task contrasts (e.g. Panel J), the MOTOR CUE (Panel K) and MOTOR AVG (Panel L) contrasts, and less activated in the LANGUAGE STORY-MATH contrast (Panel I). **TPOJ1's** border with PHT was covered previously (Section #14 Lateral Temporal Cortex). In the right hemisphere relative to inferior neighbor STSvp, area **TPOJ1**, has more myelin (Panel B) and differs in functional connectivity (Panel D). Relative to its inferior neighbor STSdp, area **TPOJ1** has more myelin (Panel B), differs in functional connectivity (Panel D), and is more activated in the MOTOR AVG (Panel L, more on the left than the right) and the FACES-SHAPES (Panel O) contrasts and less activated in the LANGUAGE STORY-MATH contrast (Panel I). Relative to

anterior neighbor A5, area **TPOJ1** has more myelin (Panel B), differs in functional connectivity (Panel D), is deactivated vs activated in the TOOL-AVG contrast, more activated in the MOTOR CUE (Panel K) contrast, less activated in the STORY-MATH (Panel I) contrast, and activated vs deactivated in the TOM-RANDOM (Panel N) and FACES-SHAPES (Panel O) contrasts. Relative to its supero-anterior neighbor A4, area **TPOJ1** differs in functional connectivity (Panel D), is more activated in the MOTOR CUE contrast (Panel K), activated vs deactivated in the FACE-AVG, TOM-RANDOM (Panel N) and FACES-SHAPES (Panel O) contrasts, and deactivated vs activated in the TOOL-AVG contrast. The border of **TPOJ1** with STV will be discussed below. Unlike areas TPOJ2 and TPOJ3, area **TPOJ1** is both larger and more heavily myelinated in the right hemisphere (Panel B).

The remaining two areas in this region, **STV** (Superior Temporal Visual area) and **PSL** (Peri-Sylvian Language area) have several distinctive features in addition to the typical multi-modal gradients used to define other cortical areas. In terms of functional connectivity, STV is strongly connected with PCV (Posterior Cingulate Visual area, used as a bilateral seed in Panel E), and gradients from the functional connectivity map seeded from area PCV in both hemispheres were used in its definition. Similarly, gradients from the functional connectivity map seeded from unilateral area 55b (Panel F) were used to help define PSL. PSL also contains an anterior to posterior topographic organization of connectivity (which is also present in areas 55b, SFL, and 44, see Figure 18). In contrast to most other regions, there are prominent asymmetries of some features for these two areas. Below, the criteria used for the left and right hemispheres are described separately when it improves clarity.

The border between **STV** and area A4 is moderately long in the left hemisphere, but almost nonexistent on the right. In the **left** hemisphere, **STV** is more connected with PCV than is area A4 (Panel E), is deactivated vs activated in the TOOL-AVG, LANGUAGE MATH and STORY (Panels G and H) contrasts, more activated in the MOTOR CUE-AVG contrast, and activated vs deactivated in the SOCIAL primary contrasts and the TOM-RANDOM contrast (Panel N). Relative to inferior neighbor TPOJ1 in **both** hemispheres, **STV** has less myelin (Panel B), has stronger functional connectivity with the PCV (Panel E), and is deactivated vs activated in the LANGUAGE MATH and STORY contrasts (Panels G and H). In the **left** hemisphere, STV is less activated than TPOJ1 in the GAMBLING primary contrasts and the MOTOR AVG contrast (Panel L). In the **right** hemisphere, STV is less activated than TPOJ1 in the TOM-RANDOM contrast (Panel N). Relative to its posterior neighbor PGi in **both** hemispheres, **STV** differs strongly in functional connectivity (Panel D) and is less activated in the LANGUAGE STORY and STORY-MATH contrasts (Panels H and I) and more activated in the SOCIAL RANDOM contrast. Relative to its posterior neighbor PFm in **both** hemispheres, **STV** differs strongly in functional connectivity (Panel D) and is more activated in the SOCIAL primary contrasts. Relative to its superior neighbor PSL in **both** hemispheres, area **STV** is deactivated vs activated in the working memory primary contrasts, the MOTOR AVG contrast (Panel L), the LANGUAGE MATH (Panel G) and STORY (Panel H, left hemisphere only) contrasts, and the RELATIONAL primary contrasts (e.g. Panel J). **STV** also has stronger functional connectivity with PCV (Panel E), whereas **PSL** has stronger functional connectivity with 55b in the corresponding hemisphere (Panel F).

Relative to its antero-inferior neighbor A4, area **PSL** has stronger functional connectivity with area 55b (Panel F), is activated vs deactivated in the primary contrasts (e.g. Panel J), deactivated vs activated in the TOOL-AVG contrast, and more activated in the

MOTOR AVG (Panel L). Relative to its supero-posterior neighbor PFm, area **PSL** has stronger functional connectivity with area 55b (Panel F), is more activated in the LANGUAGE MATH and STORY contrasts (Panels G and H in the left hemisphere), the MOTOR CUE (Panel K) and TOM-RANDOM (Panel N in the right hemisphere) contrasts, and the relational primary contrasts in both hemispheres (e.g. Panel J). The left **PSL** is more activated in the RELATIONAL-MATCH contrast relative to the right hemisphere **PSL**, and it is much thicker on the right than the left (Panel C). Relative to its supero-anterior neighbor PF, area **PSL** has stronger functional connectivity with area 55b (Panel F) and is less activated in the MOTOR CUE contrast on the left (Panel K, but not on the right), more activated in the LANGUAGE MATH and STORY contrast (Panels G and H, less deactivated on the right), and more activated in the TOM-RANDOM contrast in the right but not the left (Panel N). Thus, area PSL is one of a handful of strikingly functionally lateralized areas in the cerebral cortex, having a number of left/right task activation differences and belonging to the strongly lateralized language network (see Figure 18).

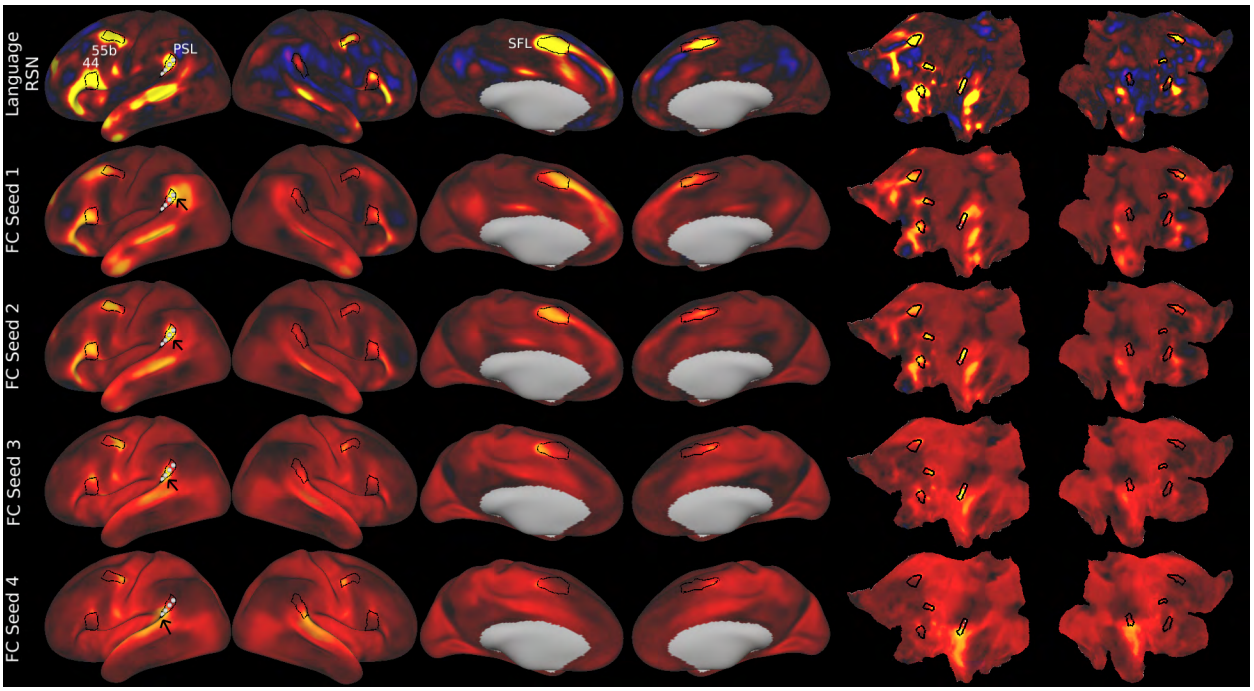

Figure 18 shows the topographic organization of the language network (Row 1 d=40 ICA RSN). Four seeds are placed along the anterior-posterior axis of area PSL in the left hemisphere (marked by black arrows from posterior to anterior). The functional connectivity pattern shows corresponding changes in the other major nodes of the language network, including 55b, SFL, and 44. The pattern is present when seeded in either hemisphere, but stronger in the left hemisphere. Data at http://balsa.wustl.edu/WNrX.

Area PSL**,** along with areas 55b, SFL, and 44, also shows topographic organization of functional connectivity along its anterior to posterior axis as illustrated in Figure 18. Row 1 shows a left-lateralized language RSN, with areas PSL, 55b, 44, and SFL outlined in white. Seed locations in left area PSL (black arrows) progressing from posterior (row 2) to anterior (rows 3 – 5) are associated with elevations in FC that progress from anterior to posterior in area 55b, inferior to superior in area 44, and anterior to posterior in area SFL in both hemispheres but more prominently on the left. In both hemispheres PSL appears in

a reasonably corresponding geographic location near the supero-posterior tip of the Sylvian fissure and extending onto the superior temporal gyrus (especially on the right), and it is functionally connected with a corresponding set of areas in each hemisphere.

16. Superior Parietal Cortex

The superior parietal region has some parallels to the cortex of the temporo-parieto-occipital junction, insofar as it lies between two major sensory modalities (in this case visual and somatosensory domains) and forms a bridge between these modalities. We include in the superior parietal region the medial bank of the intra-parietal sulcus (IPS) and superior medial parietal cortex and divided this region into ten areas: LIPv, LIPd, VIP, AIP, MIP, 7PC, 7AL, 7Am, 7PL, and 7Pm. These areas are surrounded by areas IP0, IP1, IP2, PFm, PF, PFt, 2, 5L, PCV, 7m, POS2, DVT, and IPS1. Figure 19 shows the multi-modal information used in parcellating the superior parietal cortex, with Panel A showing the areas on a folding map.

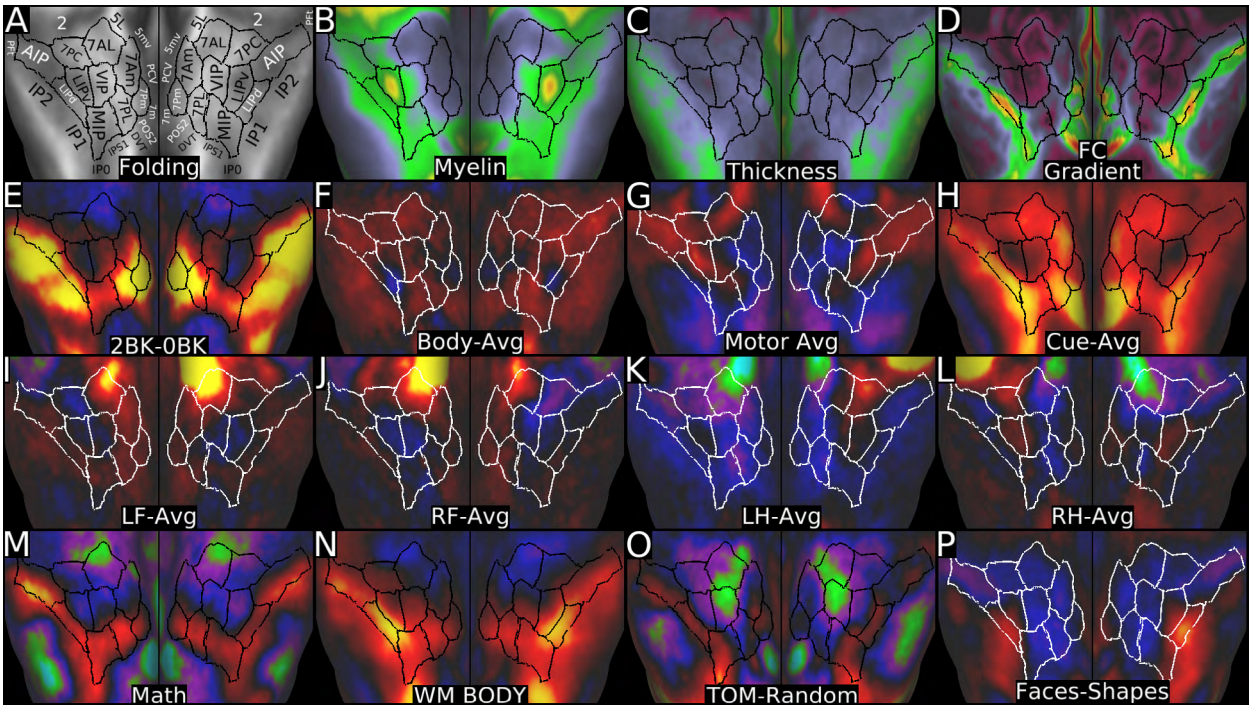

Figure 19 shows multi-modal information used in parcellating the superior parietal cortex. Panel A shows the areas on a group average folding map. Panels B and C show the myelin map and the cortical thickness map. Panel D shows the functional connectivity gradient. Panels E, F, G, and H show the working memory 2BK-0BK contrast, the BODY-AVG contrast, the MOTOR AVG contrast, and the MOTOR CUE-AVG contrast. Panels I, J, K, and L show the MOTOR LF-AVG, RF-AVG, LH-AVG, and RH-AVG contrasts. Panels M, N, O, and P show the LANGUAGE MATH, a working memory primary contrast, TOM-RANDOM contrast, and FACES-SHAPES contrast. Data at http://balsa.wustl.edu/RGGM.

Area **MIP** separates a more posterior region of the dorsal stream visual cortex from a more anterior region (containing putative homologues of macaque LIPv and VIP). We identified it as **MIP** because it is a candidate homologue of macaque **MIP**, lying between the putative LIP/VIP homologues and more posterior visual regions (Van Essen et al., 2012a).

MIP has strong functional connectivity with other areas along the medial bank of the IPS (e.g. LIPd and AIP) and less connectivity with either the posterior (e.g. IPS1, V7, V3A) or anterior portions (LIPv, VIP) of the dorsal visual stream. Area **MIP's** posterior border with IPS1 was covered previously (see Section #3 Dorsal Stream Visual Cortex). Relative to its anterior neighbors LIPv and VIP, area **MIP** is thicker (Panel C), differs in functional connectivity (Panel D), is more activated in the working memory 2BK-0BK contrast (Panel E), the MOTOR CUE-AVG contrast (Panel H), the LANGUAGE MATH (Panel M) and MATH-STORY contrasts, and the TOM-RANDOM contrast (Panel O). **MIP** also has less myelin than LIPv (Panel B). Relative to its medial neighbor 7PL, area **MIP** has more myelin (Panel B), is less activated in the working memory 2BK-0BK contrast (Panel E), more deactivated in the FACE-AVG contrast, and more activated in the TOOL-AVG and TOM-RANDOM (Panel O) contrasts. Relative to inferior neighbor IP0, **MIP** is thinner (Panel C) and differs in functional connectivity (Panel D). Relative to its lateral neighbor IP1, **MIP** has more myelin and is thinner (Panels B and C), differs strongly in functional connectivity (Panel D), is more deactivated in the FACE-AVG contrast, and is more activated in the TOOL-AVG, SOCIAL TOM, TOM-RANDOM (Panel O), and EMOTION SHAPES contrasts. Relative to its antero-lateral neighbor LIPd, **MIP** has less myelin (Panel B), differs in functional connectivity (Panel D), is less activated in the working memory and gambling primary contrasts, more activated in the BODY-AVG (Panel F) contrast, and deactivated vs activated in the FACE-AVG and FACES-SHAPES (Panel P) contrasts.

The **LIPv/VIP** complex is distinct from its neighbors both architecturally and functionally. The area names reflect a presumed homology with correspondingly named areas in the macaque, even though LIPv is on the lateral bank of the IPS in the macaque (where it is ventral to LIPd) but is on the medial bank of the IPS in humans. Thus, LIPv lies supero-medial to LIPd, reflecting the overall medial shift of parietal visual regions in humans compared to macaques. **LIPv** is heavily myelinated and **VIP** is moderately myelinated (Panel B). Both areas have much stronger functional connectivity with higher dorsal stream visual areas than do their neighbors, and they also have a distinct pattern of functional activation. Because of high intersubject variability of areal boundaries relative to cortical folds and the folding patterns themselves, this region benefits especially from areal-feature-based registration (the myelin maps presented here are much sharper than those made with folding-based registration in (Glasser and Van Essen, 2011), for example). The putative homologies are based on myelin maps that have been analyzed in macaques, chimpanzees, and humans showing a corresponding hotspot of increased myelin content in the IPS (Glasser et al., 2014). Relative to its inferolateral neighbor LIPd, area **LIPv** has more myelin, is thinner (Panels B and C), differs in functional connectivity (Panel D), is less activated in the working memory 2BK-0BK (Panel E), FACE-AVG, CUE-AVG (Panel H), LANGUAGE MATH (Panel M) and MATH-STORY contrasts, and is deactivated vs activated in the TOM-RANDOM contrast (Panel O). Relative to its anterior neighbor AIP, area **LIPv** has more myelin (Panel B), is thinner (Panel C), differs in functional connectivity (Panel D), is less activated in the working memory 2BK-0BK (Panel E), CUE-AVG (Panel H), LANGUAGE MATH (Panel M) and MATH-STORY contrasts, and is more deactivated in the TOM-RANDOM (Panel O) and RELATIONAL-MATCH contrasts. Relative to its anterior neighbor 7PC, area **LIPv** has more myelin (Panel B), is thinner (Panel C), differs in functional connectivity (Panel D), is less activated in the MOTOR CUE-AVG contrast (Panel H), but is more activated in the ipsilateral ?H-AVG contrast (Panels K and L). Relative to its medial

neighbor VIP, **LIPv** has more myelin (Panel B), differs modestly in functional connectivity (Panel D), is less activated in the working memory 2BK-0BK contrast (Panel E, more so on the right than the left), more activated in the MOTOR AVG (Panel G), ipsilateral ?H-AVG hand motor (Panels K and L), and FACES-SHAPES (Panel P) contrasts, and is less activated in the T-AVG face motor and SOCIAL RANDOM contrasts. Relative to its anterior neighbor 7AL, area **VIP** is has more myelin (Panel B), differs in functional connectivity (Panel D), is less activated in the MOTOR CUE and MOTOR AVG (Panel G) contrasts, and more activated in the EMOTION primary contrasts. Relative to its medial neighbor 7Am, area **VIP** has more myelin (Panel B), differs in functional connectivity (Panel D), is less activated in the MOTOR CUE-AVG contrast (Panel H), and more deactivated in the TOM-RANDOM contrast (Panel P). Relative to its postero-medial neighbor 7PL, area **VIP** has more myelin (Panel B), differs in functional connectivity (Panel D), is less activated in the working memory 2BK-0BK (Panel E), MOTOR CUE-AVG (Panel H), and LANGUAGE MATH (Panel M) and MATH-STORY contrasts, and is more deactivated in the TOM-RANDOM contrast (Panel O). We previously suggested (Glasser and Van Essen, 2011) that cytoarchitectonic area hIP3 (Scheperjans et al., 2008a; Scheperjans et al., 2008b) might overlap with the heavily myelinated patch now identified as LIPv (and perhaps also part of area LIPd), but confirmation would require surface based (and ideally areal feature-based alignment) of the post-mortem cytoarchitectonic data.

Areas **LIPd** and **AIP** are named after putative homologues in the macaque (Van Essen et al., 2012a), in part based on their relationship to the LIPv/VIP complex just discussed. **LIPd** is a moderately myelinated area inferolateral to area LIPv (Panel B). Relative to its lateral neighbors IP1 and IP2, **LIPd** differs strongly in functional connectivity (Panel D), is deactivated vs activated in the BODY-AVG contrast (Panel F), activated vs deactivated in the PLACE-AVG contrast, more activated in the MOTOR CUE and TOM-RANDOM contrasts (Panel O), and less activated in the RELATIONAL-MATCH contrast. Also **LIPd** was statistically more activated than IP1 and IP2 in the working memory (e.g. Panel N), gambling, and relational primary contrasts. Relative its anterior neighbor AIP, **LIPd** has more myelin (Panel B), differs in functional connectivity (Panel D), is less activated in the BODY-AVG (Panel F) and MOTOR AVG (Panel G) contrasts, more activated in the PLACE-AVG and MOTOR CUE-AVG (Panel H) contrasts, and activated vs deactivated in the FACES-SHAPES contrast (Panel P). Relative to its infero-lateral neighbor IP2, area **AIP** differs in functional connectivity (Panel D), is more activated in SOCIAL and EMOTION primary task contrasts and in the MOTOR CUE contrast, less deactivated in the FACE-AVG and LANGUAGE STORY contrasts, and more deactivated in the FACES-SHAPES contrast (Panel P). Relative to its anterior neighbor PFt, area **AIP** has more myelin (Panel B) and is more activated in several primary contrasts (e.g. Panel N). Relative to its medial neighbor 7PC, area **AIP** differs in functional connectivity (Panel D), is more activated in the primary contrasts (e.g. Panel N) and the working memory 2BK-0BK contrast (Panel E), and is deactivated vs activated in the contralateral ?H-AVG hand motor contrasts (Panels K and L).

The posterior, lateral, and anterior borders of area **7PC** have previously been covered (above and Section #6 Somatosensory and Motor Cortex). Relative to its anterior and posterior neighbors LIPv and area 2, area **7PC** has less myelin (Panel B) and has stronger functional connectivity with somatosensory area 2 than with more visually related LIPv. We assigned this name based on its location antero-lateral to areas hIP3 and

7A (Scheperjans et al., 2008a; Scheperjans et al., 2008b). Relative to its medial neighbor 7AL, area **7PC** has more myelin (Panel B), differs in functional connectivity (Panel D), is less activated in the MOTOR CUE and bilateral ?F-AVG foot MOTOR contrasts (Panels I and J), more activated in bilateral ?H-AVG hand MOTOR contrasts (Panels K and L), and less deactivated in the TOM-RANDOM contrast (Panel O). We identified medial and lateral subdivisions **7Am** and **7AL** of area 7A (though our area VIP may also overlap with the region identified as 7A by (Scheperjans et al., 2008a; Scheperjans et al., 2008b) and the anterior corner of **7AL** may overlap with 5L as well). Most of **7AL's** borders have already been covered (above and Sections #6 Somatosensory and Motor Cortex and #7 Paracentral Lobular and Mid Cingulate Cortex). Relative to posterior neighbor VIP and anterior neighbor area 2, area **7AL** has less myelin but is comparable in myelin content to its medial neighbors 5L and 7Am (Panel B). Its strongest distant functional connectivity is with superior premotor cortex. Relative to its medial neighbor 7Am, area **7AL** has slightly more myelin (Panel B), differs in functional connectivity (Panel D), is more activated in the MOTOR AVG contrast (Panel G) and more deactivated in the TOM-RANDOM contrast (Panel O). Area **7Am's** border with 5L has been covered previously (Section #7 Paracentral Lobular and Mid Cingulate Cortex). Relative to its infero-medial neighbor PCV, area **7Am** has less myelin (Panel B), is thinner (Panel C), differs in functional connectivity (Panel D), is more activated in the working memory 2BK-0BK (Panel E), MOTOR CUE-AVG (Panel H), and MATH-STORY contrasts (Panel M), and is activated vs deactivated in the FACES-SHAPES contrast (Panel P). Relative to its postero-lateral neighbor 7PL, area **7Am** has less myelin (Panel B), differs in functional connectivity (Panel D), is less activated in the primary contrasts (e.g. Panel N), working memory 2BK-0BK (Panel E), and LANGUAGE MATH (Panel M) and MATH-STORY contrasts. Relative to its postero-medial neighbor 7Pm, area **7Am** is thinner (Panel C), differs in functional connectivity (Panel D), is less activated in the working memory 2BK-0BK contrast (Panel E), deactivated vs activated in the RELATIONAL-MATCH contrast, and more deactivated in the FACES-SHAPES contrast (Panel P).

We identified medial and lateral areas **7Pm** and **7PL** within the region identified as area 7P by (Scheperjans et al., 2008a; Scheperjans et al., 2008b), lying posterior to 7A, medial to the intra-parietal sulcus (IPS), anterior to the partieto-occipital sulcus (POS), and superior to 7m. Relative to its anterior neighbor PCV, area **7Pm** has less myelin (Panel B), differs in functional connectivity (Panel D), is more activated in the working memory 2BK-0BK (Panel E), LANGUAGE MATH (Panel M), MATH-STORY, and RELATIONAL-MATCH contrasts, and is deactivated vs activated in the BODY-AVG contrast (Panel F). Relative to its inferior neighbor 7m, area **7Pm** differs in functional connectivity (Panel D), is deactivated vs activated in the BODY-AVG contrast (Panel F), less activated in the FACE-AVG and FACES-SHAPES (Panel P) contrasts, more activated in the PLACE-AVG and MATH-STORY contrasts, and less deactivated in the TOOL-AVG contrast. Relative to its infero-posterior neighbor POS2, area **7Pm** has less myelin (Panel B), is thicker (Panel C), differs in functional connectivity (Panel D), is more activated in some of the primary contrasts (SOCIAL and EMOTION) and the working memory 2BK-0BK contrast (Panel E), is deactivated vs activated in the BODY-AVG contrast (Panel F), is activated vs deactivated in the PLACE-AVG, LANGUAGE MATH (Panel M), and TOM-RANDOM (Panel O) contrasts, is less activated in the MOTOR CUE-AVG contrast (Panel H), and is less deactivated in the LANGUAGE STORY contrast. Relative to its supero-lateral neighbor 7PL, area **7Pm** has less

myelin (Panel B), is thicker (Panel C), differs in functional connectivity (Panel D), is deactivated vs activated in the BODY-AVG contrast (Panel F), and is less activated in the EMOTION and SOCIAL primary contrasts. Relative to its postero-inferior neighbor POS2, area **7PL** has less myelin (Panel B), differs in functional connectivity (Panel D), is more activated in some of the primary contrasts (SOCIAL and EMOTION), is activated vs deactivated in the PLACE-AVG, LANGUAGE MATH (Panel M), and TOM-RANDOM (Panel O) contrasts, and is less deactivated in the LANGUAGE STORY contrast. Finally, relative to its postero-inferior neighbor DVT, area **7PL** differs in functional connectivity (Panel D), is more activated in the working memory 2BK-0BK contrast (Panel E), is locally activated vs deactivated in the BODY-AVG contrast (Panel F), LANGUAGE MATH (Panel M), and MATH-STORY contrasts, less deactivated in the FACE-AVG contrast, and less activated in the PLACE-AVG contrast.

17. Inferior Parietal Cortex

The inferior parietal cortex is an association region similar in several respects to the lateral temporal cortex discussed previously. It is predominantly lightly myelinated (Panel B), moderately thick cortex (Panel C), and includes some areas strongly associated with the task positive network and others with the task negative network. Like the lateral temporal cortex, this region has expanded dramatically in humans relative to macaques and chimpanzees (Glasser et al., 2014; Hill et al., 2010). We identified ten areas in this region: PGp, PGs, PGi, PFm, PF, PFt, PFop, IP0, IP1, and IP2. The names reflect correspondences with areas identified by (Caspers et al., 2008; Caspers et al., 2006; Choi et al., 2006), except that their PF likely extends into portions of our PSL and STV, their PGa is subdivided into PGi and PGs (which also may include some of their PGp, as our PGp is somewhat smaller). Area IP0 is a new area posterior to IP1 along the lateral bank of the posterior IPS. These areas are surrounded by PFcm, OP4, 1, 2, AIP, LIPd, MIP, IPS1, V3B, V3CD, LO3, TPOJ1, TPOJ2, TPOJ3, STV, and PSL. Figure 20 shows multi-modal information used to parcellate this region, with the areas shown on a folding map in Panel A.

Area **PGp** is a transitional area insofar as its myelin content (Panel B) and thickness (Panel C) are similar to the rest of the inferior parietal cortex, but it has stronger functional connectivity with other transitional regions (e.g. the dorsal visual transitional area—DVT) and with higher visual cortex than does the rest of the inferior parietal cortex. Area **PGp's** posterior and inferior borders were previously covered in Sections #5 MT+ Complex and Neighboring Visual Areas (V3CD, LO3), and #15 Temporal-Parietal-Occipital Junction (TPOJ3). Relative to its supero-anterior neighbor PGs, area **PGp** differs strongly in functional connectivity (Panel D), is deactivated vs activated in the FACE-AVG contrast, and is activated vs deactivated in the PLACE-AVG, SOCIAL RANDOM, and MOTOR CUE-AVG (Panel F, deactivated on the left, less activated on the right and only assessed statistically) contrasts. Our area PGp corresponds to area PGp from (Caspers et al., 2008; Caspers et al., 2006), though it is somewhat smaller. Area **IP0** lies in the posterior IPS, and its borders with V3CD, V3B, and IPS1 were discussed previously (Sections #3 Dorsal Stream Visual Cortex and #5 MT+ Complex and Neighboring Visual Areas). Relative to its supero-lateral neighbor PGp, area **IP0** has more myelin (Panel B), is thinner (Panel C), differs modestly in functional connectivity (Panel D), and is more activated in primary contrasts (e.g. Panel I) and the FACES-SHAPES contrast (Panel J). Relative to its antero-superior neighbor IP1,

area **IP0** differs in functional connectivity (Panel D), is more activated in many primary contrasts (e.g. Panel I), is deactivated vs activated in the FACE-AVG and RELATIONAL-MATCH contrasts, activated vs deactivated in the PLACE-AVG contrast, and less deactivated in the LANGUAGE STORY contrast (Panel G).

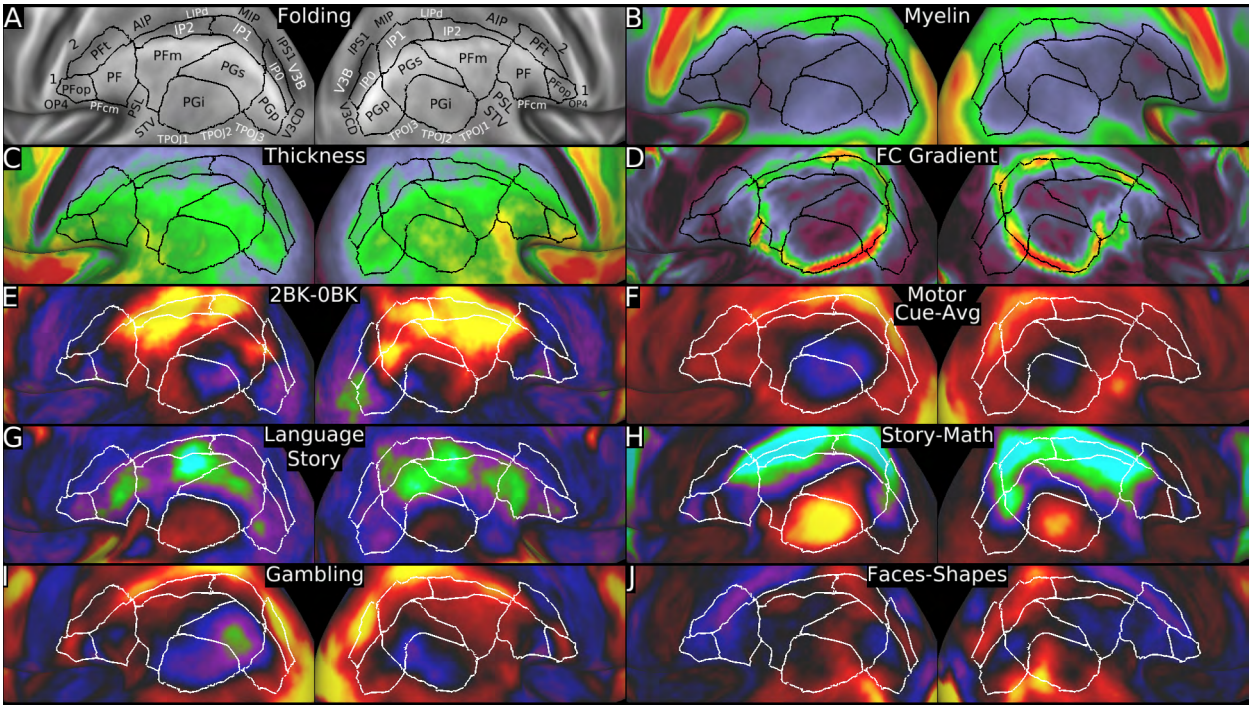

Figure 20 shows the multi-modal information used to parcellate the inferior parietal cortex. Panel A shows the areas on a folding map. Panels B and C show the myelin and cortical thickness maps. Panel D shows the resting state functional connectivity gradient. Panels E and F show the working memory 2BK-0BK contrast and the MOTOR CUE-AVG contrast. Panels G and H show the LANGUAGE STORY and STORY-MATH contrasts. Panels I and J show the GAMBLING PRIMARY contrast and the FACES-SHAPES contrasts. Data at http://balsa.wustl.edu/WL0P.

We identified two areas on the lateral bank of the intraparietal sulcus that correspond to areas **IP1** and **IP2** reported by (Choi et al., 2006). Relative to their neighbors on the medial bank (MIP, LIPd, and AIP), **IP1** and **IP2** differ strongly in functional connectivity (Panel D) and in various task contrasts (see Section #16 Superior Parietal Cortex). Relative to their lateral neighbors PGs and PFm, **IP1** and **IP2** have more myelin (Panel B) and differ modestly in functional connectivity (Panel D). Also, **IP1** is more activated in primary contrasts (e.g. Panel I), the MOTOR CUE-AVG contrast (Panel F), the LANGUAGE MATH contrast, less deactivated in the LANGUAGE STORY contrast (Panel G), and more activated in the FACES-SHAPES contrast (Panel J). Relative to its infero-lateral neighbor PGs, **IP1** is also more deactivated in the language STORY-MATH contrast (Panel H). Relative to its infero-lateral neighbor PFm, **IP2** is also more activated in the MOTOR CUE-AVG contrast (Panel F). Relative to its anterior neighbor IP2, area **IP1** differs modestly in functional connectivity (Panel D), is modestly more activated in RELATIONAL primary contrasts and FACES-SHAPES contrast (Panel J), and is less deactivated in the LANGUAGE STORY contrast (Panel G). Relative to anterior neighbor PF, area **IP2** differs in functional connectivity (Panel D) and in the FACES-SHAPES contrast (Panel J).

We subdivided classical area PF (BA 40) into 5 areas sufficiently similar to those identified by (Caspers et al., 2008; Caspers et al., 2006) that we use the same names: **PF**, **PFt**, **PFop**, PFm, and PFcm (previously covered in Section #9 Posterior Opercular Cortex). The three most anterior areas (PFt, PFop, and PF) have strong functional connectivity with other portions of the task positive network. Their superior (AIP), anterior (1, 2, OP4), and inferior borders (PFcm, PSL) have been covered previously in Sections #16 Superior Parietal Cortex, #6 Somatosensory and Motor Cortex, #9 Posterior Opercular Cortex, and #15 Temporal Parietal Occipital Junction. Relative to its posterior neighbor PF and inferior neighbor PFop, area **PFt** has more myelin and is thinner (Panels B and C), differs in functional connectivity (Panel D), and is less deactivated in the LANGUAGE STORY contrast (Panel G), more activated in the SOCIAL RANDOM contrast, and more deactivated in the FACES-SHAPES contrast (Panel J). **PFt** is also more activated than PF in the EMOTION SHAPES contrast. Relative to its posterior neighbor PF, area **PFop** is modestly thicker (Panel C), differs in functional connectivity (Panel D), and is less activated in the contralateral and ipsilateral ?F-AVG foot motor contrasts. Relative to its posterior neighbor PFm, area **PF** is thicker (Panel C), differs in functional connectivity (Panel D), and is more activated in the MOTOR CUE and SOCIAL TOM contrasts. Our areas PFop and PF may correspond to areas 72 and 88 from the Vogt-Vogt school (Nieuwenhuys et al., 2015).

The remaining three areas in the inferior parietal cortex are **PFm**, **PGi**, and **PGs**. Area **PFm** is a transitional region between PF, which is a major node in the task positive network, and **PGi** and **PGs**, which are major nodes in the task negative network. All three areas are lightly myelinated relative to most of their neighbors (Panel B) and are moderately thick (Panel C). Many of the outer borders of these areas were covered above or in Section #15 Temporal Parietal Occipital Junction (TPOJ1, TPOJ2, TPOJ3, STA, and PSL). Internally, these areas all differ from one another in functional connectivity (Panel D). Relative to its postero-inferior neighbor PGi, area **PFm** also has modestly less myelin (Panel B). Relative to PGi and posterior neighbor PGs, area **PFm** is also more activated in the working memory 2BK-0BK (Panel E), MOTOR CUE-AVG (Panel F), and the GAMBLING primary contrasts (Panel I), and is more deactivated in the STORY-MATH contrast (Panel H). Relative to PFm and superior-medial neighbor PGs, area **PGi** is more activated in the FACE-AVG, LANGAUGE STORY (Panel G) (only assessed statistically on the right), and the STORY-MATH (Panel H) contrasts. Our areas PGi and PGs correspond to area PGa from (Caspers et al., 2008; Caspers et al., 2006). Our areas PFm and PGi plus PGs may correspond to areas 89 and 90 from the Vogt-Vogt school (Nieuwenhuys et al., 2015).

18. Posterior Cingulate Cortex

The posterior cingulate cortex contains a diversity of architecturally and functionally distinct areas that we group together based on geographic proximity rather than functional similarity. It includes 14 areas: DVT, ProS, POS1, POS2, RSC, v23ab, d23ab, 31pv, 31pd, 31a, 23d, 23c, PCV, and 7m, which are surrounded by areas PreS, V2, V1, V6, V6A, IPS1, 7PL, 7Pm, 7Am, 5mv, 24dd, 24dv, p24pr, and 33pr. Figure 21 shows the multi-modal information used to parcellate this region. Panel A shows the areas on a group average folding map.

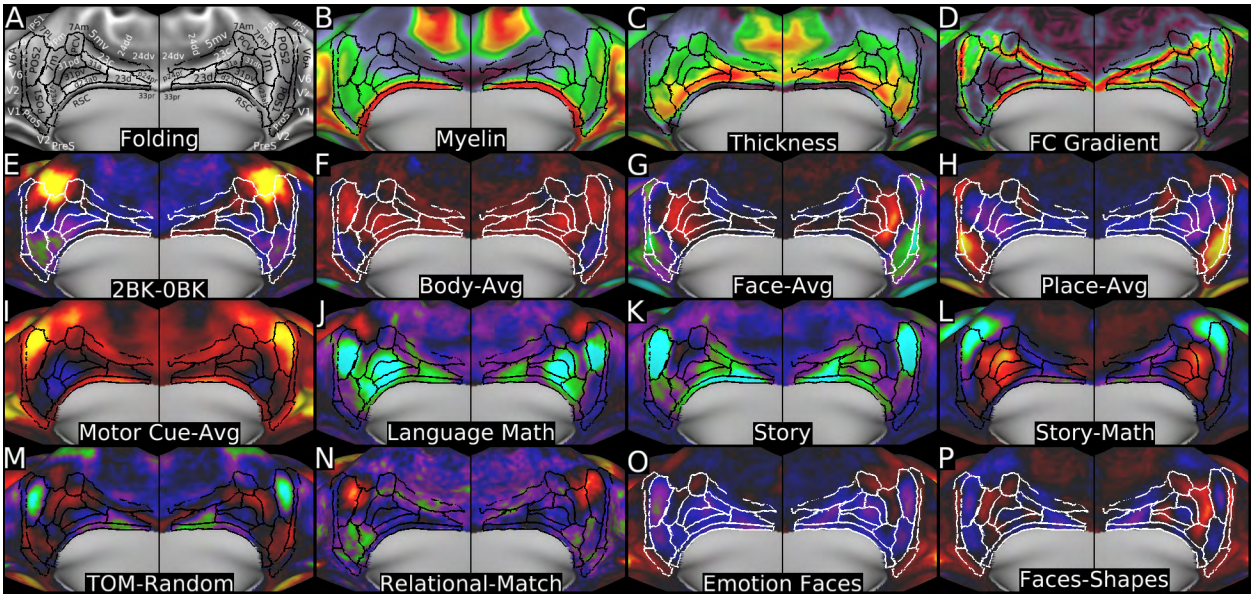

Figure 21 shows the multi-modal information used to parcellate the posterior cingulate cortex. Panel A shows the areas on a folding map. Panels B and C show the myelin and cortical thickness maps. Panel D shows the resting state functional connectivity gradients. Panels E, F, G, and H show the working memory 2BK-0BK, BODY-AVG, FACE-AVG, and PLACE-AVG contrasts. Panel I shows the MOTOR CUE-AVG contrast. Panels J, K, and L show the LANGUAGE MATH, STORY, and STORY-MATH contrasts. Panels M, N, O, and P show the TOM-RANDOM, RELATIONAL-MATCH, EMOTION FACES primary, and FACES-SHAPES contrasts. Data at http://balsa.wustl.edu/Jp5j.

The anterior bank of the parietal-occipital sulcus (POS) is an intriguing but poorly understood region that is transitional between early visual cortex and posterior cingulate association cortex. It includes 3 newly identified areas (though see (Glasser and Van Essen, 2011), where we suggested the existence of POS1 and POS2 based on myelin maps alone), plus one previously described area. The Dorsal Visual Transitional cortex (**DVT**) and Prostriate (**ProS**) cortex are transitional areas having architectural properties similar to their anterior neighbors and functional and connectional patterns more similar to their posterior neighbors (analogous to area 52 in Section #12 Insular and Frontal Opercular Cortex). The prostriate cortex **ProS** lies anterior to V1 (Sanides, 1970; Sanides and Vitzthum, 1965; Vogt, 2001), and its borders with V1, V2, and PreS were covered previously (Sections #1 Primary Visual Cortex (V1), #2 Early Visual Cortex, and #13 Medial Temporal Cortex). Despite its dramatically lower myelin content (Panel B), area **ProS** has strong functional connectivity with the early visual cortex. Relative to its superior neighbor POS1, area **ProS** is more lightly myelinated (Panel B), differs in functional connectivity (Panel D), and is more activated in the working memory primary contrasts and the FACES-SHAPES contrast (Panel P). Relative to its superior neighbor **DVT**, area **ProS** has less myelin (Panel B), is more activated in the working memory and relational primary contrasts, and is locally less deactivated in the FACE-AVG contrast (Panel G). Area **DVT's** posterior and superior borders were covered previously (Sections #2 Early Visual Cortex, #3 Dorsal Stream Visual Cortex, and #16 Superior Parietal Cortex). Although area **DVT** appears to be a very narrow strip when viewed on the inflated surface, it actually spans the entire fundus of the superior POS and is only slightly narrower than neighboring area V6. **DVT** has strong functional connectivity with higher dorsal stream visual cortex

and posterior superior parietal cortex, and weaker connectivity with its anterior neighbors POS1 and POS2. Relative to its antero-medial neighbor POS1, area **DVT** has less myelin (Panel B), is thinner (Panel C), differs in functional connectivity (Panel D), and is more activated in the working memory PLACE primary contrast. Relative to its antero-medial neighbor POS2, **DVT** has less myelin (Panel B), is thinner (Panel C), differs dramatically in functional connectivity (Panel D), is activated vs deactivated in the PLACE-AVG contrast (Panel H), EMOTION primary contrasts (e.g. Panel O), and FACES-SHAPES contrast (Panel P), is less deactivated in the LANGUAGE STORY and STORY-MATH contrasts (Panels K and L), is more activated in the SOCIAL primary contrasts, and is less deactivated in the TOM-RANDOM contrast (Panel M).

Area **POS2** is a highly distinctive area, as it differs dramatically from its neighbors in the four major feature categories (myelin, thickness, resting state connectivity, and task activations). Additionally, **POS2** has notably large BOLD fluctuations, and thus high Contrast to Noise Ratio (CNR) in functional neuroimaging. Particularly distinctive is the strong functional connectivity of POS2 with the retrosplenial complex (RSC). Because of its distinctiveness, the area is an excellent candidate for more detailed study with neuroanatomically informed and careful functional neuroimaging methods. The borders of **POS2** with DVT postero-laterally and 7PL and 7Pm superiorly have already been described (above and in Section #16 Superior Parietal Cortex). Relative to its antero-medial neighbor 7m, area **POS2** has more myelin (Panel B), is thinner (Panel C), differs strongly in functional connectivity (Panel D), is less activated in the FACE-AVG contrast (Panel G), and is more deactivated in the LANGUAGE MATH and STORY (Panels J and K), TOM-RANDOM (Panel M), and FACES-SHAPES (Panel P) contrasts. Relative to its inferior neighbor POS1, area **POS2** has more myelin (Panel B), is thinner (Panel C), differs in functional connectivity (Panel D), is activated vs deactivated in the BODY-AVG (Panel F) and FACE-AVG contrasts (Panel G), is deactivated vs activated in the PLACE-AVG contrast (Panel H), is more activated in the MOTOR CUE-AVG (Panel I) contrast, is more deactivated in the LANGUAGE MATH and STORY contrasts (Panels J and K), and is strongly deactivated vs activated in the TOM-RANDOM contrast (Panel M).

Relative to its supero-medial neighbor 7m, area **POS1** has more myelin (Panel B), differs in functional connectivity (Panel D), is strongly deactivated vs mixed activated/deactivated in the working memory 2BK-0BK contrast (Panel E), is deactivated vs activated in the FACE-AVG (Panel G) and FACES-SHAPES (Panel P) contrasts, is activated vs deactivated in the PLACE-AVG contrast (Panel H), is more deactivated in the LANGUAGE STORY contrast (Panel K), is deactivated vs activated in the STORY-MATH contrast (Panel L), and is more deactivated in the RELATIONAL-MATCH contrast (Panel N). Relative to its antero-medial neighbor v23ab, **POS1** differs in functional connectivity (Panel D), is deactivated vs activated in the FACE-AVG contrast (Panel G), activated vs deactivated in the PLACE-AVG contrast (Panel H), less deactivated in the MOTOR CUE-AVG contrast (Panel I), and deactivated vs activated in the STORY-MATH (Panel L) and FACES-SHAPES (Panel P) contrasts. Finally, relative to its antero-medial neighbor, the retrosplenial complex (RSC), area **POS1** has much less myelin (Panel B), is much thicker (Panel C), differs in functional connectivity (Panel D), is deactivated vs activated in the BODY-AVG contrast (Panel F), more activated in the PLACE-AVG contrast (Panel H), and less activated in the MOTOR CUE-AVG contrast (Panel I). Given the strong activation of area **POS1** in the PLACE-AVG task contrast, it likely corresponds to the scene-selective region identified as 'retrosplenial

cortex' in some neuroimaging studies (e.g., (Nasr et al., 2011)). However, it is a misnomer to call this region retrosplenial cortex, perhaps fostered by Brodmann's schematic drawing in which cortex behind the splenium of the corpus callosum was expanded so that areas 29 and 30 within the callosal sulcus could be more easily viewed. In reality these areas do not actually extend onto the anterior bank of the parietal occipital sulcus where POS1 resides (Palomero-Gallagher et al., 2009; Vogt, 2009).

The real retrosplenial complex (**RSC**) is a very distinct complex of areas (including Brodmann's areas 29 and 30, (Palomero-Gallagher et al., 2009; Vogt, 2009) that lies within the posterior callosal sulcus. Besides being very tightly coupled with area POS2, the RSC is dramatically more heavily myelinated and thinner than most of its neighbors (Panels B, C, and (Glasser and Van Essen, 2011)). The border between RSC and PreS inferiorly was already covered (Section #13 Medial Temporal Cortex). Relative to its posterior neighbor area v23ab, the **RSC** has more myelin (Panel B), is thinner (Panel C), differs in functional connectivity (Panel D), is less deactivated in the working memory 2BK-0BK (Panel E) and GAMBLING primary contrasts, is activated vs deactivated in the MOTOR CUE-AVG contrast (Panel I), is more deactivated in the LANGUAGE STORY contrast (Panel K), and is deactivated vs activated in the STORY-MATH contrast (Panel L). Relative its superior neighbor d23ab, the **RSC** is more heavily myelinated (Panel B), thinner (Panel C), differs in functional connectivity (Panel D), is activated vs deactivated in the 2BK-0BK (Panel E) and GAMBLING primary contrasts, is more activated in the MOTOR-AVG contrast, is more deactivated in the LANGUAGE STORY contrast (Panel K), is deactivated vs activated in the LANGUAGE STORY-MATH contrast (Panel L), and is more deactivated in the TOM-RANDOM contrast (Panel M). Relative to its superior neighbor 23d, the **RSC** has more myelin (Panel B), is thinner (Panel C), differs in functional connectivity (Panel D), is more activated in the MOTOR CUE-AVG contrast (Panel I) and more deactivated in the LANGUAGE STORY-MATH contrast (Panel L). Relative to its anterior neighbor 33pr, the **RSC** has more myelin (Panel B), differs in functional connectivity (Panel D), is more activated in the MOTOR CUE-AVG contrast (Panel I) and is more deactivated in the LANUGAGE STORY (Panel K) and TOM-RANDOM (Panel M) contrasts. Like POS2, the real retrosplenial cortex is an excellent candidate for further neuroimaging study using methods that accurately align cortical areas across subjects and avoid excessive spatial blurring.

The most superior portion of the medial parietal cortex was already covered in Section #16 Superior Parietal Cortex (7PL, 7Pm, 7Am), but two areas, **7m** and **PCV** remain to be covered here. Area **7m**, corresponding to area 7m of (Scheperjans et al., 2008a; Scheperjans et al., 2008b), has strong functional connectivity with task negative network areas PGi and PGs in lateral parietal cortex. Its posterior and superior borders with POS2, POS1, and 7Pm have been covered already (above and in Section #16 Superior Parietal Cortex). Relative to its inferior neighbor v23ab, area **7m** is less myelinated (Panel B), is more activated in the working memory 2BK-0BK (Panel E) and TOM-RANDOM (Panel M) contrasts and in the RELATIONAL and EMOTION primary contrasts (e.g. Panel O), is less deactivated in the LANGUAGE MATH contrast (Panel J), and is activated vs deactivated in the LANGUAGE STORY contrast (Panel K). Relative to its anterior neighbor 31pd, area **7m** is thicker (Panel C), differs in functional connectivity (Panel D), is more activated in the working memory 2BK-0BK (Panel E), FACE-AVG (Panel G), and FACES-SHAPES (Panel P) contrasts, is less deactivated in the LANGUAGE MATH contrast (Panel J), and is activated vs deactivated in the LANGUAGE STORY contrast (Panel K, in the right hemisphere). Relative

to its superior neighbor **PCV**, area **7m** differs in functional connectivity (Panel D), is more activated in the FACE-AVG (Panel G), STORY-MATH (Panel L), and FACES-SHAPES (Panel P) contrasts, and more deactivated in the PLACE-AVG contrast (Panel H). The newly identified PreCuneus Visual area, **PCV,** is distinctive in its strong functional connectivity with areas STV, TPOJ3, and DVT. Area **PCV's** superior (7Am), posterior (7Pm), and anterior neighbors (5mv) have already been covered in Sections #16 Superior Parietal Cortex and #7 Paracentral Lobular and Mid Cingulate Cortex. Relative to its inferior neighbor 31pd, area **PCV** differs strongly in functional connectivity (Panel D), is less activated in the STORY-MATH contrast (Panel L), and is more activated in the EMOTION primary contrasts (e.g. Panel O). Relative to its anterior neighbor 31a, area **PCV** is more heavily myelinated (Panel B), is thinner (Panel C), differs strongly in functional connectivity, is activated instead of deactivated in the FACE-AVG contrast (Panel G), is less activated in the PLACE-AVG contrast (Panel H), and is activated/less deactivated in the STORY-MATH (Panel L) contrast. Relative to its anterior neighbor 23c, area **PCV** has more myelin (Panel B), differs in functional connectivity (Panel D), is more activated in the FACE-AVG (Panel G) and STORY-MATH (Panel L) contrasts, is less activated in the PLACE-AVG contrast (Panel H), and is activated vs deactivated in the FACES-SHAPES contrast (Panel P). Area PCV likely corresponds to a precuneus ('PrCu') visual area showing retinotopic organization (Sereno et al., 2013). Also, it is noteworthy that the functional connectivity gradients in this region are strikingly affected by global or mean grey signal regression, which shifts the gradient ridge that lies along the inferior and posterior border (Panel D) towards the center of area **PCV**.

Brodmann's area 23 in posterior cingulate cortex has been subdivided in a variety of ways in previous architectonic studies. Our parcellation agrees most closely with that of (Palomero-Gallagher et al., 2009; Vogt, 2009), in which 23a and 23b were combined into 23ab, but then split into inferior and superior subdivisions, which we identify respectively as **v23ab** and **d23ab**. (Vogt's parcellation of area 23 also includes areas 23c and 23d discussed below.) The posterior (7m), inferior (POS1), and anterior (RSC) borders of area **v23ab** were already covered above. Relative to its superior neighbor 31pd, area **v23ab** is thicker (Panel C), differs modestly in functional connectivity (Panel D), is less activated in the STORY-MATH contrast (Panel L), and is more deactivated in the RELATIONAL-MATCH contrast (Panel N). Relative to its superior neighbor area 31pv, area **v23ab** is thicker (Panel C), differs modestly in functional connectivity (Panel D), is more deactivated in the RELATIONAL-MATCH contrast (Panel N), and is locally deactivated vs activated in the FACES-SHAPES contrast (Panel P). Relative to its supero-anterior neighbor area d23ab, area **v23ab** differs modestly in functional connectivity (Panel D) and is more deactivated in the RELATIONAL-MATCH contrast (Panel N). Relative to superior neighbor area 31pv, area **d23ab** is dramatically thicker (Panel C), as was previously shown in (Glasser and Van Essen, 2011). Relative to its anterior neighbor area 23d, area **d23ab** differs in functional connectivity (Panel D), is deactivated vs activated in the working memory 2BK-0BK contrast (Panel E), and is less deactivated in the STORY-MATH (Panel L), TOM-RANDOM (Panel M), and FACES-SHAPES (Panel P) contrasts.

Superior to areas v23ab and d23ab is area 31 (Palomero-Gallagher et al., 2009; Vogt, 2009), which we have divided into three areas, **31pv**, **31pd**, and **31a**. Relative to is supero-posterior neighbor area 31pd, area **31pv** has more myelin (Panel B), is thicker (Panel C), is more deactivated in the LANGUAGE STORY contrast (Panel K), and is deactivated vs

activated in the TOM-RANDOM contrast (Panel M). Relative to its superior neighbor area 31a, area **31pv** has more myelin (Panel B), differs modestly in functional connectivity (Panel D), is more activated in the BODY-AVG contrast (Panel F), is activated vs deactivated in the FACE-AVG (Panel G) and STORY-MATH (Panel L) contrasts, and is deactivated vs activated in the PLACE-AVG (Panel H) and TOM-RANDOM (Panel M) contrasts. The borders of area **31pd** with area v23ab, 7m, and PCV were already described above. Relative to its anterior neighbor area 31a, area **31pd** has more myelin (Panel B), is thinner (Panel C), differs modestly in functional connectivity (Panel D), and is less activated in the BODY-AVG contrast (Panel F), is more activated in the FACE-AVG contrast (Panel G), is deactivated vs activated in the PLACE-AVG contrast (Panel H), is more deactivated in the LANGUAGE MATH contrast (Panel J), and is activated vs deactivated in the STORY-MATH contrast (Panel L). Relative to its superior neighbor area 23c, area **31a** is thicker (Panel C), differs dramatically in functional connectivity (Panel D), and is less activated in the MOTOR CUE-AVG contrast (Panel I). Relative to its anterior neighbor area 23d, area **31a** differs modestly in functional connectivity (Panel D), and is less activated in the BODY-AVG contrast (Panel F), is deactivated vs activated in the FACE-AVG contrast (Panel G), is activated vs deactivated in the PLACE-AVG (Panel H), TOM-RANDOM (Panel M), and FACES-SHAPES (Panel P) contrasts, and is less deactivated in the LANGUAGE MATH contrast (Panel J).

Areas **23c** and **23d** both lie superior and anterior to the other areas in the posterior cingulate region (Palomero-Gallagher et al., 2009; Vogt, 2009). Area **23d** is a very thick (Panel C), lightly myelinated area (Panel B) that differs strongly from its superior neighbors in functional connectivity (Panel D). Relative to its anterior neighbor p24pr, area **23d** differs in functional connectivity (Panel D), and is deactivated vs weakly activated in the TOOL-AVG contrast, is less activated in the CUE-AVG contrast (Panel I), is more deactivated in the LANGUAGE MATH contrast (Panel J), is activated vs deactivated in the SOCIAL primary contrasts, and is deactivated vs activated in the FACES-SHAPES contrast (Panel P). Area **23d** is also statistically more heavily myelinated (Panel B) and more activated in the LANGUAGE STORY contrast (Panel K) than p24pr. Relative to its superior neighbor area **23c**, area **23d** is thicker (Panel C), differs strongly in functional connectivity (Panel D), and is less activated in the CUE-AVG contrast (Panel I) and deactivated vs activated in the TOM-RANDOM contrast (Panel M). Area **23c** is a lightly myelinated (Panel B), moderately thick area (Panel C) that lies between the task negative posterior cingulate cortex and the sensorimotor cortex that has strong functional connectivity with the task positive network. Most of its borders have already been covered (above or in Section #7 Paracentral Lobular and Mid Cingulate Cortex: 5mv, 24dd, 24dv). Relative to its anterior neighbor p24pr, area **23c** is more heavily myelinated (Panel B) and thinner (Panel C).

19. Anterior Cingulate and Medial Prefrontal Cortex

The anterior cingulate and medial prefrontal cortex, lying along the medial aspect of each hemisphere and anterior to motor/premotor areas, is generally lightly myelinated and thick. It has functional connectivity with a variety of networks and differential functional activations in many different tasks. We divided this region into 15 areas: 33pr, p24pr, a24pr, p24, a24, p32pr, a32pr, d32, p32, s32, 8BM, 9m, 10v, 10r, and 25, surrounded by areas RSC, 23d, 23c, 24dv, SCEF, SFL, 8BL, 9a, 9p, 10d, 10pp, OFC, and pOFC. The

organization of the region reflects two dominant principles: 1) Architecturally, there are three major bands of cingulate cortex: a narrow strip of thin and lightly myelinated periallocortex (classical area 33) lying inferiorly; a very thick, very lightly myelinated proisocortex (classical area 24) in the middle; and a thick, lightly myelinated paralimbic region (classical area 32) superiorly (Glasser and Van Essen, 2011; Paus, 2001). The medial prefrontal cortex lies outside these regions superiorly, anteriorly, and inferiorly. 2) Based on functional connectivity, there is a very strong gradient ridge that runs obliquely, from supero-posterior to antero-inferior. Behind this transition (posterior and inferior) cortex is more connected with higher somatosensory and motor regions and the task positive network. In front of the transition, cortex is strongly associated with the task negative network. The multi-modal information used to parcellate the anterior cingulate and medial prefrontal cortex is shown in Figure 22. Panel A shows the areas on a folding map.

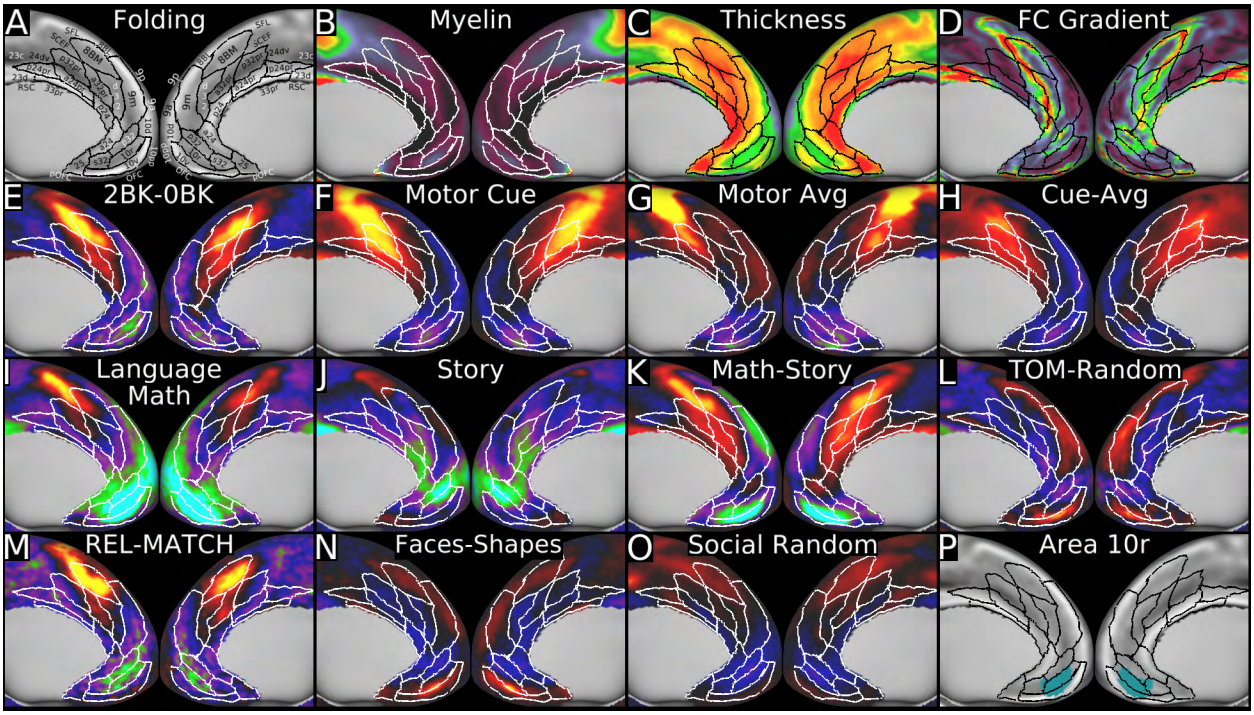

Figure 22 shows multi-modal information used to parcellate the anterior cingulate cortex. Panel A shows the areas on a group average folding map. Panels B and C show the myelin and cortical thickness maps. Panel D shows the resting state functional connectivity gradients. Panels E, F, G, and H show the working memory 2BK-0BK, MOTOR CUE, AVG, and CUE-AVG task contrasts. Panels I, J, K, and L show the LANGUAGE MATH, STORY, MATH-STORY and SOCIAL TOM-RANDOM contrasts. Panels M, N, and O show the RELATIONAL-MATCH and EMOTION FACES-SHAPES contrasts and the SOCIAL RANDOM primary contrast. Panel P shows area 10r from the (Ongur et al., 2003) publication. Data at http://balsa.wustl.edu/Q9xk.

The periallocortex (classical area 33) is a thin (Panel C), lightly myelinated strip (Panel B) that lies in front of the retrosplenial cortex (RSC). Vogt recognized three subdivisions of area 33: area 33 proper plus a33' and p33' (Vogt, 2009). Our data provides evidence for a single area in this region that we identify as **33pr** (pr represents ' because the latter is a reserved character in many programming languages), corresponding to the location of Vogt's a33' and p33'. The more anterior area 33 subdivision of Vogt may be

largely excluded from the grayordinates space established by the medial wall mask (though part of it may be visible in the right hemisphere), which likely also encroaches on part of 33pr (more so in the left hemisphere). A future higher resolution standard grayordinates space would benefit from improvements to the medial wall mask here (as well as exclusion of the hippocampal complex, as noted above). The posterior border of area **33pr** with the RSC was covered in Section #18 Posterior Cingulate Cortex. Relative to its superior neighbor p24pr, area **33pr** is much thinner (Panel C), has slightly more myelin (Panel B), differs modestly in resting state functional connectivity (Panel D), is less deactivated in the LANGUAGE MATH contrast (Panel I), and is more activated in the MATH-STORY contrast (Panel K). Relative to its superior neighbor a24pr, area **33pr** (Panel C) is again much thinner (Panel C) and has slightly more myelin (Panel B). It also is modestly activated vs deactivated in the TOM-RANDOM contrast (Panel L) and is less deactivated in the LANGUAGE STORY contrast (Panel J). In both cases, cortical thickness was a primary criterion for delineating the border using the semi-automated border optimize tool. Our 33pr may correspond to area 16 from the Vogt-Vogt school (Nieuwenhuys et al., 2015).

The proisocortex (area 24) is a thick (Panel C), very lightly myelinated (Panel B) strip that lies superior to area 33. Vogt (Vogt, 2009) recognized three subdivisions of area 24 (area 24 proper and a24' and p24'). We identified four areas, including a more anterior pair (a24 and p24, which are anterior and posterior subdivisions of Vogt's area 24 proper) and a more posterior pair (**a24pr** and **p24pr**, corresponding to Vogt's a24' and p24', with pr substituting for '). Vogt also identified a more superior triplet, areas 24c, a24c', and p24c', and these areas likely partially overlap with our areas p24, a24, a24pr, and p24pr. The borders of the most posterior subdivision, **p24pr** with area 23d, 23c, and 24dv were already covered (Sections #18 Posterior Cingulate Cortex and #7 Paracentral Lobular and Mid Cingulate Cortex). Relative to its anterior neighbor a24pr, area **p24pr** differs in functional connectivity (Panel D), is less activated in the MOTOR CUE (Panel F) and CUE-AVG (Panel H) contrasts, is less deactivated in the contralateral ?H-AVG hand motor and LANGUAGE STORY contrasts (Panel J), is deactivated vs activated in the T-AVG face motor contrast, and is activated vs deactivated in the SOCIAL RANDOM primary contrast (Panel O). Moving anteriorly, relative to its superior neighbor p32pr, area **a24pr** has dramatically less myelin (Panel B), is less activated in the MOTOR CUE (Panel F), AVG (Panel G), and LANGUAGE MATH-STORY (Panel K) contrasts and in a variety of primary contrasts (e.g. Panel O), is deactivated vs activated in the LANGUAGE MATH contrast (Panel I), and is more deactivated in the LANGUAGE STORY contrast (Panel J). Relative to its superior neighbor a32pr, area **a24pr** has dramatically less myelin (Panel B), differs in functional connectivity (Panel D), and is deactivated vs activated in the LANUAGE MATH (Panel I) and RELATIONAL-MATCH (Panel M) contrasts and the SOCIAL RANDOM primary contrast (Panel O). Relative to its anterior neighbor p24, area **a24pr** differs in functional connectivity (Panel D), is more activated in the MOTOR CUE contrast (Panel E), is weakly activated vs weakly deactivated in the MOTOR AVG contrast (Panel F), and is less deactivated in the LANGUAGE STORY contrast (Panel J).

Further anteriorly, relative to its superior neighbor a32pr, area **p24** has less myelin (Panel B), is thicker (Panel C), differs in functional connectivity (Panel D), is less activated in the working memory 2BK-0BK contrast (Panel E), is deactivated vs activated in the LANGUAGE MATH (Panel I) and RELATIONAL-MATCH (Panel M) contrasts and in primary contrasts such as the SOCIAL RANDOM contrast (Panel O), and is less activated in the

LANGUAGE MATH-STORY contrast (Panel K). Relative to its superior neighbor d32, area **p24** has less myelin (Panel B), is thicker (Panel C), differs strongly in functional connectivity (Panel D), and is more activated in the MOTOR CUE (Panel F) and CUE-AVG (Panel H) contrasts. Relative to its anterior neighbor a24, area **p24** differs strongly in functional connectivity (Panel D), is activated vs deactivated in the MOTOR CUE (Panel F) and CUE-AVG (Panel H) contrasts, and is less deactivated in the LANGUAGE MATH contrast (Panel I). Further anteriorly, relative to its superior neighbor 9m, area **a24** has less myelin (Panel B), is thicker (Panel C), differs modestly in functional connectivity (Panel D), is more deactivated in the LANGUAGE STORY contrast (Panel J), and is deactivated vs activated in the TOM-RANDOM (Panel L) and FACES-SHAPES (Panel N) contrasts. Relative to its anterior neighbor p32, area **a24** has less myelin (Panel B), is thicker (Panel C) and differs in functional connectivity (Panel D). Relative to its inferior neighbor s32, area **a24** has less myelin (Panel B), is thicker (Panel C), and differs in functional connectivity (Panel D). Relative to its posterior neighbor 25, area **a24** has less myelin (Panel B) and differs in functional connectivity (Panel D).

The paralimbic cortex (area 32) is a thick (Panel C), lightly myelinated (Panel B) strip that surrounds the area 24 complex on its superior and anterior sides. Vogt recognized four subdivisions of area 32: area 32' most posteriorly followed by areas d32, p32, and s32 progressing anteriorly then inferiorly (Vogt, 2009). We subdivide area 32 into five subdivisions that are split by area 9m (see below). The three most posterior areas are **p32pr**, **a32pr** (posterior and anterior subdivisions of Vogt's 32') and **d32** (overlapping with d32 of Vogt). Anterior to 9m we identified areas p32 and s32 (overlapping with p32 and s32 of Vogt). Our areas 32 may include portions of Vogt's areas 24c, a24c', and p24c'. The borders of the most posterior subdivision of area 32, **p32pr**, with areas 24dv and SCEF were already covered (Section #7 Paracentral Lobular and Mid Cingulate Cortex), and its border with a24pr was covered above. Relative to its anterior neighbor a32pr, area **p32pr** differs in functional connectivity (Panel D), is more activated in the MOTOR CUE (Panel F), MOTOR AVG (Panel G), and EMOTION primary contrasts and in the RELATIONAL REL-MATCH contrast (Panel M). Moving anteriorly and relative to its superior neighbor 8BM, area **a32pr** differs strongly in functional connectivity (Panel D), is more activated in the working memory 2BK-0BK (Panel E), MOTOR CUE (Panel F), and CUE-AVG (Panel H) contrasts, is less activated in the SOCIAL primary contrasts (e.g. Panel O) and RELATIONAL-MATCH contrast (Panel M), and is deactivated vs activated in the FACES-SHAPES contrast (Panel N). Relative to its anterior neighbor d32, area **a32pr** differs strongly in functional connectivity (Panel D), is more activated in the MOTOR CUE (Panel F) and CUE-AVG (Panel H) contrasts and in the RELATIONAL primary contrasts. Further anterior and relative to its superior neighbor 8BM, area **d32** has modestly less myelin (Panel B), differs modestly in functional connectivity (Panel D), is less activated in the working memory 2BK-0BK contrast (Panel E) and in the SOCIAL and RELATIONAL primary contrasts (e.g. Panel O), is more deactivated in the LANGUAGE STORY contrast (Panel J), is strongly activated vs weakly activated or deactivated in the RELATIONAL-MATCH contrast (Panel M), and is deactivated vs activated in the FACES-SHAPES contrast (Panel N). Relative to its anterior neighbor 9m, area **d32** has modestly more myelin on the left (Panel B), differs in functional connectivity (Panel D), is activated vs deactivated in the working memory 2BK-0BK (Panel E) and LANGUAGE MATH-STORY (Panel K) contrasts, and is deactivated vs activated in the TOM-RANDOM contrast (Panel L).

In our parcellation, and contrary to Vogt's parcellation, we find a region of cortex that intercedes between area d32 and area **p32** that is more similar to area 9m than to either area d32 or p32. There may be substantially inter-individual heterogeneity in this region, as this portion of cortex shares some properties with d32 as well. Further anteriorly and relative to its superior neighbor 9m, area **p32** differs in functional connectivity (Panel D), is activated vs deactivated in the MOTOR CUE-AVG (Panel H) and LANGUAGE MATH-STORY (Panel K) contrasts, is strongly deactivated vs weakly deactivated or activated in the LANGUAGE STORY contrast (Panel J), and is deactivated vs activated in the TOM-RANDOM (Panel L) and FACES-SHAPES (Panel N) contrasts. Relative to its anterior neighbor 10d, area **p32** has less myelin (Panel B), is thicker (Panel C), differs in functional connectivity (Panel D), and is activated vs deactivated in the MOTOR CUE-AVG (Panel H) and MATH-STORY (Panel K) contrasts. Relative to its inferior neighbor 10r, area **p32** is more lightly myelinated (Panel B), thicker (Panel C), differs in functional connectivity (Panel D), and is activated vs deactivated in the MOTOR CUE-AVG (Panel H) and LANGUAGE MATH-STORY (Panel K) contrasts. Relative to its inferior neighbor s32, area **p32** differs in functional connectivity (Panel D), is weakly activated/deactivated vs strongly deactivated in the LANGUAGE MATH-STORY contrast (Panel K) and deactivated vs activated in the TOM-RANDOM contrast (Panel L). Moving inferiorly and relative to its anterior neighbor 10r, area **s32** has less myelin (Panel B), is thicker (Panel C), differs modestly in functional connectivity (Panel D), and is less deactivated in the CUE-AVG contrast (Panel H). Relative to its inferior neighbor 10v, area **s32** has more myelin (Panel B) and differs modestly in functional connectivity (Panel D). Relative to its posterior neighbor 25, area **s32** has less myelin (Panel B) and is thinner (Panel C).

The remaining areas in this region are largely medial or orbital prefrontal areas. Most superior and posterior is area **8BM**, whose posterior border with SCEF was covered in Section #7 Paracentral Lobular and Mid Cingulate Cortex and whose inferior borders were covered above. Area 8BM is so named because it overlaps with the medial portion of area 8B from (Petrides and Pandya, 1999). Relative to its supero-posterior neighbor SFL, area **8BM** differs strongly in functional connectivity (Panel D), is more activated in the working memory 2BK-0BK (Panel E) and MATH-STORY (Panel K) contrasts, and is more activated in the RELATIONAL-MATCH contrast (areas are more different on the right, Panel M). Relative to its supero-lateral neighbor 8BL, area **8BM** is thicker (Panel C), differs in functional connectivity (Panel D), is activated vs deactivated in the working memory 2BK-0BK (Panel E), MOTOR CUE-AVG (Panel H), LANGUAGE MATH-STORY (Panel K), and RELATIONAL-MATCH (Panel M) contrasts. Relative to its superior neighbor 9m, area **8BM** has more myelin (Panel B), differs in functional connectivity (Panel D), is activated vs deactivated in the working memory 2BK-0BK (Panel E), MOTOR CUE (Panel F) and CUE-AVG (Panel H), LANGUAGE MATH (Panel I) and MATH-STORY (Panel K), and RELATIONAL-MATCH (Panel M) contrasts, and is deactivated vs activated in the TOM-RANDOM contrast (Panel L).

Also lying mostly on the medial surface is area **9m,** the medial portion of area 9 from (Petrides and Pandya, 1999). The inferior borders of area **9m** with 8BM, d32, a24, and p24 were covered above. Relative to its posterior neighbor 8BL, area **9m** has modestly less myelin (Panel B), differs modestly in functional connectivity (Panel D), is more activated in the TOM-RANDOM contrast (Panel L), and is deactivated vs activated in the RELATIONAL-MATCH contrast (Panel M). Relative to its superior neighbor 9p, area **9m** has

less myelin (Panel B), is much thicker (Panel C), differs modestly in functional connectivity (Panel D), is activated/less deactivated vs more deactivated in the LANGUAGE STORY contrast (Panel J), and is more activated in the TOM-RANDOM contrast (Panel L). Relative to its lateral neighbor 9a, area **9m** has less myelin (Panel B), is thicker (Panel C), and differs in functional connectivity (Panel D) in the right hemisphere and is deactivated instead of activated in the RELATIONAL-MATCH contrast in the left hemisphere (Panel M). Relative to its antero-lateral neighbor 10d, area **9m** has less myelin (Panel B), is thicker (Panel C), and differs in functional connectivity (Panel D).

We identified two medial subdivisions of area 10 (in contrast to (Ongur et al., 2003), who reported three, and the most posterior of theirs overlaps most with our area 25 and s32). The first area, **10r**, corresponds reasonably closely to area 10r as mapped by (Ongur et al., 2003) (Panel P). The posterior and superior borders of area **10r** with s32 and p32 were covered above. Relative to its superior neighbor 10d, area **10r** differs in functional connectivity (Panel D) and is more deactivated in the working memory 2BK-0BK (Panel E) and MOTOR CUE-AVG (Panel H) contrasts. Relative to its inferior neighbor 10v, area **10r** has more myelin (Panel B), is thinner (Panel C), differs modestly in functional connectivity (Panel D), is activated/less deactivated vs more deactivated in the LANGUAGE MATH-STORY contrast (Panel K), is deactivated vs activated in the TOM-RANDOM contrast (Panel L), and is more deactivated in the RELATIONAL-MATCH contrast (Panel M). Relative to its superior neighbor 10d, area **10v** is thicker (Panel B), differs in functional connectivity (Panel D), is more deactivated in the LANGUAGE MATH-STORY contrast (Panel K), is activated vs deactivated in the TOM-RANDOM contrast (Panel L), and is more activated in the FACES-SHAPES contrast (Panel N). Relative to its antero-lateral neighbor 10pp, area **10v** has less myelin (Panel B, in the left hemisphere), is thicker (Panel C), differs in functional connectivity (Panel D), and is more deactivated in the MATH-STORY contrast (Panel K). Relative to its infero-lateral neighbor OFC, area **10v** has less myelin (Panel B) and is thicker (Panel C, left border defined primarily using thickness). In the orbito-frontal complex, signal loss greatly reduced the quality of resting state and task fMRI data. This region will need to be revisited in the future, once MR technology allows improved signal quality (e.g. by better shimming or by using spin echo fMRI). Relative to its posterior neighbor 25, area **10v** has less myelin (Panel B) and is thinner (Panel C). Area **25** is a very thick (Panel C), lightly myelinated (Panel B) cortical area beneath the genu of the corpus callosum. Its borders with a24, s32, and 10v have been covered above. Its borders with OFC and pOFC are primarily delineated by a difference in cortical thickness (Panel C), given the above issue with signal loss. The area is so named because of its similarity in position to area 25 in Vogt's parcellation (Vogt, 2009). Area **25** also appears to be in a similar location to that reported in (Palomero-Gallagher et al., 2015). Their s24 may correspond to our a24 and their s32 to our s32. One difference is that they usually find at least a narrow strip of s24 between 25 and s32, which we did not observe. An alternative explanation is that the medial wall mask that defines the grayordinates space may exclude a portion or even most of area 25 (in addition to their anterior area 33, which is definitely excluded) and that what we call area 25 is their s24 (Palomero-Gallagher et al., 2015). Importantly, this region is also challenging to map because the functional imaging modalities are lower in quality in this region, which is strongly effected by b0-related gradient echo fMRI signal loss. Future studies with an expanded grayordinates space and better MRI acquisitions may revisit the parcellation and areal identifications in the subgenual cingulate region.

20. Orbital and Polar Frontal Cortex

The orbital and polar frontal cortex contains cortical areas with a variety of architectural and functional properties. We have subdivided this region into 11 areas and complexes: 47s, 47m, a47r, 11l, 13l, a10p, p10p, 10pp, 10d, OFC, and pOFC. They are surrounded by areas 25, 10v, 10r, p32, 9m, 9a, 9-46d, a9-46v, p47r, 47l, AVI, AAIC, and Pir. The (Ongur et al., 2003) surface-based parcellation aided in naming many of these areas (Ongur et al., 2003); see Panel O). The multi-modal information used to parcellate the orbital and polar frontal cortex is shown in Figure 23. Panel A shows the areas on a folding map.

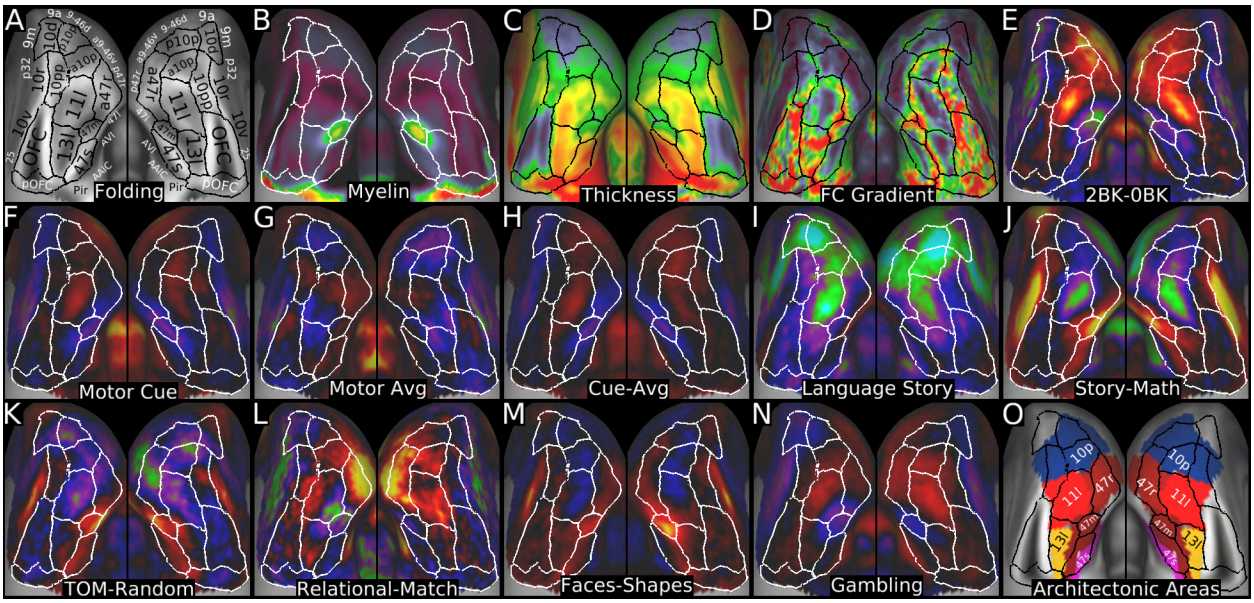

Figure 23 shows the multi-modal information that was used to parcellate the orbital and polar frontal cortex. Panel A shows the areas on a folding map. Panels B and C show myelin and cortical thickness maps. Panel D shows the resting state functional connectivity gradient. Panel E shows the working memory 2BK-0BK contrast. Panels F, G, and H show the MOTOR CUE, AVG, and CUE-AVG contrasts. Panels I and J show the LANGUAGE STORY and STORY-MATH contrasts. Panels K, L, M, and N show the TOM-RANDOM, RELATIONAL-MATCH, FACES-SHAPES, and GAMBLING primary contrasts. Panel O shows some areas (13l, 11l, 47m, 47s, 47r, and 10p) from the (Ongur et al., 2003) parcellation that were used to name areas in our parcellation. Data at http://balsa.wustl.edu/RkD2.

As mentioned in the preceding section, substantial b0-releated fMRI signal loss in the orbitofrontal cortex was an impediment to a fine-grained parcellation of this region. Using mainly architectural criteria, we identified two distinct complexes, the orbitofrontal complex (**OFC**) and the posterior orbitofrontal complex (**pOFC**) that include multiple architectonic areas by other parcellations (e.g. (Ongur et al., 2003). In particular, pOFC overlaps with areas 13a and 14c, and OFC overlaps with areas 11m, 13b, 13m, and 14r of (Ongur et al., 2003). With improved fMRI data quality (e.g. better shimming or spin echo fMRI), this region should be revisited. The medial borders of OFC and pOFC with 10v and 25 were covered previously in Section #20 Anterior Cingulate and Medial Prefrontal Cortex. Relative to its posterior neighbor pOFC, the **OFC** is thinner (Panel C) and has less myelin (Panel B), with cortical thickness being primarily used to delineate the boundary.

Relative to its lateral neighbor Pir, the **pOFC** is thicker (Panel C) and has less myelin (Panel B). Relative to its anterior neighbor 13l and antero-lateral neighbor 47s, the **pOFC** is thicker (Panel C) and has more myelin (Panel B). Relative to its lateral neighbor 13l, the **OFC** is thinner (Panel C) and has less myelin (Panel B). Relative to anterior-lateral neighbor 11l, the **OFC** is thinner (Panel C) and has slightly less myelin (Panel B). Relative to its antero-superior neighbor 10pp, the **OFC** is thinner (Panel C) and has slightly more myelin near the border (Panel B). The relative thinness of the OFC does not appear to be artifactual, insofar as histological studies also report this region to be thinner (Triarhou, 2007a, b; von Economo and Koskinas, 1925). Nonetheless, some of OFC cortex (particularly on inferiorly facing gyral crowns) may still be impacted by signal loss in the gradient echo T1w image, leading to artifactually thinner cortex. Artifacts in the myelin maps in this region were reduced relative to our previous study (Glasser and Van Essen, 2011) by using readout distortion correction of the T1w and T2w images so that they are not distorted relative to one another (Glasser et al., 2013), though signal loss in the T1w image likely still produces some artifacts on the inferiorly facing gyral crowns. Within this region, OFC and pOFC overlap with Fo1 and Fo2, though the boundary between OFC and pOFC is posterior to the boundary between Fo1 and Fo2 (Henssen et al., 2016).

Lateral to OFC, we identified areas **13l** and **11l**, based on their overlap with areas reported by (Ongur et al., 2003) (Panel O). Relative to its postero-lateral neighbor 47s, area **13l** differs in functional connectivity (Panel D) and is less activated in the TOM-RANDOM contrast (Panel K). Relative to its heavily myelinated lateral neighbor 47m, area **13l** has less myelin (Panel B), is thicker (Panel C), differs in functional connectivity (Panel D), is less deactivated in the MOTOR CUE-AVG contrast (Panel H), and is less activated in the LANGUAGE STORY-MATH (Panel J), TOM-RANDOM (Panel K), and FACES-SHAPES (Panel M) contrasts. Relative to its anterior neighbor 11l, area **13l** differs in functional connectivity (Panel D), is deactivated vs activated in the MOTOR CUE (Panel F) contrast, and is activated vs deactivated in the TOM-RANDOM (Panel K) and LANGUAGE STORY-MATH contrasts (Panel J). Relative to its postero-lateral neighbor 47m, area **11l** has much less myelin (Panel B), is thicker (Panel C), differs in functional connectivity (Panel D), is activated vs deactivated in the MOTOR CUE (Panel F) and CUE-AVG contrasts (Panel H), is more deactivated in the LANGUAGE STORY contrast (Panel I), is deactivated vs activated in the TOM-RANDOM contrast (Panel K), and is less activated/deactivated vs strongly activated in the FACES-SHAPES contrast (Panel M). Relative to its lateral neighbor a47r, area **11l** is thicker (Panel C), differs in functional connectivity (Panel D), is activated vs deactivated in the MOTOR CUE-AVG contrast (Panel H), and is deactivated vs activated in the LANGUAGE STORY-MATH (Panel J) and FACES-SHAPES (Panel M) contrasts. Relative to its superior neighbor a10p, area **11l** has less myelin near the border (Panel B), is thicker (Panel C), differs in functional connectivity (Panel D), and is more deactivated in the LANGUAGE STORY-MATH contrast (Panel J). Relative to its supero-medial neighbor 10pp, area **11l** is thicker (Panel C), differs in functional connectivity (Panel D), is more activated in the working memory 2BK-0BK contrast (Panel E), and is more deactivated in the STORY-MATH contrast (Panel J). These areas overlap extensively with area Fo3 (Henssen et al., 2016).

We subdivided area 47 into five areas, three of which (**47s**, **47m**, and **a47r**) are covered in this section, with the remaining two (47l, p47r) covered in the next Section #21 Inferior Frontal Cortex. The names of these areas reflect correspondences with the (Ongur

et al., 2003) parcellation, though in our parcellation, 47m does not extend as far posteriorly, and 47s extends more medially and does not extend as far laterally (Panel O). The most anterior area is **47s**, a lightly myelinated (Panel B), thick area (Panel C) that is connected to the language network and is more activated in the language task contrasts than many of its neighbors (Panels I and J). Its posterior borders with AAIC and AVI were covered in Section #12 Insular and Frontal Opercular Cortex, and its borders with 13l and pOFC were covered above. Relative to its superior neighbor 47m, area **47s** has less myelin (Panel B), differs in functional connectivity (Panel D), and is less activated by the STORY-MATH (Panel J), TOM-RANDOM (Panel K), and FACES-SHAPES (Panel M) contrasts. Relative to its supero-lateral neighbor 47l, area **47s** is thicker (Panel C), differs in functional connectivity (Panel D), and is less activated by the LANGUAGE STORY contrast (Panel I). Area **47m** is one of the more distinctive areas in the cerebral cortex. Unlike the rest of prefrontal cortex, area 47m is a hot spot of heavily myelination (Panel B), as we have noted previously (Glasser and Van Essen, 2011). It has strong functional connectivity with areas 10r and s32, and it shows more pronounced differential activation in various category task contrasts (BODY-AVG, FACE-AVG, PLACE-AVG, and TOOL-AVG) than do other prefrontal cortical areas (except perhaps area 10r). The borders of area 47m with 47s, 13l, and 11l have already been described above. Relative to its lateral neighbor 47l, area **47m** has more myelin (Panel B), differs in functional connectivity (Panel D), is deactivated vs activated in the LANGUAGE STORY contrast (Panel I), and is more activated in the FACES-SHAPES contrast (Panel M). Relative to its antero-lateral neighbor a47r, area **47m** has more myelin (Panel B), differs in functional connectivity (Panel D), is more deactivated in the LANGUAGE MATH contrast, and is more activated in the FACES-SHAPES contrast (Panel M).

Relative to its posterior neighbor 47l, area **a47r** differs in functional connectivity (Panel D), is deactivated vs activated in the LANGUAGE STORY contrast (Panel I), is less activated/deactivated vs activated in the LANGUAGE STORY-MATH (Panel J) and TOM-RANDOM (Panel K) contrasts, is activated vs deactivated in the RELATIONAL primary contrasts, and is more activated in the RELATIONAL-MATCH contrast (Panel L). Relative to its superior neighbor p47r, area **a47r** is more lightly myelinated (Panel B), thicker (Panel C), differs in functional connectivity (Panel D), and is more deactivated in the LANGUAGE MATH contrast, and is less deactivated in the STORY-MATH contrast (Panel J). Relative to its supero-medial neighbor a9-46v, area **a47r** differs in functional connectivity (Panel D), is modestly less activated in the working memory 2BK-0BK contrast (Panel E), is deactivated vs activated in the MOTOR CUE contrast (Panel F), less deactivated in the LANGUAGE STORY-MATH contrast (Panel J), and is activated vs deactivated in the FACES-SHAPES contrast (Panel M). The topology of area **a47r**'s superior border differs in the left and right hemispheres, as it adjoins both a10p and p10p in the right hemisphere, but only a10p on the left. Interestingly the (Yeo et al., 2011) functional network parcellation shows an analogous asymmetry in this region. Relative to its medial neighbor a10p, area **a47r** differs in functional connectivity (Panel D), differs in the MOTOR CUE-AVG contrast (Panel H, deactivated vs activated on the left and less activated on the right), and is less deactivated in the LANGUAGE STORY-MATH contrast (Panel J), is more activated in the RELATIONAL-MATCH contrast (Panel L), and is activated vs deactivated in the FACES-SHAPES contrast (Panel M). In the right hemisphere relative to its postero-medial neighbor p10p, area **a47r** differs in functional connectivity (Panel D), is more activated in the

primary GAMBLING contrasts (e.g. Panel N) and the RELATIONAL-MATCH (Panel L) contrasts and is less activated in the MOTOR CUE-AVG (Panel H).

We now discuss the remaining four subdivisions of area 10: **10pp**, **a10p**, **p10p** and **10d**. These largely overlap with area Fp1 of (Bludau et al., 2014), whereas areas 10r and 10v (covered in Section #19 Anterior Cingulate and Medial Prefrontal Cortex) largely overlap with Fp2 (though 10d likely also overlaps partly with Fp2). Our polar divisions of area 10 overlap extensively with area 10p in (Ongur et al., 2003) (which was incompletely defined along its superior extent). The most polar subdivision of area 10, 10pp, has medial (10v), inferior (OFC), and lateral (11l) borders that were covered already (above or in Section #19 Anterior Cingulate and Medial Prefrontal Cortex). Relative to its lateral neighbor a10p, area **10pp** differs in functional connectivity (Panel D), is less activated in the working memory 2BK-0BK contrast (Panel E), and is activated vs deactivated in the LANGUAGE STORY-MATH (Panel J), TOM-RANDOM (Panel K), and FACES-SHAPES (Panel M) contrasts. Relative to its superior neighbor 10d, area **10pp** differs in functional connectivity (Panel D) and is activated vs deactivated in many primary task contrasts (e.g. Panel N). Parcellation of cortex in the vicinity of area 10pp should be revisited once better methods of suppressing susceptibility-induced signal loss from the frontal sinus are available, as this process may affect its borders. The lateral (a47r), inferior (11l), and medial (10pp) borders of area **a10p** were already covered above. Relative to supero-posterior neighbor p10p, area **a10p** is thicker (Panel C), differs in functional connectivity (Panel D), and is activated vs deactivated in the GAMBLING primary contrasts (e.g. Panel N). Corresponding to the above asymmetry in areal topology of a47r, area **a10p** adjoins area a9-46v only in the left hemisphere. In the left hemisphere relative to posteriorly bordering area a9-46v, area **a10p** differs in functional connectivity (Panel D), is less deactivated in the LANGUAGE STORY-MATH contrast (Panel J), and is more activated in the RELATIONAL primary contrasts. Relative to its lateral neighbor a9-46v, area **p10p** differs in functional connectivity (Panel D), is deactivated vs activated in the GAMBLING and EMOTION primary contrasts (e.g. Panel N), and is less deactivated in the STORY-MATH contrast (Panel J). Relative to its posterior neighbor 9-46d, area **p10p** is thinner (Panel C), differs in functional connectivity (Panel D), is deactivated vs activated in the GAMBLING and EMOTION primary contrasts (Panel N), is more activated in the MOTOR CUE contrast (Panel F), and is less deactivated in the LANGUAGE STORY-MATH contrast (Panel J). Relative to its postero-medial neighbor 9a, area **p10p** has more myelin (Panel B), differs in functional connectivity (Panel D), is activated vs deactivated in the working memory 2BK-0BK contrast (Panel E), and is deactivated vs activated in the MOTOR AVG contrast (Panel G). Relative to its medial neighbor 10d, area **p10p** differs in functional connectivity (Panel D), is activated vs deactivated in the working memory 2BK-0BK contrast (Panel E) and the MOTOR CUE-AVG contrast (Panel H), and is deactivated vs activated in the LANGUAGE STORY-MATH contrast (Panel J). Relative to its posterior neighbor 9a, area **10d** has more myelin (Panel B), differs in functional connectivity (Panel D), and is more deactivated in the GAMBLING primary contrasts (Panel N).

21. Inferior Frontal Cortex

The inferior frontal cortex contains language-associated areas, including Broca's area, plus a number of moderately myelinated areas in the inferior frontal sulcus. We

subdivided inferior frontal cortex into eight areas: 44, 45, IFJp, IFJa, IFSp, IFSa, 47l, and p47r, which are surrounded by areas FOP4, FOP5, AVI, 47s, 47m, a47r, a9-46v, 46, p9-46v, 8C, PEF, and 6r. Figure 24 shows multi-modal information used to parcellate the inferior frontal cortex. Panel A shows the areas on a folding map.

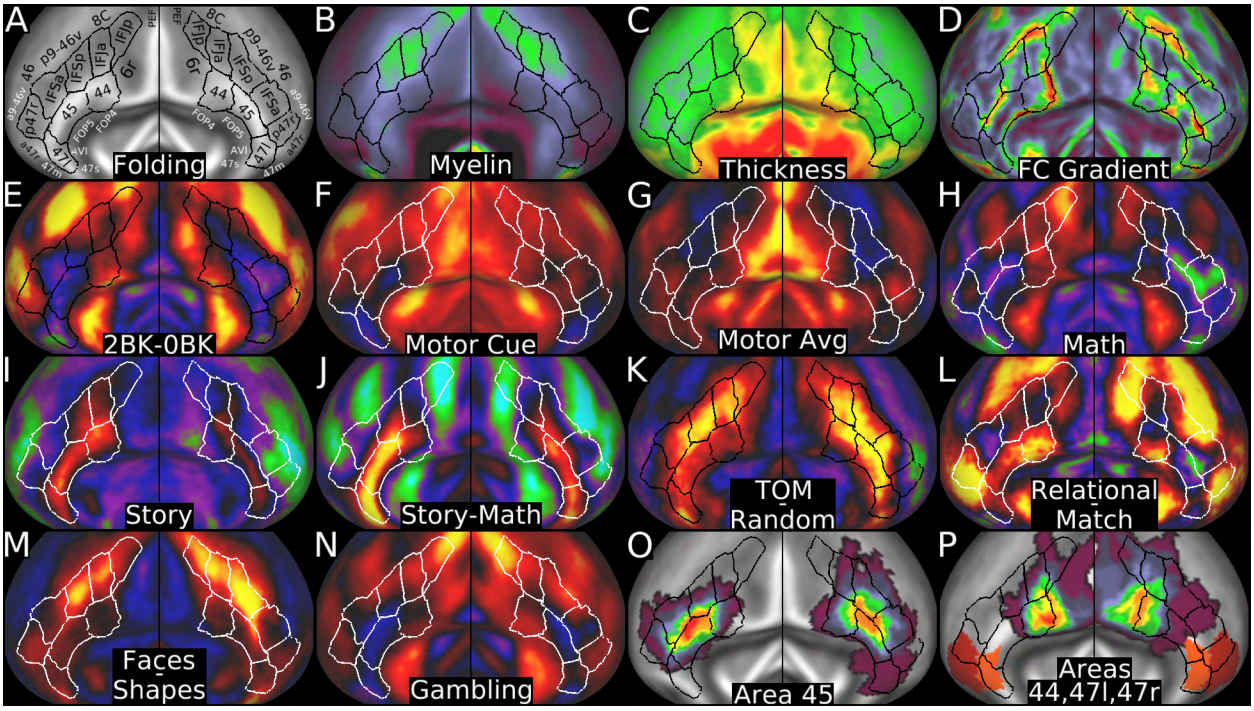

Figure 24 shows multi-modal information used to parcellate the inferior frontal cortex. Panel A shows the areas on a folding map. Panels B and C show myelin and cortical thickness maps. Panel D shows the resting state functional connectivity gradients. Panels E, F, G, and H show the working memory 2BK-0BK contrast, the MOTOR CUE contrast, the MOTOR AVG contrast, and the LANGUAGE MATH contrast. Panels I, J, K and L show the LANGUAGE STORY contrast, the STORY-MATH contrast, the SOCIAL TOM-RANDOM contrast, and the RELATIONAL-MATCH contrast. Panels M and N show the EMOTION FACES-SHAPES contrast and a GAMBLING primary contrast. Panel O shows the surface-based probabilistic map of area 45 from (Fischl et al., 2008). Panel P shows the surface-based probabilistic map of area 44 from (Fischl et al., 2008) and maps of area 47l and 47r from (Ongur et al., 2003). While the parcellation is reasonably symmetric (parcel boundaries in the same locations relative to folding and areal features) the probabilistic maps have some asymmetries, suggesting that registration drift may contribute to some of the mismatches. Data at http://balsa.wustl.edu/W0Nl.

Areas **44**, 45, and 47l are so named because of their substantial overlap with correspondingly named areas in previous studies (Panels O and P, (Amunts et al., 1999; Fischl et al., 2008; Ongur et al., 2003), though the overlap is not perfect. Broca's area is commonly described as including Brodmann's areas 44 and 45 (Amunts et al., 2010; Amunts et al., 1999). In the LANGUAGE STORY primary contrast (Panel I) and STORY-MATH contrast (Panel J), the strongest activations in the inferior frontal region included areas 44, 45, and 47l on the left, with more modest activations of areas 45 and 47l on the right. These three areas also show strong functional connectivity with one another and with other areas activated in the language task contrasts. Area **44**'s posterior border with 6r was covered in Section #8 Premotor Cortex and its borders with FOP4 and FOP5 were covered in Section #12 Insular and Frontal Opercular Cortex. Relative to its superior

neighbor IFJa, area **44** has less myelin (Panel B), is thicker (Panel C), differs modestly in functional connectivity (Panel D), is more activated in the RELATIONAL-MATCH contrast in the left hemisphere (Panel L) and less activated in the FACES-SHAPES contrast (Panel M). Relative to its antero-superior neighbor IFSp, area **44** has less myelin (Panel B), is thicker (Panel C), differs modestly in functional connectivity (Panel D), is more activated in the working memory 2BK-0BK (Panel E) and MOTOR AVG (Panel G) contrasts, and is less activated in the FACES-SHAPES contrast (Panel M). In the left hemisphere, area **44** is also more activated in the LANGUAGE STORY (Panel I) and RELATIONAL-MATCH (Panel L) contrasts and less activated in the TOM-RANDOM (Panel K) contrast relative to area IFSp. Relative to its anterior neighbor 45, area **44** has modestly less myelin (Panel B), is thicker (Panel C), differs in functional connectivity in the right hemisphere (Panel D), is activated vs deactivated in primary task contrasts (e.g. Panel N) and in the working memory 2BK-0BK (Panel E) and LANGUAGE MATH (Panel H) contrasts, and is less activated in the LANGUAGE STORY-MATH contrast (Panel J). Area **44** shows strongly lateralized functional activation in the LANGUAGE STORY contrast (Panel I) and to some extent in the RELATIONAL-MATCH task contrast (Panel L). Areas 44 and 45 have been subdivided respectively into cytoarchitectonic areas 44d and 44v and 45a and 45p (Amunts et al., 2010). We found intra-areal heterogeneity in the right hemisphere consistent with similar subdivisions of both areas 44 and 45, but not in the left hemisphere (Panel D; see also panel L) in our in vivo multi-modal data.

Relative to its supero-posterior neighbor IFSp, area **45** has less myelin (Panel B), is thicker (Panel C), differs modestly in functional connectivity (Panel D), is more activated in the LANGUAGE STORY contrast (Panel I, more on the right), and is less activated in the FACES-SHAPES contrast (Panel M). Area **45** is activated in the RELATIONAL-MATCH contrast in the left hemisphere (Panel L), but mainly deactivated in the right hemisphere, whereas IFSp is more activated on the right. Relative to its superior neighbor IFSa, area **45** differs in functional connectivity (Panel D), is activated vs deactivated in the LANGUAGE STORY (Panel I) and STORY-MATH (Panel J) contrasts, and in the RELATIONAL-MATCH contrast in the left hemisphere (Panel L). Relative to its supero-anterior neighbor p47r, area **45** differs in functional connectivity (Panel D), is deactivated vs activated in many primary task contrasts (e.g. Panel N) and in the working memory 2BK-0BK (Panel E) and LANGUAGE STORY (Panel I) contrasts, is activated vs deactivated in the LANGUAGE STORY-MATH contrast (Panel J), and is less activated in the TOM-RANDOM (Panel K) and RELATIONAL-MATCH (Panel L) contrasts. Relative to its inferior neighbor 47l, area **45** has more myelin (Panel B), differs in functional connectivity (in the right hemisphere only, Panel D), is more activated in the MOTOR CUE contrast (Panel F), and is deactivated vs activated in the EMOTION SHAPES primary contrast. Relative to its supero-anterior neighbor p47r, area **47l** is thicker (Panel C), differs in functional connectivity (Panel D), is deactivated vs activated in the working memory 2BK-0BK contrast (Panel E), is activated vs deactivated in the LANGUAGE STORY (Panel I) and STORY-MATH (Panel J) contrasts, and is less activated in the RELATIONAL-MATCH contrast (Panel L). The remaining borders of **47l** (with a47r, 47m, and 47s anteriorly and inferiorly, and with AVI and FOP5 posteriorly and inferiorly) were covered in Sections #20 Orbital and Polar Frontal Cortex and #12 Insular and Frontal Opercular Cortex.

The inferior frontal sulcus includes areas **IFJp**, **IFJa**, IFSp, IFSa that are named because of their similarity in location to areas ifj2, ifj1, ifs2, and ifs1 that were partly

described in (Amunts et al., 2010), but with some differences in relation to a future, yet to be published parcellation (Katrin Amunts, personal communication). It also includes area p47r, so named because it overlaps with the posterior part of area 47r of (Ongur et al., 2003) (Panel P). Area **IFJp's** posterior borders with PEF and 6r were discussed in Section #8 Premotor Cortex. Relative to its superior neighbor 8C, area **IFJp** has more myelin (Panel B), differs in functional connectivity (Panel D), is more activated in primary task contrasts (e.g. Panel N) and in the PLACE-AVG, TOM-RANDOM (Panel K), and FACES-SHAPES (Panel M) contrasts, and is more deactivated in the FACE-AVG and LANGUAGE STORY-MATH (Panel J) contrasts. Relative to its anterior neighbor IFJa, area **IFJp** is thicker (Panel C), differs in functional connectivity (Panel D), is deactivated vs activated in the FACE-AVG contrast, is less activated in the LANGUAGE STORY contrast (Panel I), is strongly deactivated vs weakly activated in the STORY-MATH contrast (Panel J), and is more activated in the RELATIONAL-MATCH contrast (Panel L, particularly on the right). Relative to its superior neighbor 8C, area **IFJa** has more myelin (Panel B), differs in functional connectivity (Panel D), is more activated in the MOTOR CUE (Panel F), TOM-RANDOM (Panel K) and FACES-SHAPES (Panel M) contrasts, and is less activated in the RELATIONAL-MATCH contrast (Panel L). Relative to its anterior neighbor IFSp, area **IFJa** is thicker (Panel C), differs in functional connectivity (Panel D), is more activated in the MOTOR AVG contrast (Panel G), and is weakly deactivated vs activated in the RELATIONAL-MATCH contrast (Panel L).

Further anterior and relative to its supero-posterior neighbor 8C, area **IFSp** has more myelin (Panel B), differs in functional connectivity (Panel D), is activated vs deactivated in the LANGUAGE STORY contrast in the left hemisphere (Panel I), is more activated in the TOM-RANDOM (Panel K) and FACES-SHAPES (Panel M) contrasts, and is less activated in the RELATIONAL-MATCH contrast in the left hemisphere (Panel L). Relative to its superior neighbor p9-46v, area **IFSp** has more myelin (Panel B), differs in functional connectivity (Panel D), is deactivated vs strongly activated in the working memory 2BK-0BK contrast (Panel E), is more activated in the LANGUAGE STORY contrast in the left hemisphere (Panel I) and in the TOM-RANDOM (Panel K) and FACES-SHAPES (Panel M) contrasts, and is less activated in the RELATIONAL-MATCH contrast (Panel L). Relative to its anterior neighbor IFSa, area **IFSp** has more myelin (Panel B), differs in functional connectivity (Panel D), is deactivated vs activated in the MOTOR AVG contrast (Panel G), is activated/less deactivated vs more deactivated in the LANGUAGE STORY contrast (Panel I), and is more activated in the FACES-SHAPES contrast (Panel M). Further anterior and relative to its supero-posterior neighbor p9-46v, area **IFSa** differs in functional connectivity (Panel D), is activated vs deactivated in the working memory 2BK-0BK contrast (Panel E), is more activated in the TOM-RANDOM contrast (Panel K), and is deactivated vs activated in the RELATIONAL-MATCH contrast in the left hemisphere (Panel L). Relative to its superior neighbor 46, area **IFSa** has more myelin (Panel B), differs in functional connectivity (Panel D), is more activated in the 2BK-0BK (Panel E) and FACES-SHAPES (Panel M) contrasts, and is activated vs deactivated in the TOM-RANDOM contrast (Panel K). Relative to its antero-superior neighbor a9-46v, area **IFSa** differs in functional connectivity (Panel D), is deactivated vs activated in the working memory 2BK-0BK contrast (Panel E), is less deactivated in the STORY-MATH contrast (Panel J), and is activated vs deactivated in the TOM-RANDOM contrast (Panel K). Relative to its anterior neighbor p47r, area **IFSa** has more myelin (Panel B), differs in functional connectivity

(Panel D), is deactivated vs activated in the working memory 2BK-0BK (Panel E) and RELATIONAL-MATCH (Panel L) contrasts, is more deactivated in the LANGUAGE MATH contrast (Panel H), and is less deactivated in the LANGUAGE STORY-MATH contrast (Panel J). Finally, relative to its superior neighbor a9-46v, area **p47r** differs in functional connectivity (Panel D), is activated/less deactivated vs more deactivated in the LANGUAGE MATH (Panel H) and STORY contrasts on the left (Panel I), is more activated in the RELATIONAL-MATCH contrast (Panel L), and is activated vs deactivated in the FACES-SHAPES contrast (Panel M). The anterior border of **p47r** with area a47r was covered in Section #20 Orbital and Polar Frontal Cortex.

22. DorsoLateral Prefrontal Cortex

The dorsolateral prefrontal cortex is one of the larger and more functionally heterogeneous regions of human neocortex, and thus the often-used term "DLPFC" is not a particularly specific spatial localization. The DLPFC region is generally lightly myelinated, of moderate thickness, participates strongly in both the task positive and task negative networks, and shows substantial heterogeneity in functional contrasts. Thus it has many similarities with the inferior parietal cortex and lateral temporal cortex, as well as with the other prefrontal regions (including inferior frontal, orbital and polar frontal, and medial frontal). Like lateral temporal cortex and inferior parietal cortex, the dorsolateral prefrontal cortex has also expanded dramatically in humans relative to monkeys and apes (Glasser et al., 2014; Hill et al., 2010). We have subdivided DLPFC into 13 areas: 8C, 8Av, i6-8, s6-8, SFL, 8BL, 9p, 9a, 8Ad, p9-46v, a9-46v, 46, and 9-46d. They are surrounded by areas 55b, FEF, 6a, 6ma, SCEF, 8BM, 9m, 10d, p10p, a10p, a47r, p47r, IFSa, IFSp, IFJa, IFJp, and PEF. Figure 25 shows the multi-modal information used to parcellate this region of cortex. Panel A shows the areas on a cortical folding map.

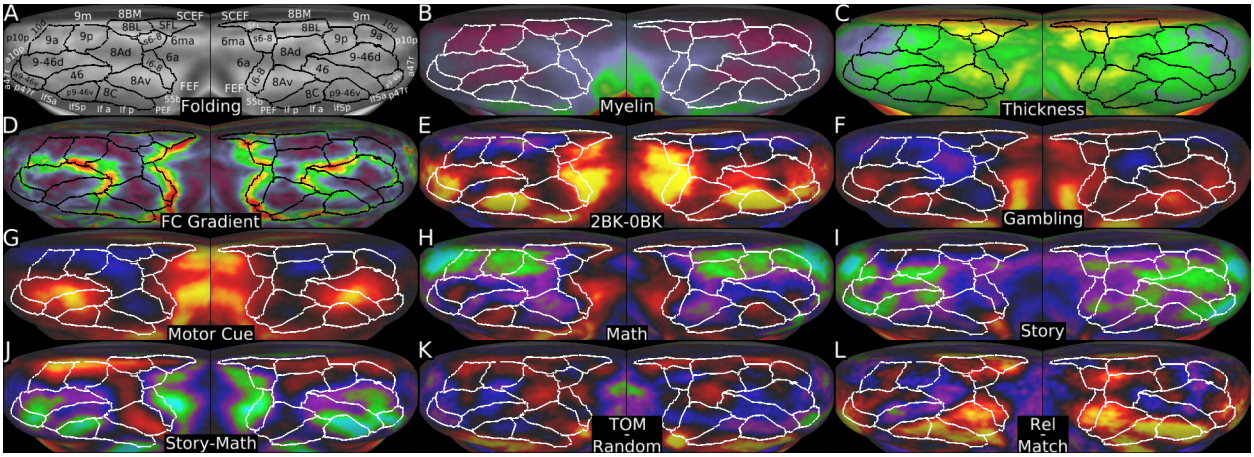

Figure 25 shows multi-modal information used to parcellate the dorsolateral prefrontal cortex. Panel A shows the areas on a group average folding map. Panels B and C show the myelin and cortical thickness maps. Panel D shows the resting state functional connectivity gradient map. Panels E and F show the working memory 2BK-0BK contrast and a GAMBLING primary contrast. Panels G, H, and I show the MOTOR CUE contrast, the LANGUAGE MATH contrast, and the LANGUAGE STORY contrast. Panels J, K, and L show the STORY-MATH contrast, the TOM-RANDOM contrast, and the RELATIONAL-MATCH contrast. Data at http://balsa.wustl.edu/Q2LG.

A notably distinct area in dorsolateral prefrontal cortex is the hemispherically asymmetric Superior Frontal Language (**SFL**) area, located posteriorly on the superior frontal gyrus. The **SFL** area is larger on the left, shows more activation in the LANGUAGE STORY contrast in the left hemisphere (Panel I), and strong activation in the RELATIONAL-MATCH contrast in the left hemisphere compared with deactivation in the right hemisphere (Panel L). It is also part of the language network in the left hemisphere and the corresponding network in the right hemisphere (see Supplementary Figure 4 in the Supplementary Results and Discussion). The lateral (6ma) and medial (SCEF and 8BM) borders of area **SFL** were already covered (in Sections #8 Premotor Cortex and #19 Anterior Cingulate and Medial Prefrontal Cortex). Relative to its anterior neighbor 8BL, area **SFL** is thicker (Panel C), differs in functional connectivity (Panel D), is less deactivated in the LANGUAGE MATH contrast (Panel H), and is more activated in the LANGUAGE STORY contrast (particularly on the left, Panel I), in the TOM-RANDOM contrast (in the right hemisphere, Panel K), and in the RELATIONAL-MATCH contrast in the left hemisphere (Panel L). Relative to its lateral neighbor s6-8, area **SFL** is thicker (Panel C), differs in functional connectivity (Panel D), is less activated in the working memory 2BK-0BK contrast in the right hemisphere (Panel E), is activated (left) or activated/deactivated (right) vs strongly deactivated in the LANGUAGE STORY (Panel I) and STORY-MATH (Panel J) contrasts, is activated vs deactivated in the TOM-RANDOM contrast in the right hemisphere (Panel K), and is deactivated vs activated in the RELATIONAL-MATCH contrast in the right hemisphere (Panel L).

We identified two areas, **s6-8** and **i6-8**, in a transitional region similar to the transitional region of cortex between areas FB (BA6) and FC (BA8) in the von Economo and Koskinas parcellation (Talavage and Hall, 2012; Triarhou, 2007a, b; von Economo and Koskinas, 1925). We consider the region transitional because of differences across task contrasts as to whether their strongest gradient is located at the anterior or posterior border of the region. The posterior borders of area **s6-8** with 6ma and 6a were covered in Section #8 Premotor Cortex. Relative to its medial neighbor 8BL, area **s6-8** has more myelin (Panel B), differs in functional connectivity (Panel D), is activated vs deactivated in the working memory 2BK-0BK (Panel E), MOTOR CUE (Panel G), and CUE-AVG contrasts, is activated/deactivated vs strongly deactivated in the LANGAUGE MATH (Panel H) contrast, and is deactivated vs activated in the STORY-MATH contrast (Panel J). Relative to its anterior neighbor 8Ad, area **s6-8** differs in functional connectivity (Panel D), is more activated in the working memory 2BK-0BK contrast (Panel E), is activated vs deactivated in the MOTOR CUE contrast (Panel G), is less deactivated in the LANGUAGE MATH contrast (Panel H), and is deactivated vs activated in the STORY-MATH contrast (Panel J). Relative to its infero-lateral neighbor i6-8, area **s6-8** has less myelin (Panel B), differs in functional connectivity (Panel D), and is less activated in the RELATIONAL primary contrasts. Relative to its anterior neighbor 8Ad, area **i6-8** differs in functional connectivity (Panel D), is activated vs deactivated in many primary task contrasts (e.g. Panel F), is more activated in the working memory 2BK-0BK (Panel E), MOTOR CUE (Panel G), CUE-AVG and LANGUAGE MATH contrasts (Panel H), and is deactivated vs activated in the LANGAUGE STORY-MATH contrast (Panel J). Relative to its antero-lateral neighbor 8Av, area **i6-8** differs in functional connectivity (Panel D), is more activated in the working memory 2BK-0BK contrast (Panel E), and is deactivated vs activated in the STORY-MATH contrast (Panel J).

Anterior to the 6-8 transitional areas are five subdivisions of area 8 (8BM, 8BL, 8Ad, 8Av, and 8C), whose names largely reflect correspondences with architectonic areas defined by (Petrides and Pandya, 1999), except that their 8Av is subdivided into 8Av plus a new area 8C and their 8B is subdivided into 8BM and 8BL. Area 8BM was covered previously in Section #19 Anterior Cingulate and Medial Prefrontal Cortex. The medial and posterior borders of **8BL** with 8BM, 9m, SFL, and s6-8 were covered in #19 Anterior Cingulate and Medial Prefrontal Cortex or above. Relative to its anterior neighbor 9p, area **8BL** is thicker (Panel C), is more activated/less deactivated in the LANGUAGE STORY contrast (Panel I), and is more activated in the RELATIONAL-MATCH contrast in the left hemisphere (Panel L) and in the TOM-RANDOM (Panel K) and FACES-SHAPES contrasts in the right hemisphere. Relative to its inferior neighbor 8Ad, area **8BL** has less myelin (Panel B), is thicker (Panel C), differs in functional connectivity (Panel D), is deactivated vs activated in the working memory 2BK-0BK contrast (Panel E) and activated vs deactivated in the RELATIONAL-MATCH contrast in the left hemisphere (Pane L). Relative to its anterior neighbor 9p, area **8Ad** has more myelin (Panel B), is thicker (Panel C), differs in functional connectivity (Panel D), is more deactivated in the GAMBLING primary contrasts (e.g. Panel F), and is less activated/deactivated vs activated in the MOTOR AVG contrast. Relative to its anterior neighbor 9-46d, area **8Ad** differs strongly in functional connectivity (Panel D), is less activated in the working memory 2BK-0BK contrast (Panel E), and is deactivated vs activated in the GAMBLING and RELATIONAL primary contrasts (e.g. Panel F) and in the MOTOR CUE (Panel G) and CUE-AVG contrasts. Relative to its antero-lateral neighbor 46, area **8Ad** has more myelin (Panel B), is thicker (Panel C), differs strongly in functional connectivity (Panel D), and is deactivated vs activated in the MOTOR CUE (Panel G) and CUE-AVG contrasts. Relative to its infero-lateral neighbor 8Av, area **8Ad** differs in functional connectivity (Panel D), is deactivated vs activated in the working memory, GAMBLING, and RELATIONAL primary contrasts (e.g. Panel F), and is deactivated/less activated vs more activated in the RELATIONAL-MATCH contrast (Panel L). Relative to its postero-lateral neighbor 55b, area **8Av** differs in functional connectivity (Panel D), is less activated in the STORY (Panel I) and MOTOR CUE contrasts (Panel G), and is less activated in the TOM-RANDOM contrast in the right hemisphere only (Panel K). Relative to its anterior neighbor 46, area **8Av** differs in functional connectivity (Panel D), is deactivated vs activated in the MOTOR CUE (Panel G) and CUE-AVG contrasts, and is activated vs deactivated in the RELATIONAL-MATCH contrast (Panel L). Relative to its infero-lateral neighbor 8C, area **8Av** differs modestly in functional connectivity (Panel D), is less activated in the working memory 2BK-0BK contrast (Panel E), is deactivated vs activated in the MOTOR CUE (Panel G) and CUE-AVG contrasts, and is activated vs deactivated in the STORY-MATH contrast (Panel J). Relative to its antero-medial neighbor 46, area **8C** has more myelin (Panel B), differs strongly in functional connectivity (Panel D), and is locally more activated in the 2BK-0BK contrast (Panel E), is less activated in the MOTOR CUE (Panel G) and CUE-AVG contrasts, and is activated vs deactivated in the RELATIONAL-MATCH contrast (Panel L). Relative to its anterior neighbor p9-46v, area **8C** differs in functional connectivity (Panel D), is less activated in primary contrasts (e.g. Panel F) and in the MOTOR CUE (Panel G) and CUE-AVG contrasts, and is deactivated vs activated in the LANGUAGE MATH contrast (Panel H). Relative to its posterior neighbor 55b, area **8C** differs strongly in functional connectivity (Panel D) and is deactivated/less-activated in the LANGUAGE STORY contrast (Panel I). The inferior borders of area **8C** with PEF, IFJp, IFJa,

and IFSp were covered previously (Sections #8 Premotor Cortex and #21 Inferior Frontal Cortex).

We subdivided area 9 into three areas: 9m (covered previously in Section #19 Anterior Cingulate and Medial Prefrontal Cortex) and areas **9p** and **9a** (based on splitting the lateral portion of area 9 of (Petrides and Pandya, 1999). The medial (9m) and posterior (8BL, 8Ad) borders of area **9p** have already been covered (Section #19 Anterior Cingulate and Medial Prefrontal Cortex and above). Relative to its infero-lateral neighbor 9-46d, area **9p** has less myelin (Panel B), differs strongly in functional connectivity (Panel D), is deactivated vs activated in the working memory 2BK-0BK (Panel E), MOTOR CUE (Panel G, assessed only statistically) and CUE-AVG contrasts, and is mostly activated vs deactivated in the STORY-MATH contrast (Panel J). Relative to its anterior neighbor 9a, area **9p** is slightly thicker (Panel C), differs modestly in functional connectivity (Panel D), is deactivated vs activated in the SOCIAL primary contrasts in the left hemisphere, is less activated in the TOM-RANDOM contrast in the right hemisphere (Panel K), is mainly deactivated vs activated in the left hemisphere, and is mainly activated vs deactivated in the right hemisphere in the RELATIONAL-MATCH contrast (Panel L). Relative to its infero-lateral neighbor 9-46d, area **9a** has less myelin (Panel B), differs strongly in functional connectivity (Panel D), is deactivated vs activated in the working memory and RELATIONAL primary contrasts and in the working memory 2BK-0BK (Panel E), MOTOR CUE (Panel G), and CUE-AVG contrasts, and is activated vs deactivated in the STORY-MATH contrast (Panel J). The medial (9m) and anterior (10d and p10p) borders of **9a** have already been covered (Sections #19 Anterior Cingulate and Medial Prefrontal Cortex and #20 Orbital and Polar Frontal Cortex).

We identified four areas in the central portion of the dorsolateral prefrontal cortex region: **9-46d**, **46**, **a9-46v**, and **p9-46v**. The names are based on approximate correspondences with areas 9-46d, 46, and 9-46v of (Petrides and Pandya, 1999) except that we identify discontinuous anterior and posterior subdivisions of their area 9-46v. The anterior (p10p, a10p, a47r) and inferior (p47r) borders of area **a9-46v** were covered already (Sections #20 Orbital and Polar Frontal Cortex and #21 Interior Frontal Cortex). Relative to its superior neighbor 9-46d, area **a9-46v** differs in functional connectivity (Panel D), is deactivated vs activated in the SOCIAL TOM primary contrast, and is more deactivated in the TOM-RANDOM contrast (Panel K). Relative to its posterior neighbor 46, area **a9-46v** has slightly more myelin (Panel B), differs modestly in functional connectivity (Panel D), is more activated in the working memory, GAMBLING, and RELATIONAL primary contrasts (e.g. Panel F) and in the working memory 2BK-0BK contrast in the left hemisphere (Panel E), is more deactivated in the LANGUAGE STORY-MATH contrast in the left hemisphere (Panel J) and in the TOM-RANDOM contrast in both hemispheres (Panel K), and is more activated in the RELATIONAL-MATCH contrast in the left hemisphere (Panel L). The borders of **p9-46v** inferiorly with IFSa and IFSp and posteriorly with 8C were already covered (Section #21 Interior Frontal Cortex and above). Relative to its superior neighbor 46, area **p9-46v** has more myelin (Panel B), differs in functional connectivity (Panel D), is more activated in the working memory 2BK-0BK contrast (Panel E) and in the working memory, GAMBLING, and RELATIONAL primary task contrasts (e.g. Panel F), is activated vs deactivated in the LANGUAGE MATH (Panel H) and RELATIONAL-MATCH (Panel L) contrasts, and is more deactivated in the STORY-MATH contrast (Panel J). In the left hemisphere, the primary contrasts and RELATIONAL-MATCH contrasts were only

assessed statistically. Relative to its supero-medial neighbor 9-46d in the left hemisphere, area **46** has less myelin (Panel B), differs modestly in functional connectivity (Panel D), and is less activated in the working memory, GAMBLING, and RELATIONAL primary task contrasts (e.g. Panel F) and in the working memory 2BK-0BK (Panel E) and LANGUAGE MATH (Panel H) contrasts, is more deactivated in the STORY-MATH contrast (Panel J), and is deactivated vs activated in the RELATIONAL-MATCH contrast (Panel L). Relative to area 9-46d in the right hemisphere, area **46** differs modestly in functional connectivity (Panel D), is modestly less deactivated in the LANGUAGE STORY-MATH contrast (Panel J), and is modestly more deactivated in the RELATIONAL-MATCH contrast (Panel L). This central region of the DLPFC (including area 46) is also a hotspot of individual variability, including topologically incompatible areal configurations (Rajkowska and Goldman-Rakic, 1995a, b).

Table 1 lists the 180 areas of the cortical parcellation with index number, short name, description, whether or not the area is new or not, the sections the area is described in, synonyms or 'quasi-synonyms' for the area, and key studies used for the area's identification. A "Yes" in the 'New?' column signifies an area that was not previously described in the neuroanatomical literature as far as we are aware. For some areas, "Yes*" signifies subdivisions of a previously described area, homologues, or similarity to a previously described area but not the same. "No" means that the area was previously described in a very similar form to what we found here. The **bold** section number is the primary section in which the area is described. **Bold** studies are those that had surface-mapped data available for us to make direct comparisons on the same atlas mesh.

Parcel Index	Area Name	Area Description	New?	Sections	Other Names	Key Studies
1	V1	Primary Visual Cortex	No	**1**,2	17, hOC1, OC, BA17	Amunts et al 2000, **Fischl et al 2008**, **Abdollahi et al 2014**
2	MST	Medial Superior Temporal Area	No	**5**,15	MSTv, hOC5, hOC5v	**Abdollahi et al 2014**, Kolster et al 2010, Malikovic et al 2007, **Fischl et al 2008**
3	V6	Sixth Visual Area	No	2,**3**,18	112	Pitzalis et al 2006, Pitzalis et al 2013, Sereno et al 2012, Nieuwenhuys et al 2014
4	V2	Second Visual Area	No	1,**2**	18, hOC2, OB, BA18	Amunts et al 2000, **Fischl et al 2008**, Schira et al 2009, **Abdollahi et al 2014**, Wang et al 2015, Wandell and Winawer 2011
5	V3	Third Visual Area	No	**2**	V3d, V3v, VP, hOC3d, hOC3v	**Abdollahi et al 2014**, Rottschy et al 2007, Schira et al 2009, Kujovic et al 2012, Wang et al 2015, Wandell and Winawer 2011
6	V4	Fourth Visual Area	No	**2**,3,4,5	V4d, V4v, hV4, hOC4v, hOC4lp, LO1	Hansen et al 2007, **Abdollahi et al 2014**, Rottschy et al 2007, Malikovic et al 2015
7	V8	Eighth Visual Area	No	2,**4**,5	VO1	Hadjikhani et al 1998, **Abdollahi et al 2014**
8	4	Primary Motor Cortex	No	**6**,7,8,9	BA4, 4a, 4p, M1, PMC, F1	**Fischl et al 2008,** Geyer et al 1996
9	3b	Primary Sensory Cortex	No	**6**,7,9	S1, 3	**Fischl et al 2008,** Geyer et al 1999, Geyer et al 2000
10	FEF	Frontal Eye Fields	No	6,**8**,22		**Glasser and Van Essen 2011**, Amiez and Petrides 2009
11	PEF	Premotor Eye Field	No	6,**8**,21,22	6v2	Amiez and Petrides 2009, Amunts et al 2010
12	55b	Area 55b	No	6,**8**,22		Hopf 1956
13	V3A	Area V3A	No	2,**3**	V3D, hOC4d	**Abdollahi et al 2014**, Swisher et al 2007, Kujovic et al 2012, Wandell and Winawer 2011, Larsson and Heeger 2006, Tootell et al 1997
14	RSC	RetroSplenial Complex	No	13,**18**	29,30	**Glasser and Van Essen 2011,** Vogt, 2009, Palomero-Gallagher et al 2009
15	POS2	Parieto-Occipital Sulcus Area 2	Yes*	16,**18**		**Glasser and Van Essen 2011**
16	V7	Seventh Visual Area	No	**3**	IPS0	**Abdollahi et al 2014**, Swisher et al 2007, Larsson and Heeger 2006, Tootell et al 1998, Hagler et al 2007, Wang et al., 2015
17	IPS1	IntraParietal Sulcus Area 1	No	**3**,16,17		Swisher et al 2007, Wang et al., 2015, Hagler et al 2007
18	FFC	Fusiform Face Complex	No	**4**,5,14	FFA, FG2	**Glasser and Van Essen 2011,** Kanwisher and Yovel, 2006, Caspers et al 2013, Weiner et al 2014
19	V3B	Area V3B	No	**3**,5,17	V3C	**Abdollahi et al 2014**, Larsson and Heeger 2006, Swisher et al 2007, Wandell and Winawer 2011, Smith et al 1998
20	LO1	Area Lateral Occipital 1	No	2,**5**	LO2, hOC4la	**Abdollahi et al 2014,** Hansen et al 2007, Malikovic et al 2015, Larsson and Heeger 2006
21	LO2	Area Lateral Occipital 2	No	2,4,**5**	LO1, hOC4la	**Abdollahi et al 2014,** Hansen et al 2007, Malikovic et al 2015, Larsson and Heeger 2006
22	PIT	Posterior InferoTemporal	No	2,**4**,5	phPITv, phPITd, OFA, hOC4la	**Abdollahi et al 2014,** Kolster et al 2010, Malikovic et al 2015, Kanwisher and Yovel, 2006, Tsao et al 2008

		Complex				
23	MT	Middle Temporal Area	No	**5**,15	hOC5, hOC5d	**Abdollahi et al 2014**, Kolster et al 2010, Malikovic et al 2007, **Fischl et al 2008**
24	A1	Primary Auditory Cortex	No	10	Core, R1, TC, TE1.0, TE1.1, 41	**Glasser and Van Essen 2011**, Moerel et al 2014, von Economo and Koskinas 1925, Triarhou 2007, Morosan et al 2001
25	PSL	PeriSylvian Language Area	Yes	9,10,11, **15**,17		
26	SFL	Superior Frontal Language Area	Yes	7,19,**22**		
27	PCV	PreCuneus Visual Area	No	7,16,**18**	PrCu	Sereno et al 2012
28	STV	Superior Temporal Visual Area	Yes	11,**15**,17		
29	7Pm	Medial Area 7P	Yes	**16**,18	7P	Scheperjans et al 2008a, Scheperjans et al 2008b
30	7m	Area 7m	No	16,**18**		Scheperjans et al 2008a, Scheperjans et al 2008b
31	POS1	Parieto-Occipital Sulcus Area 1	Yes*	**18**	"Retrosplenial Cortex"	**Glasser and Van Essen 2011**
32	23d	Area 23d	No	**18**,19		Vogt, 2009, Palomero-Gallagher et al 2009
33	v23ab	Area ventral 23 a+b	No	**18**	23a, 23b, v23	Vogt, 2009, Palomero-Gallagher et al 2009
34	d23ab	Area dorsal 23 a+b	No	**18**	23a, 23b, d23	Vogt, 2009, Palomero-Gallagher et al 2009
35	31pv	Area 31p ventral	Yes*	**18**	31, 31d, 31v	Vogt, 2009, Palomero-Gallagher et al 2009
36	5m	Area 5m	No	6,**7**		Scheperjans et al 2008a, Scheperjans et al 2008b
37	5mv	Area 5m ventral	Yes*	**7**,16,18	5ci	Scheperjans et al 2008a, Scheperjans et al 2008b
38	23c	Area 23c	No	**7**,18,19		Vogt, 2009, Palomero-Gallagher et al 2009
39	5L	Area 5L	No	6,**7**,16		Scheperjans et al 2008a, Scheperjans et al 2008b
40	24dd	Dorsal Area 24d	No	6,**7**,18	24d	Palomero-Gallagher et al 2009, Vogt and Vogt 2003
41	24dv	Ventral Area 24d	No	**7**,19	24d	Palomero-Gallagher et al 2009, Vogt and Vogt 2003
42	7AL	Lateral Area 7A	Yes*	6,7,**16**		Scheperjans et al 2008a, Scheperjans et al 2008b
43	SCEF	Supplementary and Cingulate Eye Field	Yes*	**7**,19,22	SEF, CEF, 6, SMA, SMAr	Amiez and Petrides 2009
44	6ma	Area 6m anterior	Yes*	**7**,8,22	SMAr, 6, SMA	**Fischl et al 2008**, Vorobiev et al 1998, Geyer 2004
45	7Am	Medial Area 7A	Yes*	7,**16**,18		Scheperjans et al 2008a, Scheperjans et al 2008b
46	7Pl	Lateral Area 7P	Yes*	**16**,18		Scheperjans et al 2008a, Scheperjans et al 2008b
47	7PC	Area 7PC	No	6,**16**		Scheperjans et al 2008a, Scheperjans et al 2008b
48	LIPv	Area Lateral IntraParietal ventral	Yes*	**16**	hIP3	**Van Essen et al 2012a**, Scheperjans et al 2008a, Scheperjans et al 2008b
49	VIP	Ventral IntraParietal Complex	Yes*	**16**		**Van Essen et al 2012a**
50	MIP	Medial IntraParietal Area	Yes*	3,**16**,17		**Van Essen et al 2012a**
51	1	Area 1	No	**6**,7,9,17		**Fischl et al 2008,** Geyer et al 1999, Geyer et al 2000
52	2	Area 2	No	**6**,7,16,17		**Fischl et al 2008,** Grefkes et al 2000
53	3a	Area 3a	No	**6**,7,9,17		**Fischl et al 2008,** Geyer et al 1999, Geyer et al 2000
54	6d	Dorsal area 6	Yes*	6,7,**8**	6, 6aα	**Fischl et al 2008,** Geyer 2004, Geyer et al 2000
55	6mp	Area 6mp	Yes*	6,**7**,8	SMAc, 6, SMA	**Fischl et al 2008**, Vorobiev et al 1998, Geyer 2004
56	6v	Ventral Area 6	No	6,**8**,9	6, 6v1	**Fischl et al 2008**, Amunts et al 2010, Geyer 2004
57	p24pr	Area Posterior 24 prime	No	7,18,**19**	p24'	Vogt, 2009
58	33pr	Area 33 prime	No	18,**19**	33', 16	Vogt, 2009, Nieuwenhuys et al 2014
59	a24pr	Anterior 24 prime	No	**19**	a24'	Vogt, 2009
60	p32pr	Area p32 prime	Yes*	7,**19**	32'	Vogt, 2009
61	a24	Area a24	Yes*	**19**	24, s24	Vogt, 2009, Palomero-Gallagher et al 2015
62	d32	Area dorsal 32	No	**19**	32	Vogt, 2009
63	8BM	Area 8BM	Yes*	7,**19**,22	8B	Petredes and Pandya 1999
64	p32	Area p32	No	**19**,20	32ac, 32	**Van Essen et al 2012b,** Ongur et al 2003**,** Vogt, 2009, Palomero-Gallagher et al 2009
65	10r	Area 10r	Yes*	**19**,20		**Van Essen et al 2012b,** Ongur et al 2003
66	47m	Area 47m	No	**20**,21		**Van Essen et al 2012b,** Ongur et al 2003, **Glasser and Van Essen 2011**
67	8Av	Area 8Av	Yes*	8,**22**		Petredes and Pandya 1999
68	8Ad	Area 8Ad	Yes*	**22**		Petredes and Pandya 1999

69	9m	Area 9 Middle	Yes*	**19**,20,22	9	Petredes and Pandya 1999
70	8BL	Area 8B Lateral	Yes*	19,**22**	8B	Petredes and Pandya 1999
71	9p	Area 9 Posterior	Yes*	19,**22**	9	Petredes and Pandya 1999
72	10d	Area 10d	Yes*	19,**20**,22	10, Fp1, Fp2	Petredes and Pandya 1999, Bludau et al 2014
73	8C	Area 8C	Yes*	8,21,**22**	8Av	Petredes and Pandya 1999
74	44	Area 44	No	8,12,**21**	44d, 44v	**Fischl et al 2008,** Amunts et al 1999, Amunts et al 2010
75	45	Area 45	No	12,**21**	45a, 45p	**Fischl et al 2008,** Amunts et al 1999, Amunts et al 2010
76	47l	Area 47l (47 lateral)	No	12,20,**21**		**Van Essen et al 2012b,** Ongur et al 2003
77	a47r	Area anterior 47r	Yes*	20,**21**,22	47r	**Van Essen et al 2012b,** Ongur et al 2003
78	6r	Rostral Area 6	No	**8**,9,12,21		Amunts et al 2010
79	IFJa	Area IFJa	Yes	8,**21**,22		
80	IFJp	Area IFJp	Yes	8,**21**,22		
81	IFSp	Area IFSp	Yes	**21**,22		
82	IFSa	Area IFSa	Yes	**21**,22		
83	p9-46v	Area posterior 9-46v	Yes*	21,**22**	9-46v	Petredes and Pandya 1999
84	46	Area 46	No	21,**22**		Petredes and Pandya 1999, Rajkowska and Goldman-Rakic 1995a, Rajkowska and Goldman-Rakic 1995b
85	a9-46v	Area anterior 9-46v	Yes*	20,21,**22**	9-46v	Petredes and Pandya 1999
86	9-46d	Area 9-46d	No	20,**22**		Petredes and Pandya 1999
87	9a	Area 9 anterior	Yes*	19,20,**22**	9	Petredes and Pandya 1999
88	10v	Area 10v	Yes	**19**,20	10, Fp2	Bludau et al 2014
89	a10p	Area anterior 10p	Yes*	**20**,22	10p, 10, Fp1	**Van Essen et al 2012b,** Ongur et al 2003, Bludau et al 2014
90	10pp	Polar 10p	Yes*	19,**20**	10p, 10, Fp1	**Van Essen et al 2012b,** Ongur et al 2003, Bludau et al 2014
91	11l	Area 11l	No	**20**	Fo3	**Van Essen et al 2012b,** Ongur et al 2003, Henssen et al 2016
92	13l	Area 13l	No	**20**	Fo3	**Van Essen et al 2012b,** Ongur et al 2003, Henssen et al 2016
93	OFC	Orbital Frontal Complex	Yes*	19,**20**	11m, 13b, 13m, 14r, Fo1	**Van Essen et al 2012b,** Ongur et al 2003, Henssen et al 2016
94	47s	Area 47s	No	12,**20**		**Van Essen et al 2012b,** Ongur et al 2003
95	LIPd	Area Lateral IntraParietal dorsal	Yes*	**16**,17		**Van Essen et al 2012a**
96	6a	Area 6 anterior	Yes	7,**8**,22	6, 6aβ	**Fischl et al 2008,** Geyer 2004, Geyer et al 2000
97	i6-8	Inferior 6-8 Transitional Area	Yes*	8,**22**	FC(B)	von Economo and Koskinas 1925, Triarhou 2007
98	s6-8	Superior 6-8 Transitional Area	Yes*	7,8,**22**	FC(B)	von Economo and Koskinas 1925, Triarhou 2007
99	43	Area 43	No	6,8,**9**,12	41	Brodmann 1909, Brodmann 2007, Nieuwenhuys et al 2014
100	OP4	Area OP4/PV	No	6,**9**,17	68	Eickhoff et al 2006a, Eickhoff et al 2006b, Nieuwenhuys et al 2014
101	OP1	Area OP1/SII	No	**9**,10		Eickhoff et al 2006a, Eickhoff et al 2006b
102	OP2-3	Area OP2-3/VS	Yes*	**9**,10,12	OP2,OP3	Eickhoff et al 2006a, Eickhoff et al 2006b
103	52	Area 52	No	**10**,12	IBT	Brodmann 1909, Brodmann 2007, von Economo and Koskinas 1925, Triarhou 2007
104	RI	RetroInsular Cortex	No	9,**10**,12,15	reI, reIt, RetroInsular, Belt, TD	**Glasser and Van Essen 2011,** Pandya and Sanides 1973, Kurth et al 2009,von Economo and Koskinas 1925, Triarhou 2007
105	PFcm	Area PFcm	No	9,**10**,15,17		Caspers et al 2006, Caspers et al 2008
106	PoI2	Posterior Insular Area 2	Yes*	**12**	Id1, Id2, Id3	Kurth et al 2009, Morel et al 2013
107	TA2	Area TA2	No	10,**11**,12	TE1.2	von Economo and Koskinas 1925, Triarhou 2007, Morosan et al 2001
108	FOP4	Frontal OPercular Area 4	Yes	9,**12**,21		
109	MI	Middle Insular Area	Yes*	**12**	Ial	**Van Essen et al 2012b,** Ongur et al 2003

110	Pir	Pirform Cortex	No	**12**,14,20	Poc	**Glasser and Van Essen 2011**, Ding et al 2009, Morel et al 2013
111	AVI	Anterior Ventral Insular Area	Yes*	**12**,20,21	Iai	**Van Essen et al 2012b,** Ongur et al 2003
112	AAIC	Anterior Agranular Insula Complex	Yes*	**12**,20	Iai, Ial	**Van Essen et al 2012b,** Ongur et al 2003
113	FOP1	Frontal OPercular Area 1	Yes	8,**9**,12		
114	FOP3	Frontal OPercular Area 3	Yes	**12**		
115	FOP2	Frontal OPercular Area 2	Yes	9,**12**		
116	PFt	Area PFt	No	6,16,**17**		Caspers et al 2006, Caspers et al 2008
117	AIP	Anterior IntraParietal Area	Yes*	6,**16**,17		**Van Essen et al 2012a**
118	EC	Entorhinal Cortex	No	**13**	28	**Fischl et al 2009**
119	PreS	PreSubiculum	No	2,**13**,18	Sub, Subicular	**Glasser and Van Essen 2011,** Amunts et al 2005
120	H	Hippocampus	No	**13**		
121	ProS	ProStriate Area	No	1,2,13,**18**		**Glasser and Van Essen 2011**, Vogt et al 2001, Sanides and Vitzthum 1965, Sanides, 1970
122	PeEc	Perirhinal Ectorhinal Cortex	Yes*	**13**,14	ATFP, AFP1, Ectorhinal, Perirhinal, 35, 36	Augustinack et al 2013, Ding et al 2009, Ding and Van Hoesen 2010, Rajimehr et al 2009, Tsao et al 2008
123	STGa	Area STGa	Yes	**11**,12,14		
124	PBelt	ParaBelt Complex	Yes*	**10**,11	ParaBelt, TA1	Moerel et al 2014, von Economo and Koskinas 1925, Triarhou 2007
125	A5	Auditory 5 Complex	Yes	**11**,15		
126	PHA1	ParaHippocampal Area 1	Yes	2,4,**13**		
127	PHA3	ParaHippocampal Area 3	Yes	4,**13**,14		
128	STSda	Area STSd anterior	Yes	**11**,14		
129	STSdp	Area STSd posterior	Yes	**11**,15		
130	STSvp	Area STSv posterior	Yes	**11**,14,15		
131	TGd	Area TG dorsal	Yes*	11,12,13,**14**	TG	Ding et al 2009, von Economo and Koskinas 1925, Triarhou 2007
132	TE1a	Area TE1 anterior	Yes*	11,**14**		von Economo and Koskinas 1925, Triarhou 2007
133	TE1p	Area TE1 posterior	Yes*	5,11,**14**		von Economo and Koskinas 1925, Triarhou 2007
134	TE2a	Area TE2 anterior	Yes*	**14**		von Economo and Koskinas 1925, Triarhou 2007
135	TF	Area TF	No	4,**13**,14		von Economo and Koskinas 1925, Triarhou 2007
136	TE2p	Area TE2 posterior	Yes*	4,5,**14**		von Economo and Koskinas 1925, Triarhou 2007
137	PHT	Area PHT	No	5,11,**14**,15		von Economo and Koskinas 1925, Triarhou 2007
138	PH	Area PH	No	4,**5**,14		von Economo and Koskinas 1925, Triarhou 2007
139	TPOJ1	Area TemporoParietoOccipital Junction 1	Yes	11,14,**15**,17		
140	TPOJ2	Area TemporoParietoOccipital Junction 2	Yes	5,14,**15**,17		
141	TPOJ3	Area TemporoParietoOccipital Junction 3	Yes	5,**15**,17		
142	DVT	Dorsal Transitional Visual Area	Yes	2,3,16,**18**		
143	PGp	Area PGp	No	5,15,**17**	39,PG	Caspers et al 2006, Caspers et al 2008
144	IP2	Area IntraParietal 2	No	16,**17**		Choi et al 2006
145	IP1	Area IntraParietal 1	No	16,**17**		Choi et al 2006
146	IP0	Area IntraParietal 0	Yes	3,5,16,**17**		
147	PFop	Area PF opercular	No	6,9,**17**	40, 72	Caspers et al 2006, Caspers et al 2008, Nieuwenhuys et al 2014
148	PF	Area PF Complex	No	9,15,**17**	40, 88	Caspers et al 2006, Caspers et al 2008, Nieuwenhuys et al 2014

149	PFm	Area PFm Complex	No	15,**17**	40, 89	Caspers et al 2006, Caspers et al 2008, Nieuwenhuys et al 2014
150	PGi	Area PGi	No	15,**17**	PGa, 39, PG, 90	Caspers et al 2006, Caspers et al 2008, Nieuwenhuys et al 2014
151	PGs	Area PGs	No	15,**17**	PGa, 39, PG, 90	Caspers et al 2006, Caspers et al 2008, Nieuwenhuys et al 2014
152	V6A	Area V6A	No	**3**,18	112	Pizalis et al 2013, Nieuwenhuys et al 2014
153	VMV1	VentroMedial Visual Area 1	Yes*	2,**4**,13	PHC2, PHC-2	Arcaro et al 2009, Wang et al 2015
154	VMV3	VentroMedial Visual Area 3	Yes*	2,**4**,13	VO2	Arcaro et al 2009, Wang et al 2015, Wandell and Winawer 2011
155	PHA2	ParaHippocampal Area 2	Yes	4,**13**		
156	V4t	Area V4t	No	**5**	LO2	**Abdollahi et al 2014,** Kolster et al 2010, Larsson and Heeger 2006
157	FST	Area FST	No	**5**,14,15		**Abdollahi et al 2014,** Kolster et al 2010
158	V3CD	Area V3CD	Yes	2,3,**5**,17	V3A,V3B, hOC4la	**Abdollahi et al 2014,** Malikovic et al 2015
159	LO3	Area Lateral Occipital 3	Yes	**5**,15,17	hOC4la	
160	VMV2	VentroMedial Visual Area 2	Yes*	2,**4**,13	PHC1, PHC-1	Arcaro et al 2009, Wang et al 2015
161	31pd	Area 31pd	Yes*	**18**	31, 31d, 31v	Vogt, 2009, Palomero-Gallagher et al 2009
162	31a	Area 31a	Yes*	**18**	31, 31d, 31v	Vogt, 2009, Palomero-Gallagher et al 2009
163	VVC	Ventral Visual Complex	Yes*	**4**,13,14	VO1, VO2, PHC1, PHC2, PHC-1, PHC-2, FG1	Arcaro et al 2009, Wang et al 2015, Wandell and Winawer 2011, Caspers et al 2013, Weiner et al 2014
164	25	Area 25	No	**19**,20		Vogt, 2009, Palomero-Gallagher et al 2015
165	s32	Area s32	No	**19**	32pl, 32	Vogt, 2009, Palomero-Gallagher et al 2015, **Van Essen et al 2012b**, Ongur et al 2003
166	pOFC	posterior OFC Complex	Yes*	12,**19**,20	13a, 14c, Fo2	**Van Essen et al 2012b,** Ongur et al 2003, Henssen et al 2016
167	PoI1	Area Posterior Insular 1	Yes*	**12**	Id1, Id2, Id3	Kurth et al 2009, Morel et al 2013
168	Ig	Insular Granular Complex	Yes*	9,**12**	Ig1, Ig2	Kurth et al 2009, Morel et al 2013
169	FOP5	Area Frontal Opercular 5	Yes	**12**,21	PrCO	**Glasser and Van Essen 2011**
170	p10p	Area posterior 10p	Yes*	**20**,22	10p, 10, Fp1	**Van Essen et al 2012b,** Ongur et al 2003, Bludau et al 2014
171	p47r	Area posterior 47r	Yes*	20,**21**,22	47r	**Van Essen et al 2012b,** Ongur et al 2003
172	TGv	Area TG Ventral	Yes*	13,**14**		Ding et al 2009, von Economo and Koskinas 1925, Triarhou 2007
173	MBelt	Medial Belt Complex	Yes*	**10**,12	Belt, TB	Moerel et al 2014, von Economo and Koskinas 1925, Triarhou 2007
174	LBelt	Lateral Belt Complex	Yes*	**10**	Belt, TB	Moerel et al 2014, von Economo and Koskinas 1925, Triarhou 2007
175	A4	Auditory 4 Complex	Yes*	**11**,15	TE3	Morosan et al 2005
176	STSva	Area STSv anterior	Yes	**11**,14		
177	TE1m	Area TE1 Middle	Yes*	11,**14**		von Economo and Koskinas 1925, Triarhou 2007
178	PI	Para-Insular Area	No	11,**12**,14	IBT	von Economo and Koskinas 1925, Triarhou 2007, Ding et al 2009
179	a32pr	Area anterior 32 prime	Yes*	**19**	32'	Vogt, 2009
180	p24	Area posterior 24	Yes*	**19**	24	Vogt, 2009

Table 2 lists the neuroanatomical studies used to identify areas in this parcellation. Our area name is given and the study's area name is in parentheses.

Short Citation	Our Area Names (The Study's Area Names)
Abdollahi et al 2014	V1, V2, V3, V4 (V4 + LO1 + LO2 + V3A + V3B), V3A (V3D), V3B (V3C), V3CD (V3A + V3B), V7, V8 (VO1), LO1, LO2, PIT(PITd + PITv), MT, MST, FST, V4t
Amiez and Petrides 2009	SCEF (SEF + CEF), FEF, PEF
Amunts et a 2000	V1 (17), V2 (18)
Amunts et al 1999	44, 45
Amunts et al 2005	PreS (Subicular Complex)
Amunts et al 2010	6r, 6v (6v1), PEF (6v2), 44 (44d + 44v), 45 (45a + 45p)
Arcaro et al 2009	V8 (VO1), VVC (VO1 + VO2 + PH1 + PH2), VMV3 (VO2), VMV2 (PHC1), VMV1 (PHC2)
Augustinack et al 2013	PeEc (Perirhinal)
Bludau et al 2014	10pp + a10p + p10p + 10d (Fp1), 10r + 10v + 10d (Fp2)
Brodmann 1909, Brodmann 2007	43, 52, V1 (17), V2 (18), 4, 3a + 3b (3), 1, 2, A1 (41)
Caspers et al 2006	PFcm, PGp, PGs PGi (PGa), PFm, PF, PFt, PFop
Caspers et al 2008	PFcm, PGp, PGs PGi (PGa), PFm, PF, PFt, PFop
Caspers et al 2013	FFC (FG2), VVC (FG1)
Choi et al 2006	IP1, IP2
Ding et al 2009	PI, Pir, PeEc (35 + 36), TGd + TGv (TG)
Eickhoff et al 2006a	OP1, OP4, OP2-3 (OP2 + OP3)
Eickhoff et al 2006b	OP1, OP4, OP2-3 (OP2 + OP3)
Fischl et al 2008	V1 (17), V2 (18), 4 (4a + 4p), 3a, 3b, 1, 2, MT (hOC5), MST (hOC5), 44, 45, 6v (6), 55b (6), FEF (6), 6d (6), 6a (6), 6mp (6), 6ma (6), SCEF (6), SFL (6), 24dd (6)
Fischl et al 2009	EC
Geyer 2004	6v (6), 55b (6), FEF (6), 6d (6), 6a (6), 6mp (6), 6ma (6), SCEF (6), SFL (6), 24dd (6)
Geyer et al 1996	4 (4a + 4p)
Geyer et al 1999	3a, 3b, 1
Geyer et al 2000	3a, 3b, 1
Geyer et al 2000	6a (6aβ), 6d (6aα)
Glasser and Van essen 2011	FOP5 (PrCO), PreS (Sub)
Grefkes et al 2000	2
Hadjikhani et al 1998	V8
Hagler et al 2007	V7, IPS1
Hansen et al 2007	V4, LO1 + LO2 (LOC)
Henssen et al 2016	pOFC (Fo2), OFC (Fo1), 11l+13l (Fo3)
Hopf 1956	55b
Kanwisher and Yovel 2006	PIT (OFA), FFC (FFA)
Kolster et al 2010	MT (MT/V5), MST (pMST), V4t (pV4t), FST (pFST), PIT (phPITd + phPITv), LO1, LO2
Kujovic et al 2012	V3 (hOC3d), V3A (hOC4d)
Kurth et al 2009	RI (RetroInsular), Ig (Ig1 + Ig2), PoI1 + PoI2 (Id1 + Id2 + Id3)
Larsson and Heeger 2006	V3A, V3B, V7, V4 (hV4 + LO1), LO1 (LO1 + LO2), LO2 (LO1 + LO2), V4t (LO2)
Malikovic et al 2007	MT (hOC5d), MST (hOC5v)
Malikovic et al 2015	V4 (hOC4lp), V4t + LO1 + LO2 + LO3 + PIT + V3CD (hOC4la)
Moerel et al 2014	A1 (Core), MBelt (Belt), LBelt (Belt), PBelt (ParaBelt), RI (Belt)
Morel et al 2013	Ig, PoI1 + PoI2 (Id1 + Id2 + Id3), Pir (Poc)
Morosan et al 2001	A1 (TE1.0 + TE1.1), TA2 (TE1.2)
Morosan et al 2005	A4 (TE3)
Nieuwenhuys et al 2014	V6 + V6A (112), 43 (41), OP4 (68), PFop (72), PF (88), PFm (89), PGs+PGi (90), 33pr (16)
Ongur et al 2003	AAIC (Iai + Ial), AVI (Iai), MI (Ial), 10r, a10p + p10p + 10pp (10p), 47s, 47m, 47l, a47r + p47r (47r), 11l, 13l, OFC (11m + 13b + 13m + 14r), and pOFC (13a + 14c)
Palomero-Gallagher et al 2009	24dd, 24dv, v23ab (v23), d23ab (d23), 31pv (31), 31pd (31), 31a (31), 23d, 23c
Palomero-Gallagher et al 2015	25, a24 (s24), s32
Pandya and Sanides 1973	RI (reIt)
Petrides and Pandya 1999	8BM + 8BL (8B), 9m + 9a + 9p (9), 10d + 10r + 10v + a10p + p10p + 10pp (10), 8C + 8Av (8Av), 8Ad, p9-46v + a9-46v (9-46v), 46, 9-46d
Pitzalis et al 2006	V6
Pitzalis et al 2013	V6, V6A
Rajimehr et al 2009	FFC (FFA), PeEc (ATFP)
Rajkowska and Goldman-Rakic 1995a	46
Rajkowska and Goldman-Rakic 1995b	46
Rottschy et al 2007	V3 (hOC3v), V4 (hOC4v)

Sanides and Vitzthum 1965, Sanides, 1970	ProS (pStr)
Scheperjans et al 2008a	5L, 5m, 5mv (5ci), 7PC, 7AL + 7Am (7A), 7PL + 7Pm (7P), LIPv (hIP3)
Scheperjans et al 2008b	5L, 5m, 5mv (5ci), 7PC, 7AL + 7Am (7A), 7PL + 7Pm (7P), LIPv (hIP3)
Schira et al 2009	V1, V2, V3
Sereno et al 2012	V6
Smith et al 1998	V3B
Swisher et al 2007	V3A, V3B, V7, IPS1
Tootell et al 1997	V3A
Tootell et al 1998	V7
Tsao et al 2008	PIT (OFA), FFC (FFA), PeEc (ATFP)
Van Essen et al 2012a	LIPv, LIPd, VIP (VIPd + VIPv), MIP, AIP
Van Essen et al 2012b	AAIC (Iai + Ial), AVI (Iai), MI (Ial), 10r, a10p + p10p + 10pp (10p), 47s, 47m, 47l, a47r + p47r (47r), 11l, 13l, OFC (11m + 13b + 13m + 14r), and pOFC (13a + 14c)
Vogt 2009	v23ab (v23), d23ab (d23), 31pv (31), 31pd (31), 31a (31), 23d, 23c, 33pr (31a' + 31p'), p24pr (p24'), a24pr (a24'), p24 + a24 (24), p32pr + a32pr (32'), d32, p32, s32, 25
Vogt and Vogt 2003	24dd, 24dv
Vogt et al 2001	ProS
von Economo and Koskinas 1925, Triarhou 2007	V1 (OC), V2 (OB), A1 (TC), MBelt + LBelt (TB), RI (TD), PBelt (TA1), TA2, 52 + PI (IBT), TE1a + TE1m + TE1p (TE1), TE2a + TE2p (TE2), TF, PHT, PH, TGv + TGd (TG), s6-8 + i6-8 (FC(B))
Vorobiev et al 1998	6mp (SMAc), 6ma (SMAr), SCEF (SMAr)
Wandell and Winawer 2011	V1, V2, V3, V3A, V3B, V4 (hV4), V8 (VO1), VVC (VO1 + VO2), VMV3 (VO2)
Wang et al 2015	V1 (V1d + V1v), V2 (V2d + V2v), V3 (V3d +V3v), V3A, V3B, V7 (IPS0), IPS1, VVC
Weiner et al 2014	FFC (FG2), VVC (FG1)

Table 3 lists the task contrasts used above including the contrast index in the composite HCP task battery, the task name, the contrast index (cope number) within the task, the contrast name, and a brief description of the contrast.

Primary Contrast Differential Contrast Duplicate Contrast

Contrast Index	Task short name	Cope number	Task Contrast Name	Brief Description
1	WM [1]	1	2BK_BODY	Two-back task, body images(vs fixation) [2]
2	WM	2	2BK_FACE	Two-back task, face images (vs fixation)
3	WM	3	2BK_PLACE	Two-back task, place images (vs fixation)
4	WM	4	2BK_TOOL	Two-back task, tool images (vs fixation)
5	WM	5	0BK_BODY	Zero-back task, body images (vs fixation) [3]
6	WM	6	0BK_FACE	Zero-back task, face images (vs fixation)
7	WM	7	0BK_PLACE	Zero-back task, place images (vs fixation)
8	WM	8	0BK_TOOL	Zero-back task, tool images (vs fixation)
9	WM	9	2BK	Two-back task, all images (vs fixation)
10	WM	10	0BK	Zero-back task, all images (vs fixation)
11	WM	11	2BK-0BK	2BK vs 0BK
12	WM	12	neg_2BK	
13	WM	13	neg_0BK	
14	WM	14	0BK-2BK	0BK vs 2BK
15	WM	15	BODY	All body images (vs fixation)
16	WM	16	FACE	All face images (vs fixation)
17	WM	17	PLACE	All place images (vs fixation)
18	WM	18	TOOL	All tool images (vs fixation)
19	WM	19	BODY-AVG	All body images vs average of other 3 categories
20	WM	20	FACE-AVG	All face images vs average of other 3 categories
21	WM	21	PLACE-AVG	All place images vs average of other 3 categories
22	WM	22	TOOL-AVG	All tool images vs average of other 3 categories
23	WM	23	neg_BODY	
24	WM	24	neg_FACE	
25	WM	25	neg_PLACE	
26	WM	26	neg_TOOL	
27	WM	27	AVG-BODY	
28	WM	28	AVG-FACE	
29	WM	29	AVG-PLACE	
30	WM	30	AVG-TOOL	
31	GAMBLING [4]	1	PUNISH	Money loss blocks (vs fixation)
32	GAMBLING	2	REWARD	Money win blocks (vs fixation)
33	GAMBLING	3	PUNISH-REWARD	PUNISH vs REWARD
34	GAMBLING	4	neg_PUNISH	
35	GAMBLING	5	neg_REWARD	
36	GAMBLING	6	REWARD-PUNISH	REWARD vs PUNISH
37	MOTOR [5]	1	CUE	visual instruction cue (vs fixation)
38	MOTOR	2	LF	squeeze left toes (vs fixation)
39	MOTOR	3	LH	tap left fingers (vs fixation)
40	MOTOR	4	RF	squeeze right toes (vs fixation)
41	MOTOR	5	RH	tap right fingers (vs fixation)
42	MOTOR	6	T	move tongue (vs fixation)
43	MOTOR	7	AVG	Average of LF,LH,RF,RH,T (vs fixation)
44	MOTOR	8	CUE-AVG	CUE vs average of other 4 effectors
45	MOTOR	9	LF-AVG	LF vs average of other 4 effectors
46	MOTOR	10	LH-AVG	LH vs average of other 4 effectors
47	MOTOR	11	RF-AVG	RF vs average of other 4 effectors
48	MOTOR	12	RH-AVG	RH vs average of other 4 effectors
49	MOTOR	13	T-AVG	T vs average of other 4 effectors
50	MOTOR	14	neg_CUE	
51	MOTOR	15	neg_LF	

52	MOTOR	16	neg_LH	
53	MOTOR	17	neg_RF	
54	MOTOR	18	neg_RH	
55	MOTOR	19	neg_T	
56	MOTOR	20	neg_AVG	
57	MOTOR	21	AVG-CUE	
58	MOTOR	22	AVG-LF	
59	MOTOR	23	AVG-LH	
60	MOTOR	24	AVG-RF	
61	MOTOR	25	AVG-RH	
62	MOTOR	26	AVG-T	
63	LANGUAGE [6]	1	MATH	Answer arithmetic questions (vs intercept of GLM)
64	LANGUAGE	2	STORY	Listen to stories (vs intercept of GLM)
65	LANGUAGE	3	MATH-STORY	MATH vs STORY
66	LANGUAGE	4	STORY-MATH	STORY vs MATH
67	LANGUAGE	5	neg_MATH	
68	LANGUAGE	6	neg_STORY	
69	SOCIAL [7]	1	RANDOM	View randomly moving geometric objects (vs fixation)
70	SOCIAL	2	TOM	"Theory Of Mind": View "socially" interacting geometric objects (vs fixation)
71	SOCIAL	3	RANDOM-TOM	RANDOM vs TOM
72	SOCIAL	4	neg_RANDOM	
73	SOCIAL	5	neg_TOM	
74	SOCIAL	6	TOM-RANDOM	TOM vs RANDOM
75	RELATIONAL [8]	1	MATCH	Match objects based on verbal category (vs fixation)
76	RELATIONAL	2	REL	Compare featural dimensions distinguishing two pairs of objects (vs fixation)
77	RELATIONAL	3	MATCH-REL	MATCH vs REL
78	RELATIONAL	4	REL-MATCH	REL vs MATCH
79	RELATIONAL	5	neg_MATCH	
80	RELATIONAL	6	neg_REL	
81	EMOTION [9]	1	FACES	Emotional faces (vs intercept of GLM)
82	EMOTION	2	SHAPES	Neutral objects (vs intercept of GLM)
83	EMOTION	3	FACES-SHAPES	FACES vs SHAPES
84	EMOTION	4	neg_FACES	
85	EMOTION	5	neg_SHAPES	
86	EMOTION	6	SHAPES-FACES	SHAPES vs FACES

[1] WM = Working Memory
[2] Two-back: respond if current stimulus matches the item two back
[3] Zero-back: respond if current stimulus matches target cue presented at start of block
[4] adapted from (Delgado et al., 2000)
[5] adapted from (Buckner et al., 2011)
[6] Adapted from (Binder et al., 2011)
[7] Adapted from (Castelli et al., 2000; Wheatley et al., 2007)
[8] Adapted from (Smith et al., 2007)
[9] Adapted from (Hariri et al., 2002)

References

Abdollahi, R.O., Kolster, H., Glasser, M.F., Robinson, E.C., Coalson, T.S., Dierker, D., Jenkinson, M., Van Essen, D.C., Orban, G.A., 2014. Correspondences between retinotopic areas and myelin maps in human visual cortex. Neuroimage 99, 509-524.

Amiez, C., Petrides, M., 2009. Anatomical organization of the eye fields in the human and non-human primate frontal cortex. Prog Neurobiol 89, 220-230.

Amunts, K., Lenzen, M., Friederici, A.D., Schleicher, A., Morosan, P., Palomero-Gallagher, N., Zilles, K., 2010. Broca's region: novel organizational principles and multiple receptor mapping. PLoS Biol 8.

Amunts, K., Malikovic, A., Mohlberg, H., Schormann, T., Zilles, K., 2000. Brodmann's areas 17 and 18 brought into stereotaxic space-where and how variable? Neuroimage 11, 66-84.

Amunts, K., Schleicher, A., Burgel, U., Mohlberg, H., Uylings, H.B., Zilles, K., 1999. Broca's region revisited: cytoarchitecture and intersubject variability. J Comp Neurol 412, 319-341.

Arcaro, M.J., McMains, S.A., Singer, B.D., Kastner, S., 2009. Retinotopic organization of human ventral visual cortex. J Neurosci 29, 10638-10652.

Augustinack, J.C., Helmer, K., Huber, K.E., Kakunoori, S., Zollei, L., Fischl, B., 2010. Direct visualization of the perforant pathway in the human brain with ex vivo diffusion tensor imaging. Front Hum Neurosci 4, 42.

Augustinack, J.C., Huber, K.E., Stevens, A.A., Roy, M., Frosch, M.P., van der Kouwe, A.J., Wald, L.L., Van Leemput, K., McKee, A.C., Fischl, B., Alzheimer's Disease Neuroimaging, I., 2013. Predicting the location of human perirhinal cortex, Brodmann's area 35, from MRI. Neuroimage 64, 32-42.

Barch, D.M., Burgess, G.C., Harms, M.P., Petersen, S.E., Schlaggar, B.L., Corbetta, M., Glasser, M.F., Curtiss, S., Dixit, S., Feldt, C., Nolan, D., Bryant, E., Hartley, T., Footer, O., Bjork, J.M., Poldrack, R., Smith, S., Johansen-Berg, H., Snyder, A.Z., Van Essen, D.C., Consortium, W.U.-M.H., 2013. Function in the human connectome: task-fMRI and individual differences in behavior. Neuroimage 80, 169-189.

Baumann, S., Petkov, C.I., Griffiths, T.D., 2013. A unified framework for the organization of the primate auditory cortex. Front Syst Neurosci 7, 11.

Binder, J.R., Gross, W.L., Allendorfer, J.B., Bonilha, L., Chapin, J., Edwards, J.C., Grabowski, T.J., Langfitt, J.T., Loring, D.W., Lowe, M.J., 2011. Mapping anterior temporal lobe language areas with fMRI: a multicenter normative study. Neuroimage 54, 1465-1475.

Bludau, S., Eickhoff, S.B., Mohlberg, H., Caspers, S., Laird, A.R., Fox, P.T., Schleicher, A., Zilles, K., Amunts, K., 2014. Cytoarchitecture, probability maps and functions of the human frontal pole. Neuroimage 93 Pt 2, 260-275.

Brodmann, K., 1909. Vergleichende Lokalisationslehre der Grosshirnrinde in ihren Prinzipien dargestellt auf Grund des Zellenbaues. Leipzig, J.A. Barth; English translation available in Garey, L.J. Brodmann's Localization in the Cerebral Cortex (Smith Gordon, London, 1994).

Brodmann, K., 2007. Brodmann's: Localisation in the Cerebral Cortex. Springer Science & Business Media.

Buckner, R.L., Krienen, F.M., Castellanos, A., Diaz, J.C., Yeo, B.T., 2011. The organization of the human cerebellum estimated by intrinsic functional connectivity. Journal of neurophysiology 106, 2322-2345.

Burton, H., Sinclair, R.J., Wingert, J.R., Dierker, D.L., 2008. Multiple parietal operculum subdivisions in humans: tactile activation maps. Somatosens Mot Res 25, 149-162.

Caspers, J., Zilles, K., Eickhoff, S.B., Schleicher, A., Mohlberg, H., Amunts, K., 2013. Cytoarchitectonical analysis and probabilistic mapping of two extrastriate areas of the human posterior fusiform gyrus. Brain Struct Funct 218, 511-526.

Caspers, S., Eickhoff, S.B., Geyer, S., Scheperjans, F., Mohlberg, H., Zilles, K., Amunts, K., 2008. The human inferior parietal lobule in stereotaxic space. Brain Struct Funct 212, 481-495.

Caspers, S., Geyer, S., Schleicher, A., Mohlberg, H., Amunts, K., Zilles, K., 2006. The human inferior parietal cortex: cytoarchitectonic parcellation and interindividual variability. Neuroimage 33, 430-448.

Castelli, F., Happé, F., Frith, U., Frith, C., 2000. Movement and mind: a functional imaging study of perception and interpretation of complex intentional movement patterns. Neuroimage 12, 314-325.

Choi, H.J., Zilles, K., Mohlberg, H., Schleicher, A., Fink, G.R., Armstrong, E., Amunts, K., 2006. Cytoarchitectonic identification and probabilistic mapping of two distinct areas within the anterior ventral bank of the human intraparietal sulcus. J Comp Neurol 495, 53-69.

Delgado, M.R., Nystrom, L.E., Fissell, C., Noll, D., Fiez, J.A., 2000. Tracking the hemodynamic responses to reward and punishment in the striatum. Journal of neurophysiology 84, 3072-3077.

Ding, S.L., Van Hoesen, G.W., Cassell, M.D., Poremba, A., 2009. Parcellation of human temporal polar cortex: a combined analysis of multiple cytoarchitectonic, chemoarchitectonic, and pathological markers. J Comp Neurol 514, 595-623.

Eickhoff, S.B., Amunts, K., Mohlberg, H., Zilles, K., 2006a. The human parietal operculum. II. Stereotaxic maps and correlation with functional imaging results. Cereb Cortex 16, 268-279.

Eickhoff, S.B., Schleicher, A., Zilles, K., Amunts, K., 2006b. The human parietal operculum. I. Cytoarchitectonic mapping of subdivisions. Cereb Cortex 16, 254-267.

Eickhoff, S.B., Weiss, P.H., Amunts, K., Fink, G.R., Zilles, K., 2006c. Identifying human parieto-insular vestibular cortex using fMRI and cytoarchitectonic mapping. Hum Brain Mapp 27, 611-621.

Felleman, D.J., Van Essen, D.C., 1991. Distributed hierarchical processing in the primate cerebral cortex. Cereb Cortex 1, 1-47.

Fischl, B., Rajendran, N., Busa, E., Augustinack, J., Hinds, O., Yeo, B.T., Mohlberg, H., Amunts, K., Zilles, K., 2008. Cortical folding patterns and predicting cytoarchitecture. Cereb Cortex 18, 1973-1980.

Fischl, B., Stevens, A.A., Rajendran, N., Yeo, B.T., Greve, D.N., Van Leemput, K., Polimeni, J.R., Kakunoori, S., Buckner, R.L., Pacheco, J., Salat, D.H., Melcher, J., Frosch, M.P., Hyman, B.T., Grant, P.E., Rosen, B.R., van der Kouwe, A.J., Wiggins, G.C., Wald, L.L., Augustinack, J.C., 2009. Predicting the location of entorhinal cortex from MRI. Neuroimage 47, 8-17.

Gennari, F., 1782. De peculiari structura cerebri nonnullisque ejus morbis: paucae aliae anatom. observat. accedunt. ex regio typographeo.
Geyer, S., 2004. The microstructural border between the motor and the cognitive domain in the human cerebral cortex. Advances in anatomy, embryology, and cell biology 174.
Geyer, S., Ledberg, A., Schleicher, A., Kinomura, S., Schormann, T., Burgel, U., Klingberg, T., Larsson, J., Zilles, K., Roland, P.E., 1996. Two different areas within the primary motor cortex of man. Nature 382, 805-807.
Geyer, S., Schleicher, A., Zilles, K., 1999. Areas 3a, 3b, and 1 of human primary somatosensory cortex. Neuroimage 10, 63-83.
Geyer, S., Schormann, T., Mohlberg, H., Zilles, K., 2000. Areas 3a, 3b, and 1 of human primary somatosensory cortex. Part 2. Spatial normalization to standard anatomical space. Neuroimage 11, 684-696.
Glasser, M.F., Goyal, M.S., Preuss, T.M., Raichle, M.E., Van Essen, D.C., 2014. Trends and properties of human cerebral cortex: correlations with cortical myelin content. Neuroimage 93 Pt 2, 165-175.
Glasser, M.F., Sotiropoulos, S.N., Wilson, J.A., Coalson, T.S., Fischl, B., Andersson, J.L., Xu, J., Jbabdi, S., Webster, M., Polimeni, J.R., Van Essen, D.C., Jenkinson, M., Consortium, W.U.-M.H., 2013. The minimal preprocessing pipelines for the Human Connectome Project. Neuroimage 80, 105-124.
Glasser, M.F., Van Essen, D.C., 2011. Mapping human cortical areas in vivo based on myelin content as revealed by T1- and T2-weighted MRI. J Neurosci 31, 11597-11616.
Goddard, E., Mannion, D.J., McDonald, J.S., Solomon, S.G., Clifford, C.W., 2011. Color responsiveness argues against a dorsal component of human V4. Journal of vision 11, 3.
Goodale, M.A., Milner, A.D., 1992. Separate visual pathways for perception and action. Trends in neurosciences 15, 20-25.
Grefkes, C., Geyer, S., Schormann, T., Roland, P., Zilles, K., 2001. Human somatosensory area 2: observer-independent cytoarchitectonic mapping, interindividual variability, and population map. Neuroimage 14, 617-631.
Hackett, T., 2007. Organization and correspondence of the auditory cortex of humans and nonhuman primates. Evolution of the nervous system, 109-119.
Hackett, T.A., Preuss, T.M., Kaas, J.H., 2001. Architectonic identification of the core region in auditory cortex of macaques, chimpanzees, and humans. J Comp Neurol 441, 197-222.
Hadjikhani, N., Liu, A.K., Dale, A.M., Cavanagh, P., Tootell, R.B.H., 1998. Retinotopy and color sensitivity in human visual cortical area V8. Nature Neurosci 1, 235-241.
Hagler, D.J., Jr., Riecke, L., Sereno, M.I., 2007. Parietal and superior frontal visuospatial maps activated by pointing and saccades. Neuroimage 35, 1562-1577.
Hansen, K.A., Kay, K.N., Gallant, J.L., 2007. Topographic organization in and near human visual area V4. J Neurosci 27, 11896-11911.
Hariri, A.R., Tessitore, A., Mattay, V.S., Fera, F., Weinberger, D.R., 2002. The amygdala response to emotional stimuli: a comparison of faces and scenes. Neuroimage 17, 317-323.
Heinzle, J., Kahnt, T., Haynes, J.D., 2011. Topographically specific functional connectivity between visual field maps in the human brain. Neuroimage 56, 1426-1436.

Henssen, A., Zilles, K., Palomero-Gallagher, N., Schleicher, A., Mohlberg, H., Gerboga, F., Eickhoff, S.B., Bludau, S., Amunts, K., 2016. Cytoarchitecture and probability maps of the human medial orbitofrontal cortex. Cortex 75, 87-112.

Hill, J., Dierker, D., Neil, J., Inder, T., Knutsen, A., Harwell, J., Coalson, T., Van Essen, D., 2010. A surface-based analysis of hemispheric asymmetries and folding of cerebral cortex in term-born human infants. J Neurosci 30, 2268-2276.

Hopf, A., 1956. Über die Verteilung myeloarchitektonischer Merkmale in der Stirnhirnrinde beim Menschen. J Hirnforsch 2, 311-333.

Kaas, J.H., Hackett, T.A., 2000. How the visual projection map instructs the auditory computational map. J Comp Neurol 421, 143-145.

Kanwisher, N., Yovel, G., 2006. The fusiform face area: a cortical region specialized for the perception of faces. Philos Trans R Soc Lond B Biol Sci 361, 2109-2128.

Kolster, H., Peeters, R., Orban, G.A., 2010. The retinotopic organization of the human middle temporal area MT/V5 and its cortical neighbors. J Neurosci 30, 9801-9820.

Krubitzer, L., Huffman, K.J., Disbrow, E., Recanzone, G., 2004. Organization of area 3a in macaque monkeys: contributions to the cortical phenotype. Journal of Comparative Neurology 471, 97-111.

Krubitzer, L.A., Kaas, J.H., 1990. The organization and connections of somatosensory cortex in marmosets. Journal of Neuroscience 10, 952.

Kujovic, M., Zilles, K., Malikovic, A., Schleicher, A., Mohlberg, H., Rottschy, C., Eickhoff, S.B., Amunts, K., 2013. Cytoarchitectonic mapping of the human dorsal extrastriate cortex. Brain Struct Funct 218, 157-172.

Kurth, F., Eickhoff, S.B., Schleicher, A., Hoemke, L., Zilles, K., Amunts, K., 2010. Cytoarchitecture and probabilistic maps of the human posterior insular cortex. Cereb Cortex 20, 1448-1461.

Larsson, J., Heeger, D.J., 2006. Two retinotopic visual areas in human lateral occipital cortex. J Neurosci 26, 13128-13142.

Malikovic, A., Amunts, K., Schleicher, A., Mohlberg, H., Eickhoff, S.B., Wilms, M., Palomero-Gallagher, N., Armstrong, E., Zilles, K., 2007. Cytoarchitectonic analysis of the human extrastriate cortex in the region of V5/MT+: a probabilistic, stereotaxic map of area hOc5. Cereb Cortex 17, 562-574.

Malikovic, A., Amunts, K., Schleicher, A., Mohlberg, H., Kujovic, M., Palomero-Gallagher, N., Eickhoff, S.B., Zilles, K., 2015. Cytoarchitecture of the human lateral occipital cortex: mapping of two extrastriate areas hOc4la and hOc4lp. Brain Struct Funct.

Meier, J.D., Aflalo, T.N., Kastner, S., Graziano, M.S., 2008. Complex organization of human primary motor cortex: a high-resolution fMRI study. J Neurophysiol 100, 1800-1812.

Mishkin, M., Ungerleider, L.G., 1982. Contribution of striate inputs to the visuospatial functions of parieto-preoccipital cortex in monkeys. Behav Brain Res 6, 57-77.

Moerel, M., De Martino, F., Formisano, E., 2014. An anatomical and functional topography of human auditory cortical areas. Front Neurosci 8, 225.

Morecraft, R.J., Rockland, K.S., Van Hoesen, G.W., 2000. Localization of area prostriata and its projection to the cingulate motor cortex in the rhesus monkey. Cerebral Cortex 10, 192-203.

Morel, A., Gallay, M.N., Baechler, A., Wyss, M., Gallay, D.S., 2013. The human insula: Architectonic organization and postmortem MRI registration. Neuroscience 236, 117-135.

Morosan, P., Rademacher, J., Schleicher, A., Amunts, K., Schormann, T., Zilles, K., 2001. Human primary auditory cortex: cytoarchitectonic subdivisions and mapping into a spatial reference system. Neuroimage 13, 684-701.

Morosan, P., Schleicher, A., Amunts, K., Zilles, K., 2005. Multimodal architectonic mapping of human superior temporal gyrus. Anat Embryol (Berl) 210, 401-406.

Nasr, S., Liu, N., Devaney, K.J., Yue, X., Rajimehr, R., Ungerleider, L.G., Tootell, R.B., 2011. Scene-selective cortical regions in human and nonhuman primates. J Neurosci 31, 13771-13785.

Nieuwenhuys, R., Broere, C.A., Cerliani, L., 2015. A new myeloarchitectonic map of the human neocortex based on data from the Vogt-Vogt school. Brain Struct Funct 220, 2551-2573.

Ongur, D., Ferry, A.T., Price, J.L., 2003. Architectonic subdivision of the human orbital and medial prefrontal cortex. J Comp Neurol 460, 425-449.

Palomero-Gallagher, N., Eickhoff, S.B., Hoffstaedter, F., Schleicher, A., Mohlberg, H., Vogt, B.A., Amunts, K., Zilles, K., 2015. Functional organization of human subgenual cortical areas: Relationship between architectonical segregation and connectional heterogeneity. Neuroimage 115, 177-190.

Palomero-Gallagher, N., Vogt, B.A., Schleicher, A., Mayberg, H.S., Zilles, K., 2009. Receptor architecture of human cingulate cortex: evaluation of the four-region neurobiological model. Hum Brain Mapp 30, 2336-2355.

Pandya, D.N., Sanides, F., 1973. Architectonic parcellation of the temporal operculum in rhesus monkey and its projection pattern. Z Anat Entwicklungsgesch 139, 127-161.

Paus, T., 2001. Primate anterior cingulate cortex: where motor control, drive and cognition interface. Nature Reviews Neuroscience 2, 417-424.

Penfield, W., Rasmussen, T., 1950. The cerebral cortex of man; a clinical study of localization of function.

Petrides, M., Pandya, D.N., 1999. Dorsolateral prefrontal cortex: comparative cytoarchitectonic analysis in the human and the macaque brain and corticocortical connection patterns. Eur J Neurosci 11, 1011-1036.

Pitzalis, S., Galletti, C., Huang, R.S., Patria, F., Committeri, G., Galati, G., Fattori, P., Sereno, M.I., 2006. Wide-field retinotopy defines human cortical visual area v6. J Neurosci 26, 7962-7973.

Pitzalis, S., Sereno, M.I., Committeri, G., Fattori, P., Galati, G., Tosoni, A., Galletti, C., 2013. The human homologue of macaque area V6A. Neuroimage 82, 517-530.

Power, J.D., Cohen, A.L., Nelson, S.M., Wig, G.S., Barnes, K.A., Church, J.A., Vogel, A.C., Laumann, T.O., Miezin, F.M., Schlaggar, B.L., Petersen, S.E., 2011. Functional network organization of the human brain. Neuron 72, 665-678.

Rademacher, J., Caviness Jr, V., Steinmetz, H., Galaburda, A., 1993. Topographical variation of the human primary cortices: implications for neuroimaging, brain mapping, and neurobiology. Cerebral Cortex 3, 313.

Rajimehr, R., Young, J.C., Tootell, R.B., 2009. An anterior temporal face patch in human cortex, predicted by macaque maps. Proc Natl Acad Sci U S A 106, 1995-2000.

Rajkowska, G., Goldman-Rakic, P.S., 1995a. Cytoarchitectonic definition of prefrontal areas in the normal human cortex: I. Remapping of areas 9 and 46 using quantitative criteria. Cereb Cortex 5, 307-322.

Rajkowska, G., Goldman-Rakic, P.S., 1995b. Cytoarchitectonic definition of prefrontal areas in the normal human cortex: II. Variability in locations of areas 9 and 46 and relationship to the Talairach Coordinate System. Cereb Cortex 5, 323-337.

Robinson, E.C., Jbabdi, S., Glasser, M.F., Andersson, J., Burgess, G.C., Harms, M.P., Smith, S.M., Van Essen, D.C., Jenkinson, M., 2014. MSM: a new flexible framework for Multimodal Surface Matching. Neuroimage 100, 414-426.

Roland, P.E., Zilles, K., 1996. Functions and structures of the motor cortices in humans. Curr Opin Neurobiol 6, 773-781.

Rottschy, C., Eickhoff, S.B., Schleicher, A., Mohlberg, H., Kujovic, M., Zilles, K., Amunts, K., 2007. Ventral visual cortex in humans: cytoarchitectonic mapping of two extrastriate areas. Hum Brain Mapp 28, 1045-1059.

Sanides, F., 1970. Functional architecture of motor and sensory cortices in primates in the light of a new concept of neocortex evolution. The primate brain: Advances in primatology 1, 137-201.

Sanides, F., Vitzthum, H.G., 1965. Zur Architektonik der menschlichen Sehrinde und den Prinzipien ihrer Entwicklung. J, Neurology 18, 680-707.

Scheperjans, F., Eickhoff, S.B., Homke, L., Mohlberg, H., Hermann, K., Amunts, K., Zilles, K., 2008a. Probabilistic maps, morphometry, and variability of cytoarchitectonic areas in the human superior parietal cortex. Cereb Cortex 18, 2141-2157.

Scheperjans, F., Hermann, K., Eickhoff, S.B., Amunts, K., Schleicher, A., Zilles, K., 2008b. Observer-independent cytoarchitectonic mapping of the human superior parietal cortex. Cereb Cortex 18, 846-867.

Schira, M.M., Tyler, C.W., Breakspear, M., Spehar, B., 2009. The foveal confluence in human visual cortex. J Neurosci 29, 9050-9058.

Sereno, M.I., Dale, A.M., Reppas, J.B., Kwong, K.K., Belliveau, J.W., Brady, T.J., Rosen, B.R., Tootell, R.B., 1995. Borders of multiple visual areas in humans revealed by functional magnetic resonance imaging. Science 268, 889-893.

Sereno, M.I., Lutti, A., Weiskopf, N., Dick, F., 2013. Mapping the human cortical surface by combining quantitative T(1) with retinotopy. Cereb Cortex 23, 2261-2268.

Sereno, M.I., McDonald, C.T., Allman, J.M., 1994. Analysis of retinotopic maps in extrastriate cortex. Cereb Cortex 4, 601-620.

Smith, A.T., Greenlee, M.W., Singh, K.D., Kraemer, F.M., Hennig, J., 1998. The processing of first- and second-order motion in human visual cortex assessed by functional magnetic resonance imaging (fMRI). J Neurosci 18, 3816-3830.

Smith, R., Keramatian, K., Christoff, K., 2007. Localizing the rostrolateral prefrontal cortex at the individual level. Neuroimage 36, 1387-1396.

Swisher, J.D., Halko, M.A., Merabet, L.B., McMains, S.A., Somers, D.C., 2007. Visual topography of human intraparietal sulcus. J Neurosci 27, 5326-5337.

Talavage, T.M., Hall, D.A., 2012. How challenges in auditory fMRI led to general advancements for the field. Neuroimage 62, 641-647.

Tootell, R.B., Hadjikhani, N., Hall, E.K., Marrett, S., Vanduffel, W., Vaughan, J.T., Dale, A.M., 1998. The retinotopy of visual spatial attention. Neuron 21, 1409-1422.

Tootell, R.B., Mendola, J.D., Hadjikhani, N.K., Ledden, P.J., Liu, A.K., Reppas, J.B., Sereno, M.I., Dale, A.M., 1997. Functional analysis of V3A and related areas in human visual cortex. J Neurosci 17, 7060-7078.

Triarhou, L.C., 2007a. The Economo-Koskinas atlas revisited: cytoarchitectonics and functional context. Stereotact Funct Neurosurg 85, 195-203.
Triarhou, L.C., 2007b. A proposed number system for the 107 cortical areas of Economo and Koskinas, and Brodmann area correlations. Stereotact Funct Neurosurg 85, 204-215.
Tsao, D.Y., Moeller, S., Freiwald, W.A., 2008. Comparing face patch systems in macaques and humans. Proc Natl Acad Sci U S A 105, 19514-19519.
Van Essen, D., Glasser, M.F., Robinson, E., Chen, X.J., Jenkinson, M., Dierker, D., Nichols, T., Smith, S., 2014. Heritability of brain structure, function, and connectiviity in Human Connectome Project data. Annual Meeting of the Organization for Human Brain Mapping. (Hamburg, Germany; June 8-12 2014).
Van Essen, D., Newsome, W.T., Bixby, J.L., 1982. The middle temporal visual area in the macaque: myeloarchitecture, connections, functional properties and topographic organization. J Neurosci 2, 265-283.
Van Essen, D.C., Glasser, M.F., Dierker, D.L., Harwell, J., 2012a. Cortical parcellations of the macaque monkey analyzed on surface-based atlases. Cereb Cortex 22, 2227-2240.
Van Essen, D.C., Glasser, M.F., Dierker, D.L., Harwell, J., Coalson, T., 2012b. Parcellations and hemispheric asymmetries of human cerebral cortex analyzed on surface-based atlases. Cereb Cortex 22, 2241-2262.
Vogt, B., 2009. Cingulate neurobiology and disease. Oxford University Press.
Vogt, B., Nimchinsky, E., Vogt, L., Hof, P., 1995. Human cingulate cortex: surface features, flat maps, and cytoarchitecture. The Journal of comparative neurology 359, 490-506.
Vogt, B.A., Vogt, L., 2003. Cytology of human dorsal midcingulate and supplementary motor cortices. Journal of Chemical Neuroanatomy 26, 301-309.
Vogt, B.A., Vogt, L., Farber, N.B., Bush, G., 2005. Architecture and neurocytology of monkey cingulate gyrus. J Comp Neurol 485, 218-239.
Vogt, B.A., Vogt, L. J., Perl, D. P., & Hof, P. R., 2001. Cytology of human caudomedial cingulate, retrosplenial, and caudal parahippocampal cortices. J. Comp. Neurol, 438, 353-376.
von Economo, C., Koskinas, G.N., 1925. E Die Cytoarchitektonik der Hirnrinde des erwachsenen Menschen. Textband und Atlas. Wien, Springer.
Vorobiev, V., Govoni, P., Rizzolatti, G., Matelli, M., Luppino, G., 1998. Parcellation of human mesial area 6: cytoarchitectonic evidence for three separate areas. Eur J Neurosci 10, 2199-2203.
Wade, A.R., Brewer, A.A., Rieger, J.W., Wandell, B.A., 2002. Functional measurements of human ventral occipital cortex: retinotopy and colour. Philos Trans R Soc Lond B Biol Sci 357, 963-973.
Wandell, B.A., Winawer, J., 2011. Imaging retinotopic maps in the human brain. Vision Res 51, 718-737.
Wang, L., Mruczek, R.E., Arcaro, M.J., Kastner, S., 2015. Probabilistic Maps of Visual Topography in Human Cortex. Cereb Cortex 25, 3911-3931.
Weiner, K.S., Golarai, G., Caspers, J., Chuapoco, M.R., Mohlberg, H., Zilles, K., Amunts, K., Grill-Spector, K., 2014. The mid-fusiform sulcus: a landmark identifying both cytoarchitectonic and functional divisions of human ventral temporal cortex. Neuroimage 84, 453-465.
Wheatley, T., Milleville, S.C., Martin, A., 2007. Understanding animate agents distinct roles for the social network and mirror system. Psychological science 18, 469-474.

Winawer, J., Horiguchi, H., Sayres, R.A., Amano, K., Wandell, B.A., 2010. Mapping hV4 and ventral occipital cortex: the venous eclipse. J Vis 10, 1.

Yeo, B.T., Krienen, F.M., Sepulcre, J., Sabuncu, M.R., Lashkari, D., Hollinshead, M., Roffman, J.L., Smoller, J.W., Zollei, L., Polimeni, J.R., Fischl, B., Liu, H., Buckner, R.L., 2011. The organization of the human cerebral cortex estimated by intrinsic functional connectivity. J Neurophysiol 106, 1125-1165.